Universitat Autònoma de Barcelona

Modulation of cellular pathways as a therapeutic strategy in HIV infection

Sònia Pedreño López

Universitat Autònoma de Barcelona

Facultat de Medicina

Departament de Biologia Cel·lular, Fisiologia i Immunologia

Modulation of cellular pathways as a therapeutic strategy in HIV infection

Sònia Pedreño López

September 2021

Institut de Recerca de la SIDA (IrsiCaixa),

Institut d'Investigació en Ciències de la Salut Germans Trias i Pujol (IGTP)

Hospital Germans Trias i Pujol

Doctoral thesis to obtain a PhD degree in Advanced Immunology from Universitat Autònoma de Barcelona

Directora: **Dra. Cecilia Cabrera Navarro**

La Dra. Cecilia Cabrera Navarro (Directora i Tutora) investigadora de l'Institut de Recerca de la SIDA (IrsiCaixa) i de l'Institut d'Investigació en Ciències de la Salut Germans Trias i Pujol (IGTP),

Certifica:

Que el treball experimental i la redacció de la memòria de la Tesi doctoral titulada **'*Modulation of cellular pathways as a therapeutic strategy in HIV infection*'** ha estat realitzada per la Sònia Pedreño López sota la seva direcció i tutoria, i considera que és apta per a ser presentada per tal d'optar al grau de Doctora en Immunologia per la Universitat Autònoma de Barcelona.

I per tal que quedi constància, signa aquest document.

Badalona, 17 Setembre 2021.

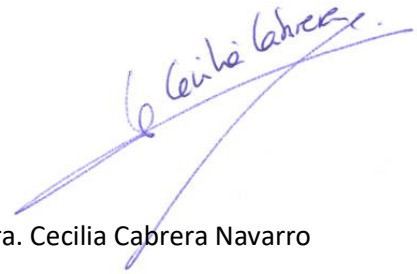

Dra. Cecilia Cabrera Navarro

This work has been supported by *'Fondo de Investigación Sanitaria (FIS)'* project PI12/02408 from 2016 to 2018, and project PI15/01053 from 2019 to 2021 from Instituto de Salud Carlos III (ISCIII) cofinanced by FEDER and by Grifols.

The printing of this thesis was possible by the financial support of the Universitat Autònoma de Barcelona.

'What we know is a drop, what we don't know is an ocean'

Isaac Newton

Per tu, avi

A la meva família i a en Francesc

INDEX

SUMMARY

The hallmarks of acquired immunodeficiency syndrome (AIDS) is a progressive depletion of $CD4^+$ T cell populations in blood and a massive destruction of these cells in lymphoid tissues. Even though $CD4^+$ T cells in blood recover progressively during the chronic phase, their destruction in lymphoid tissue continue during the course of infection and do not recover completely even with antiretroviral treatment (ART).

A complex link exists between HIV-1 and the survival and death pathways. Discordant results have been reported regarding the interrelationship between the virus and these two cellular pathways. The aim of this Thesis was to evaluate the interplay between HIV and cell survival (autophagic pathway) and cell death (apoptosis) using human lymphoid tissue cultures *ex vivo* as a model to evaluate HIV infection. Our results showed that human lymphoid aggregated cultures (HLACs) from tonsillar tissue displayed a fully functional autophagic activity. In this system, HIV infection resulted in an increase in autophagy, however, this increase was not related with a loss of autophagic functionality. Notably, we observed that both, autophagy-enhancing or blocking drugs, were able to decrease HIV-DNA levels and viral replication. Regarding cell death, our data showed that in lymphoid tissue HIV infection induce both pyroptotic (caspase-1 activation) and apoptotic (caspase-3 activation) pathways. The inhibition of caspase activation by Q-VD-OPh (a pan-caspase inhibitor) was able to prevent HIV-induced $CD4^+$ T cell depletion, but also HIV replication (in an envelope-independent manner) with a decrease in both total and integrated HIV DNA. In the evaluation of the mechanism of action of Q-VD-OPh, we observed that this drug was inducing a cellular antiviral state; decreasing cellular activation, decreasing mitochondrial membrane potential and increasing the type-I IFN response. All our data suggest that host-directed therapies are a promising emerging approach in addressing infectious diseases, and may have the potential to both interfere with host cell mechanisms hijacked by viruses for productive infection and boost innate immune defense mechanisms.

RESUM

La característica distintiva del síndrome de la immunodeficiència adquirida (SIDA) és la progressiva depleció de la població de cèl·lules T $CD4^+$ en sang i una destrucció massiva d'aquestes cèl·lules en teixit limfoide. Tot i que les cèl·lules T $CD4^+$ en sang es recuperen progressivament durant la fase crònica, la seva destrucció en teixit limfoide continua durant el curs de la infecció i no es recuperen completament ni tan sols amb tractament antirretroviral (TAR).

Existeix un vincle complex entre el VIH-1 i les vies de supervivència i mort. S'han informat de resultats discordants sobre la interrelació entre el virus i aquestes dues vies cel·lulars. L'objectiu d'aquesta Tesis era evaluar la interacció entre el VIH i la supervivència cel·lular (via autofàgica) i la mort cel·lular (apoptosis) mitjançant el cultiu de teixit limfoide humà *ex vivo* com a model per evaluar la infecció del VIH. Els nostres resultats van mostrar que els cultius limfoides humans agregats de teixit d'amígdales presentaven una activitat autofàgica completament funcional. En aquest sistema, la infecció pel VIH va donar lloc a un augment de l'autofàgia, malgrat això, aquest increment no estava relacionat amb la pèrdua de funcionalitat autofàgica. En concret, vam observar que tots dos, fàrmacs que augmenten i que bloquegen l'autofàgia, eren capaços de disminuir els nivells de ADN del VIH i la replicació viral. En relació a la mort cel·lular, les nostres dades van mostrar que en teixit limfoide la infecció pel VIH indueix tant la via de la piroptosis (caspasa-1 activa) com de l'apoptosis (caspasa-3 activa). La inhibició d'aquesta activació de caspases amb el Q-VD-Oph (un inhibidor de pan-caspases) va ser capaç de prevenir la depleció de les cèl·lules T $CD4^+$ induida pel VIH, però també la replicació del VIH (de manera independent de l'envolta) amb una disminució tant del ADN total com de l'integrat del VIH. En l'evaluació del mecanisme d'acció de Q-VD-Oph, vam observar que aquest fàrmac induïa un estat antiviral; disminuint l'activació cel·lular, reduint el potencial de membrana mitocondrial i incrementant la resposta interferó de tipus-I. Totes les nostres dades suggereixen que les teràpies dirigides a l'hoste són un enfoc emergent prometedor per fer front a les malalties infeccioses, i poden tenir el potencial tant d'interferir amb els mecanismes de les cèl·lules hostes segrestades pels virus per a una infecció productiva, com per augmentar els mecanismes de defensa del sistema immune innat.

RESUMEN

La característica distintiva del síndrome de la inmunodeficiencia adquirida (SIDA) es la progresiva depleción de la población de células T $CD4^+$ en sangre y una destrucción masiva de estas células en tejido linfoide. Aunque las células T $CD4^+$ en sangre se recuperan progresivamente durante la fase crónica, su destrucción en el tejido linfoide continua durante el curso de la infección y no se recuperan completamente ni siquiera con tratamiento antirretroviral (TAR).

Existe un vínculo complejo entre el VIH-1 y las vías de supervivencia y muerte, y se han informado de resultados discordantes sobre la interrelación entre el virus y estas dos vías celulares. El objetivo de esta Tesis era evaluar la interacción entre el VIH y la supervivencia celular (vía autofagia) y la muerte celular (apoptosis) mediante el cultivo de tejido linfoide humano *ex vivo* como modelo para evaluar la infección del VIH. Nuestros resultados mostraron que los cultivos linfoides humanos agregados de tejido de amígdala presentaban una actividad autofágica completamente funcional. En este sistema, la infección por VIH dio lugar a un aumento de la autofagia, sin embargo, este incremento no estaba relacionado con la pérdida de la funcionalidad autofágica. En concreto, observamos que ambos, fármacos que aumentan y que bloquean la autofagia, eran capaces de disminuir los niveles de ADN del VIH y la replicación viral. En relación a la muerte celular, nuestros datos mostraron que en tejido linfoide la infección por VIH induce tanto la vía de la piroptosis (caspasa-1 activa) como de la apoptosis (caspasa-3 activa). La inhibición de esta activación de caspasas con el Q-VD-OPh (un inhibidor de pan-caspasas) fue capaz de prevenir la depleción de las células T $CD4^+$ inducida por el VIH, pero también la replicación del VIH (de manera independiente de envuelta) con una disminución tanto del ADN total como del integrado del VIH. En la evaluación del mecanismo de acción de Q-VD-OPh, observamos que este fármaco inducía un estado antiviral; disminuyendo la activación celular, reduciendo el potencial de membrana mitocondrial y incrementando la respuesta interferón de tipo-I. Todos nuestros datos sugieren que las terapias dirigidas al huésped son un enfoque emergente prometedor para hacer frente a las enfermedades infecciosas, y pueden tener el potencial tanto de interferir con los mecanismos de las células huésped secuestradas por el virus para una infección productiva, como para aumentar el mecanismo de defensa del sistema inmune innato.

ABBREVIATIONS

AIDS	Acquired Immunodeficiency Syndrome
ART	Antiretroviral therapy
ATG	Autophagy-related genes
ATP	Adenosine triphosphate
AZT	Azidothymidine
CCR5	Chemokine receptor 5
cDNA	Cytoplasmic Deoxyribonucleic acid
cGAMP	Cyclic GMP-AMP
cGAS	Cyclic GMP-AMP (cGMP-AMP) synthase
CXCR4	CXC Chemokine receptor 4
Cyt c	Cytochrome C
DAMP	Damage-associated molecular pattern
DC	Dendritic cells
DNA	Deoxyribonucleic acid
EC	Elite controllers
GALT	Gut-associated lymphoid tissue
GI	Gastrointestinal
HIV	Human Immunodeficiency virus
HLAC	Human lymphoid aggregate culture
HLH	Human lymphoid histoculture
IFN-I	Interferon type 1
IL-1β	Interleukin 1 beta
IL-18	Interleukin 18
IRF	Interferon Regulatory Factor
ISG	IFN-stimulated genes
LC3	Microtubule Associated protein 1 light chain 3
LC3I	Microtubule Associated protein 1 light chain 3 Type 1
LC3II	Microtubule Associated protein 1 light chain 3 Type 2

LPS	Lipopolysaccharide
LTNP	Long term non progressors
MAVS	Mitochondrial antiviral-signaling protein
MIMP	Mitochondrial inner membrane permeabilization
MOM	Mitochondrial outer membrane
MOMP	Mitochondrial outer membrane permeabilization
mtDNA	Mitochondrial Deoxyribonucleic acid
mTOR	Mammalian target of Rapamycin
NF-κB	Nuclear factor kappa-light-chain-enhancer of activated B cells
p62	Ubiquitin-binding protein p62 or Sequestrosome-1
PAMP	Pathogen-associated molecular pattern
PBMC	Peripheral blood mononuclear cells
PCR	Polymerase chain reaction
PI3KIII	Phosphoinositide 3-kinase complex III
PI3P	Phosphatidylinositol 3-phosphate
PRR	Pattern recognition receptor
Q-VD-Oph	N-(2-Quinolyl)-L-valyl-L-aspartyl-(2,6-difluorophenoxy) methylketone
Q-VE-Oph	N-(2-Quinolyl)-L-valyl-L-glutamyl-(2,6-difluorophenoxy) methylketone
R5	Virus with tropism R5
RIG-I	Retinoic acid-inducible gene I
RNA	Ribonucleic acid
STING	Stimulator of Interferon genes
TBK1	TANK-binding kinase 1
X4	Virus with tropism X4
V-ATPase	Vacuolar H+ ATPase
z-VAD-fmk	Carbobenzoxy-valyl-alanyl-aspartyl-[O-methyl]- fluoromethylketone

INTRODUCTION

1. HUMAN IMMUNODEFICIENCY VIRUS

1.1 ORIGIN AND EPIDEMIOLOGY OF THE PANDEMIC

Human immunodeficiency virus (HIV) is a lentivirus that belongs to the *Retroviridae* family. This viral infection is characterized for causing a chronic infection with high levels of viremia that leads to an abrupt decline in the number of $CD4^+$ T lymphocytes. Without treatment, HIV produces acquired immunodeficiency syndrome (AIDS)[1], a disease which progressive failure of the immune system allows opportunistic infections to appear[2]. Although AIDS was described as a new disease that mainly affected homosexual men in 1981, it was not until two years later that the viral agent was identified as HIV type 1 (HIV-1)[3]. HIV is spread through sex, sharing needles, blood transfusion, and through vertical transmission (during pregnancy, childbirth and breastfeeding)[4].

While there are two HIV types, HIV-1 and HIV-2, HIV-1 has been described as a more virulent strain that is easily transmitted and is responsible for the majority of infections worldwide. On the contrary, HIV-2 is less transmittable and has a lower rate of disease progression. HIV-1 is closely related to a virus found in chimpanzees (subspecies *Pan troglodytes troglodytes*), which live in the forest of Central Africa. Interestingly, HIV-2 is similar to a viral strain isolated from sooty mangabey (*Cercocebus atys*) and it is mainly restrained to West Africa[3]. Since the beginning of the pandemic, 77.5 million people have become infected with HIV, 34.7 million of whom died from AIDS-related illnesses. Nowadays, there are 37.6 million people globally living with HIV-1 in 2020, 35.9 million are adults and 1.7 million are children (from 0 to 14 years old), 20 million of whom live in Africa (**Figure 1**). Even though new HIV infections have been reduced 30% since 2010, 1.5 million people became newly infected with HIV during 2020. Approximately 84% of HIV-infected people know their serostatus, which means that 16% remain unaware and, therefore, hindering the ability to control viral spread.

The availability of antiretroviral therapy (ART) has reduced mortality by AIDS. However, there are still 27.4 million people without access to this treatment on 2020[4].

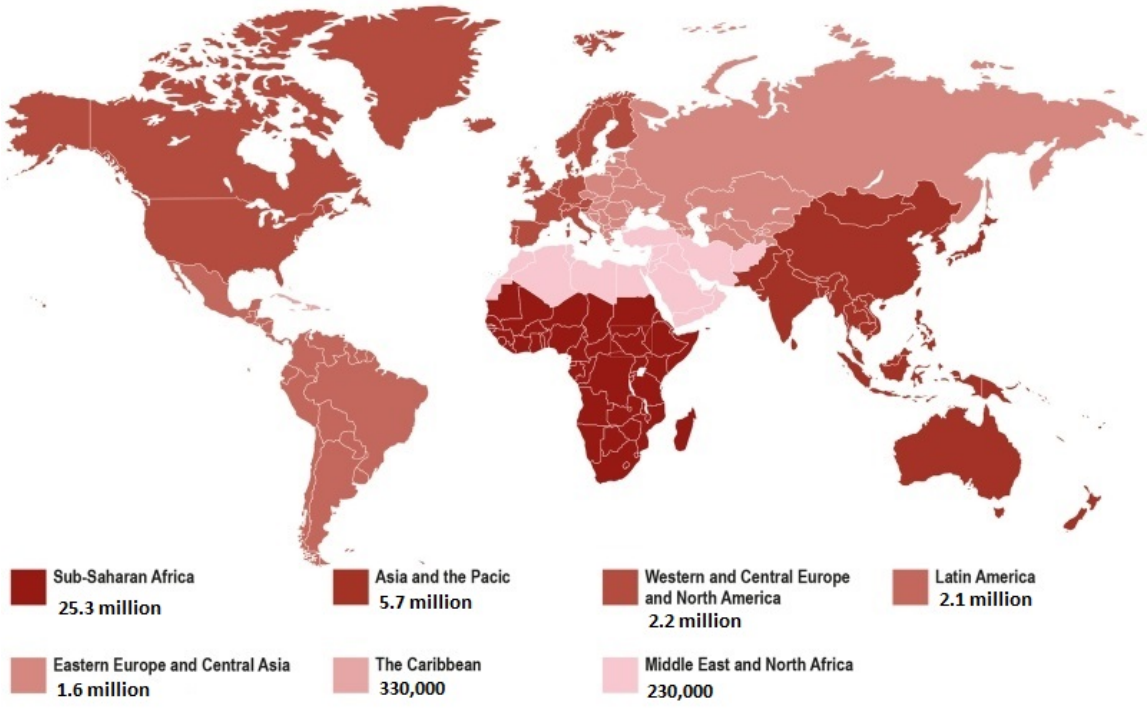

Figure 1. Estimated worldwide distribution of HIV-1 infections in 2020. Incidence of total infections worldwide. Adapted image from The Journal for unicellular biology and human disease; and numbers of infected people are extracted from the 2020 UNAIDS report.

1.2 HIV PARTICLE AND VIRAL GENOME

The mature HIV-1 particle is spherical and measures approximately 100nm in diameter. The outer lipid bilayer constituted the Envelope protein (Env, gp160), which is formed by gp120 trimers anchored to the viral membrane and the transmembrane protein gp41. Each viral particle contains two single-stranded RNA copies enclosed by a conical capsid (Gag), which includes the reverse transcriptase, protease and integrase[5]. The HIV genome contains nine genes that encode 15 viral proteins. These genes are translated as polyproteins, producing structural proteins (Gag, Pol, and Env) as well as proteins with regulatory and accessory functions (Tat, Rev, Nef, Vif, Vpr and Vpu). Particularly, Gag generates some structural proteins, such as p24, Pol enables the virus to transcribe and integrate itself into the host cell, and Env mediates CD4 binding and membrane fusion with the host cell (**Figure 2**)[6].

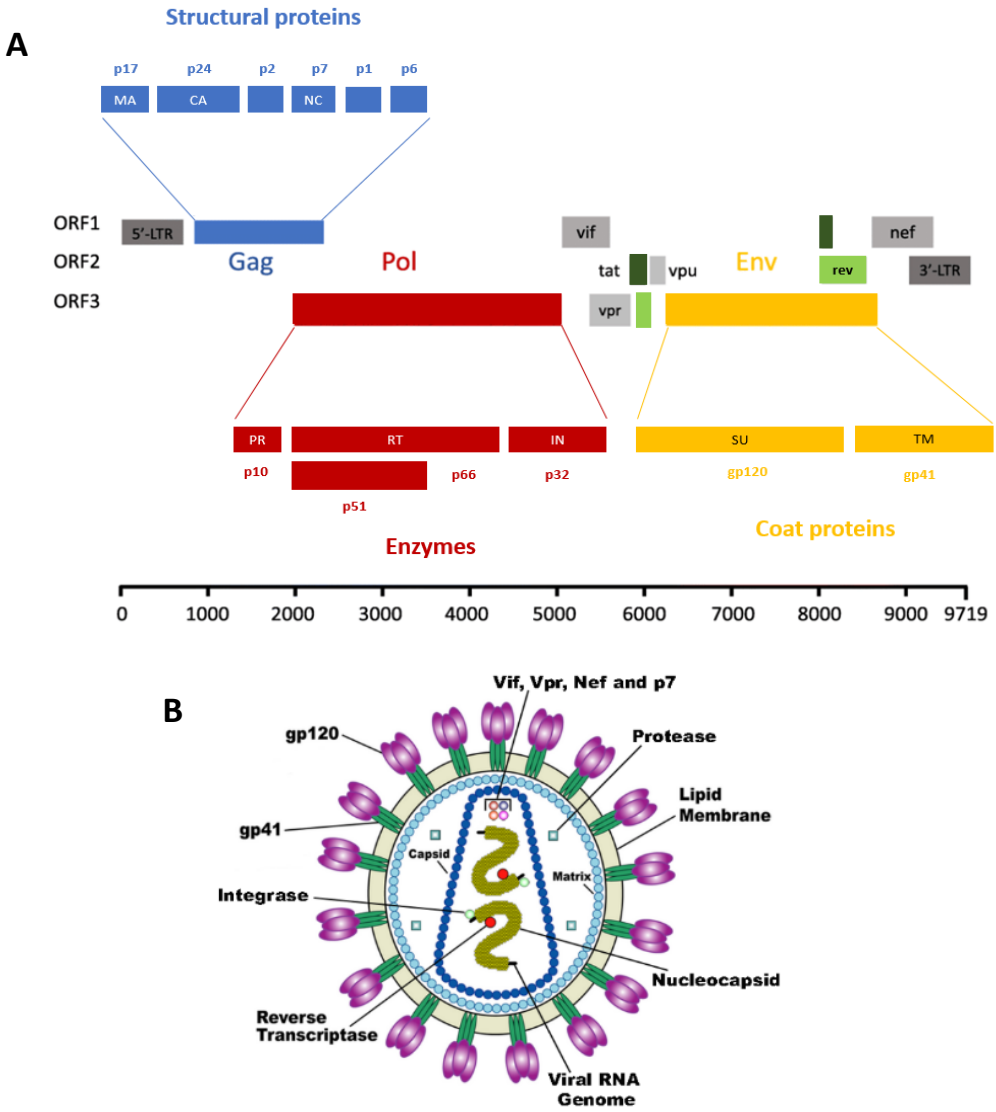

Figure 2. Genome and morphology of a HIV-1 virion. (A) HIV-1 genome is composed of 4 accessory genes in light grey, 2 regulatory genes in green and 3 structural genes: Gag (with 6 protein domains to produce structural proteins); Pol (englobing 3 protein domains to synthesize enzymes); and Env (with 2 protein domains to generate envelope proteins). **(B)** Schematic representation of a mature virion displaying its RNA genome and proteins. Virion particle adapted from US National Institute of Health, and HIV genome adapted from Cervera, L. et al., 2019[6].

1.3 HIV INFECTION AND BIOLOGIC CYCLE

The HIV life cycle includes 6 steps (**Figure 3**):

1) Entry and attachment: At the initial stages of the HIV cycle, the surface glycoprotein gp120 binds to the CD4 receptor on the host cell, which induces a conformational change in gp120, letting gp120 bind to the co-receptor (CCR5 or CXCR4) on the cell surface. After this union is completed, gp41 binds the cell membrane. Once the fusion between the cell and the viral

membranes occurs, the translocation of the viral capsid into the cytoplasm takes place, releasing all viral components inside the cell.

2) Reverse transcription: Activation of reverse transcriptase occurs inside the host cell cytoplasm, where it will reverse transcribe the single-stranded RNA of HIV genome into double-stranded DNA.

3) Integration: The double-stranded DNA reaches the nucleus, where it is integrated by the integrase into the host genome.

4) Transcription and translation: Viral replication occur alongside cellular replication. The integrated provirus is transcribed into RNA and exported to the cytoplasm, where it is translated in structural or regulatory proteins.

5) Assembly: Viral RNA and proteins are engulfed by the host cell membrane. Here it is where the immature virion obtains its lipid envelope.

6) Budding and release: Once immature virion particles are outside the cell, they will mature and target new cells[7, 8].

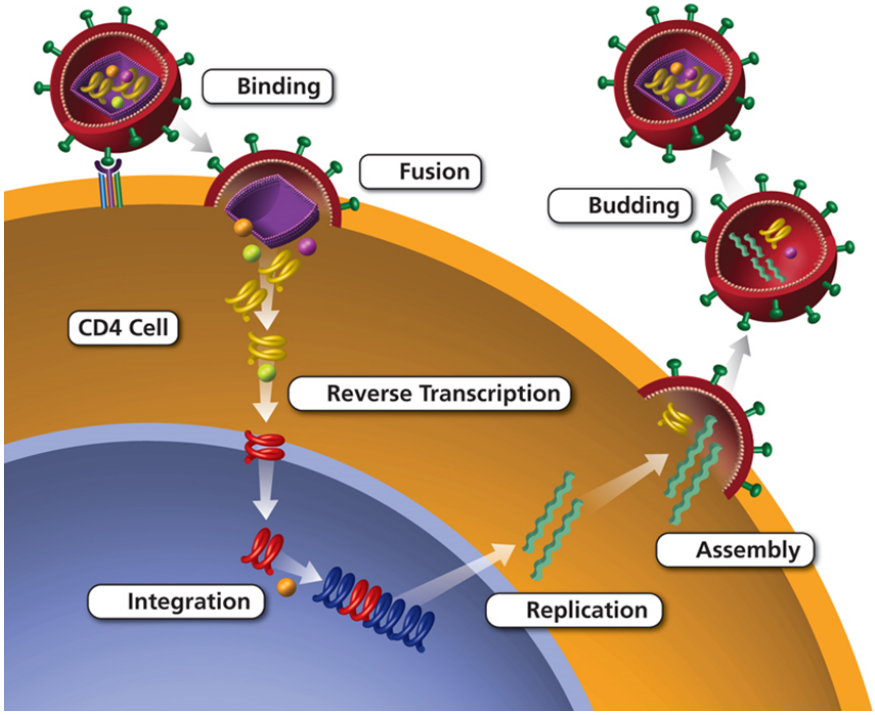

Figure 3. HIV-1 replication cycle. This image illustrates the HIV replication cycle that takes place in $CD4^+$ T cells, which consist of different steps to generate new viral particles: entry and attachment, reverse transcription, integration, transcription and translation, assembly and budding and release. Once finished, a new immature virus particle will be released and then mature. Adapted image from US National Institute of Health[9].

1.4 HIV INFECTION COURSE

The clinical course of HIV-1 infection can be divided into 3 main phases: 1) acute phase, 2) chronic phase and 3) immunodeficiency phase (AIDS)[7] (**Figure 4**).

- **Acute Phase**

Through early phase of infection, an initial peak of viremia and a massive loss of $CD4^+$ T lymphocytes are exhibited in peripheral blood, followed by an increase of specific immune responses which decline viral replication and increase $CD4^+$ T cell counts within the first weeks. During this acute phase, an abrupt loss of $CD4^+$ T cells is located in the gastrointestinal (GI)[10] tract which correlates with the high levels of viremia that are observed before its neutralization by antiviral immune responses. Around 90% of $CD4^+$ T lymphocytes in the gut-associated lymphoid tissue (GALT) are depleted during early infection.

- **Chronic Phase**

Chronic stage of HIV-1 infection can last years, however, this time lapse can vary from one individual to another. This phase is associated with no clinical symptoms and low and persistent viral replication contained by the immune system. However, HIV cytopathic effects and the constant presence of viral antigens lead to an increase in immune activation and cell death, heading to a progressive fall of $CD4^+$ T cells. Disease progression is determined either by viral factors (replicative capacity or immune escape) or host factors (age, sex or co-infections).

- **Late Phase (or AIDS)**

The late stage of HV-1 infection is characterized by a massive decline in $CD4^+$ T cell numbers and an increase in plasma viremia, due to viral replication, resulting in immunologic collapse. The increase of viral loads, either in lymphoid organs or peripheral blood, and the abrupt depletion of $CD4^+$ T cells are the main markers of disease progression. During this phase, takes place the emergence of opportunistic infections, with clear clinical symptoms. Untreated HIV-infected individuals typically progress to AIDS in approximately 8-10 years. The higher the viral loads, the faster the individual will progress to symptomatic AIDS.

1.5 HIV INFECTION IN LYMPHOID TISSUE

Plasma viremia and $CD4^+$ T cell depletion represent the most characteristic events in HIV-1 pathogenesis. A progressive and moderate decrease of $CD4^+$ T cells takes place in peripheral blood during the acute phase of HIV-1 infection. However, this is not representative of the total number of $CD4^+$ T cells, since the vast majority of $CD4^+$ T cells are localized in lymphoid tissues

(such as lymph nodes and GALT) instead of the peripheral blood[11]. Mucosal $CD4^+$ T cells consist mostly of memory $CD4^+$ T cells with an exogenous activated status. So, mucosal $CD4^+$ T cells are the principal target of HIV infection and the main active place for viral replication[10, 12]. Chronic immune activation that takes place during HIV infection is a distinctive indicator of HIV pathogenesis. Also, immune activation of $CD4^+$ T cells (determined by the expression of activation markers, i.e. Ki-67, HLA-DR, CD25 and CD38) has been associated with HIV disease progression[13]. As shown in **Figure 4**, $CD4^+$ T cell depletion in mucosal lymphoid tissue is more abrupt than in peripheral blood. Even though $CD4^+$ T cells in blood recover progressively during the chronic phase, active HIV replication and $CD4^+$ T cell destruction in lymphoid tissue continue during the course of infection and do not recover completely even during treatment with ART[14]. Nonetheless, $CD4^+$ T cell depletion in blood is still critical in HIV pathogenesis, since it is directly associated with HIV disease progression[12, 15].

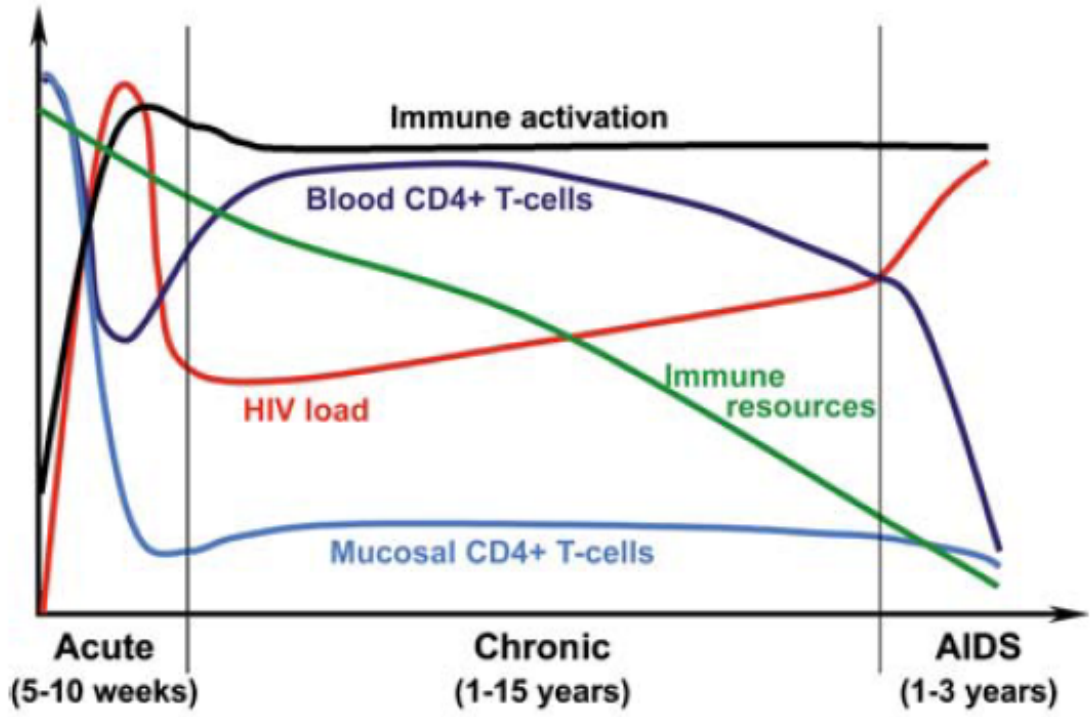

Figure 4. The course of natural HIV infection. Diagram of the temporal course of an untreated HIV infection. The time-scale is initially weeks (acute phase) and then years (chronic and late or AIDS phase). $CD4^+$ T cell counts decrease and viremia increase during the acute phase, with partial recovery during the chronic phase. Mucosal $CD4^+$ T cells do not recover during the infection time, not even during the chronic phase. Adapted from Fulop, T. et al., 2009[12].

1.5.1 *EX VIVO* CULTURES OF HUMAN LYMPHOID TISSUE: A MODEL FOR HIV PATHOGENESIS

An important development over the past decade has been the use of human tissues (mainly lymphoid and mucosal tissues) for organotypic cultures to study HIV-1 infection *ex vivo*. Although such models cannot simultaneously integrate all the physiological parameters that govern HIV-1 pathogenesis, they do permit the study of HIV-1 replication and select aspects of viral pathogenesis in the context of a complex tissue architecture that supports relevant communication between different cell types. Depending on the origin of the tissue that is used for these organotypic cultures, different aspects can be studied.

Most lymphoid organs, such as the spleen, lymph nodes and thymus, are not readily available from human donors for *ex vivo* studies. Therefore, studies of acute HIV-1 replication in lymphoid organs frequently rely on *ex vivo* tonsil cultures obtained from routine tonsillectomies. Tonsils support HIV-1 replication either as tissue blocks (known as human lymphoid histocultures (HLHs))[16, 17] or as aggregates of isolated cells (known as human lymphoid aggregate cultures (HLACs))[18]. HLHs and HLACs have been widely used to study key pathogenic parameters[16, 19-22]. In contrast to peripheral blood mononuclear cells (PBMCs), and probably due to their tissue composition and cytokine milieu, lymphoid tissue cultures support HIV-1 replication without exogenous stimulation[16, 23], and even show HIV-1 infection of resting, non-activated, target cells[24]. Although macroscopically non-inflamed parts of tonsils are used, one aspect regarding the use of HLHs and HLACs that is sometimes criticized is the fact that the inflammation that provokes the clinical manifestation and need for tonsillectomy, may influence experimental outcomes. However, HIV-1 replication is equally independent of exogenous stimulation in *ex vivo* cultures of non-inflamed spleen tissue[25].

2. CELLULAR STRESS RESPONSES: CELL SURVIVAL AND CELL DEATH

Cellular stress responses are a wide range of molecular changes, highly conserved within eukaryotes, that cells undergo in response to environmental stressors, including extreme temperatures, exposure to toxins and mechanical damage[26]. Furthermore, some viral infections can also cause cellular stress responses. Cells can respond to stress in various ways ranging from the activation of survival pathways to the initiation of cell death that eventually eliminates damaged cells. Whether cells carry out a protective or destructive stress response it depends, to a large extent, on the nature and duration of the stress, as well as the cell type. The initial cell response to a stressful stimulus is geared towards helping the cell to defend itself and recover from the stress signal. However, if the noxious stimulus is unresolved, then cells activate death

signaling pathways. The mechanism by which a cell dies (i.e., apoptosis, necrosis, pyroptosis, or autophagic cell death) depends on various exogenous factors as well as the cell ability to handle the stress to which it is exposed.

2.1 CELL SURVIVAL: AUTOPHAGY

Several cellular survival pathways help cells buffer environmental stress. Macroautophagy (hereafter referred as autophagy) is an evolutionary conserved catabolic process in all eukaryotes. The word autophagy is derived from the Greek and means to eat (phagy) oneself (auto). So, autophagy is a self-degradative cellular process by which a portion of the cytosol or entire organelles (long-lived protein, damaged organelles and malformed proteins) become sequestered in double membrane vesicles, known as autophagosomes, to get energy after fusion by lysosome degradation[27]. Autophagy can also be induced due to bacterial or virus infections and is characterized by the formation of these autophagosomes around target microorganisms and their subsequent degradation by lysosomes. Increasing evidence also suggests that microorganisms have developed strategies to use autophagy for their own benefit[28]. The autophagic process is arranged by the so-called autophagy-related proteins (Atg), which are responsible for carrying out each step of the autophagic process. Most cells types have active basal levels of autophagy, since it is suggested that autophagy maintains cell integrity by keeping balance of intracellular proteins. However, an excess of autophagic activity during an extensive period of time can lead to cell destruction called type II programmed cell death or autophagic cell death[29].

2.1.1 AUTOPHAGIC PATHWAY

The autophagic pathway can be divided into three different phases (**Figure 5**):

- Phase 1: Autophagy initiation. The degradative autophagic pathway is triggered by events that include nutrient starvation, cytokine signaling, genomic stress, unfolded proteins or pathogen infection. Many of these signals converge on the protein mTOR (mammalian target of rapamycin) that plays a crucial role in regulating protein synthesis, cellular growth and proliferation. Under normal conditions (without stress signals), mTOR is present in a phosphorylated active state resulting in autophagy suppression. On the contrary, during starvation or in response to other stress signals, mTOR is inhibited allowing autophagy initiation and phagophore formation[30]. Phagophore formation derives from the lipid bilayer of the endoplasmic reticulum and/or the trans-Golgi and endosomes.

- Phase 2: Phagophore formation and expansion. Phagophore expands to engulf intracellular cargo (like aggregated proteins, ribosomes or pathogens) inside autophagosomes. Autophagosome synthesis involves the role of more than 20 autophagy-related genes (ATG), one lipid kinase signaling complex (PI3K/Beclin-1) and two ubiquitin-like systems (Atg12-Atg5 and LC3-PE). The LC3 protein (the microtubule associated protein 1 light chain 3 or MAP1/LC3) is located in the cytoplasm in a diffuse or pro-LC3 form where, upon autophagy induction, is cleaved to LC3-I. Once LC3-I is activated, through a lipidation process, generates the LC3-II protein. LC3-II is recruited and integrated into the growing phagophore, which ends up becoming part of the inner and outer membranes of the autophagosome. Once anchored on the autophagosome, it plays a role in both selecting cargo for degradation and hemifusion of membranes. P62 (also known as Sequestrosome-1) also targets specific autophagic cargos. These cargos, tagged with ubiquitin, lead to adaptor proteins assembly such as p62, that bind to the ubiquitin chain. Once autophagosome is complete, the cargo and p62 proteins are degraded[31, 32].
- Phase 3: Lysosome fusion and degradation. Loaded autophagosome fuses with the lysosome, thereby generating single-membrane autolysosome, and degrading its content by acid proteases and hydrolases. Then, amino acids and other products obtained from that degradation are brought back to the cytoplasm by transport proteins, where they can be used again for metabolism. Degraded pathogens will provide antigens for the initiation of immune responses.

Thus, autophagy could be used to recycle cellular products to promote energy, remove non-functional or damaged proteins, as well as to initiate innate immune responses[29].

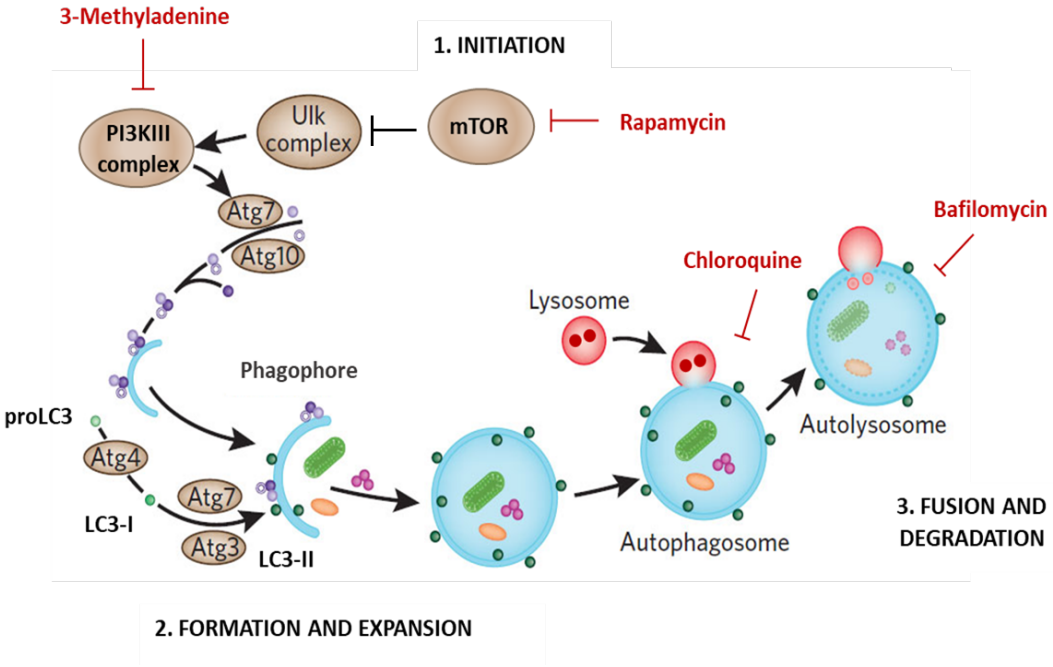

Figure 5. Autophagic pathway. Illustration where different steps of the autophagic cycle are represented: 1) Autophagy is initiated by mTOR inhibition. 2) Phagophore formation and elongation starts, and autophagosome is formed, with LC3-II protein located at its inner and outer membrane. 3) The degradation, and final step, starts with the autophagosome-lysosome fusion, generating the autolysosome, which degrades all the cargo. In red, there are different autophagy modulators, pointing at the protein or step of the cycle they modulate, like the inducer rapamycin, and inhibitors 3-methyladenine, chloroquine and bafilomycin. Adapted from Fleming, A. et al., 2011[33].

2.1.2 AUTOPHAGY MODULATION

Autophagy is involved in cell homeostasis, embryonic development and the lifespan of the individual. Nevertheless, mutations in relevant autophagic components have been related to human disorders. Malfunction of autophagy has been associated to a diverse range of clinical human disorders such as neurodegenerative disorders (like Alzheimer's, Huntington's, and Parkinson's diseases), myodegeneration, hepatic and metabolic disorders, cardiomyopathies, infectious diseases, inflammatory and autoimmune diseases (like lupus erythematosus, Chron's disease and multiple sclerosis) and aging. On the contrary, there is some controversy regarding the role that autophagy plays in cancer, suggesting that during tumor initiation autophagy suppresses tumor growth. However, autophagy has also been suggested to play an important role in tumor progression, appearance of malignancies and cancer cells survival, since it seems that helps tumor cells endure[34, 35].

Autophagy can be modulated by targeting different molecules from different steps of its pathway in order to induce or inhibit its biologic cycle (**Figure 5**). There are many autophagy activators or inhibitors used in order to treat different pathologies related to autophagy.

2.1.2.1 AUTOPHAGY INDUCERS

There are many autophagy inducers used in clinical trials as treatment for several autophagy-related disorders. In neurodegenerative diseases, nicotinamide and lithium have been used to treat Alzheimer's disease in phase I and phase II clinical trials, respectively. While curcumin and trehalose have been tested in rodent models for treatment against Parkinson's and Huntington's diseases, respectively[36]. Vitamin D and caffeine-induced autophagy has been observed to reduce hepatic steatosis in rodent models with non-alcoholic fatty liver disorder. Also, tyrosine kinase inhibitors which produce autophagy enhancement have been observed to be favorable to diabetic nephropathy and neurodegenerative disorders, and trifluoperazine and statins reduce *Salmonella* and *M. tuberculosis* infection, respectively[37]. Autophagy inducers have been also used in animal models for other multiple diseases like hepatic disorders, infectious diseases, autoinflammatory and autoimmune conditions, aging and pulmonary and renal disorders[35].

- **Rapamycin**

Rapamycin is an immunomodulatory and anti-proliferative drug that induces autophagy by mTOR inhibition (**Figure 5**). mTOR is a serine/threonine protein kinase which phosphorylates a wide number of substrates and mediates PI3 kinase signaling[38]. Rapamycin is the most widely used autophagy inducer to study the autophagic pathway.

Some neurodegenerative disorders are characterized for an accumulation of neuronal proteins, therefore, the administration of the mTOR inhibitor rapamycin, has been tested to help reduce the accumulation of these proteins by autophagy induction. For Alzheimer's and Huntington's diseases, rapamycin has been used as treatment in pre-clinical rodent models[36].

2.1.2.2 AUTOPHAGY INHIBITORS

Autophagy inhibitors target different stages of the autophagic pathway, either disabling the autophagosome formation or inhibiting autophagosome-lysosome fusion. The most commonly used early-stage inhibitors are 3-methyladenine and wortmannin; while, late stages include leupeptin, chloroquine, hydroxychloroquine, pepstatin and bafilomycin A1[39].

Autophagy inhibitors have been used in pre-clinic models and clinical trials. This is the case for everolimus, that has been used in clinical trials to treat breast, ovarian and prostate cancers[36, 40]. At the same time, in pre-clinical models, autophagy inhibition has been used as a therapeutic strategy for several infectious diseases, like hepatitis B virus and *Brucella abortus*[34].

- **3-Methyladenine**

3-Methyladenine is an autophagy inhibitor that targets both PI3K class I and III indiscriminately, which plays a role in different biological processes like autophagosome formation during autophagy (**Figure 5**). Phosphoinositide 3-kinase (PI3K) is the key element during the early steps of the autophagic cycle for phagophore formation[41].

3-methyladenine has been used as a possible treatment for some disorders. In fact, treatment of atherosclerosis with 3-methyladenine has been observed to reduce disease development and improved atherosclerotic plaque stability in rodent models[42]. In cancer therapy, 3-methyladenine has been proposed as treatment for colorectal cancer and tested in pre-clinical studies[43].

- **Chloroquine**

The anti-malaric and anti-inflammatory drug chloroquine has been used as an autophagy inhibitor of the late stages of the autophagic process. Chloroquine is a weak base that blocks the autophagosome-lysosome fusion, and so, the degradative step of autophagy (**Figure 5**). Thus, chloroquine stops the autophagic flux and accumulates autophagosome vesicles inside the cell[44].

Chloroquine and hydroxychloroquine (HCQ) have been tested in several clinical trials in combination with other drugs to treat a diverse number of cancers, from melanoma to brain metastasis, through kidney and prostate cancer. For example, chloroquine or hydroxychloroquine have been administered in combination with gemcitabine to treat pancreatic cancer, and chloroquine in combination with taxols for breast cancer. Most of these studies are in phase I and II clinical trials[36]. For SARS-Cov-2 treatment, a clinical trial was performed to determine the efficacy of early treatment with hydroxychloroquine, however no benefits were observed on patients treated with hydroxychloroquine[45].

- **Bafilomycin A1**

The macrolide antibiotic bafilomycin A1 is a potent vacuolar H+ ATPase (V-ATPase) inhibitor that increases lysosomal pH and blocks the degradation capacity in lysosomes by decreasing their acidity, and thus, inhibits the activity of resident hydrolases unable to degrade autophagosome cargo (**Figure 5**). Through this mechanism, bafilomycin inhibits autophagic flux by preventing the acidification of endosomes and lysosomes, and blocks the autophagosome-lysosome fusion[46].

Some reports claim that treatment with low-dose bafilomycin attenuates neuronal cell death *in vitro*, inducing protective effect on Parkinson's disease and other neurodegenerative diseases that disrupt protein degradation[47].

2.1.3 AUTOPHAGIC FLUX

The measurement of the balance between the rate of autophagosome formation and degradation is called autophagic flux[48]. Basal autophagy is present in most cells and tissues in the absence of a stimulus. Under basal condition, the autophagic flux can be measured by blocking the autophagosome maturation and subsequent fusion with lysosomes with chloroquine or bafilomycin. After the degradation step is blocked, an increase of autophagosome accumulation inside the cell will be observed by different detection methods, since the induction continued even without any external stimulus[49]. When cells are treated with an autophagy inducer, like rapamycin, an increase even higher of autophagosome production is observed. In order to measure the increase on the autophagic flux, after the inducer is used the degradation step must be stopped by chloroquine or bafilomycin.

2.1.4 AUTOPHAGY MONITORING

The most common approach to measure autophagy and autophagic flux is by western blot, through LC3-I and LC3-II protein detection which are the hallmark of autophagy. Another accepted marker to measure autophagy by western blot is p62 degradation, which directly binds to LC3, and is located inside the autophagosome and degraded after lysosome fusion by autophagic activity. In addition, autophagy could be also detected by visualization and counting the number of autophagosomes by electron microscopy, which allows direct visualization of the double membrane autophagosome structures. Fluorescent microscopy has been helpful for measuring autophagy through LC3-GFP detection or direct staining of the LC3 protein. The expression and modulation of autophagy-associated genes could be also detected by RT-PCR, and the silencing of some of these genes, using RNAi, has been also used as an autophagy marker (**Table 1**)[50].

Table 1. General methods for monitoring autophagy

Targeted components of autophagy	Procedure
Direct enumeration and quantification of autophagosomes. Visible as double membrane vesicles.	Electron microscopy
LC3-II to LC3-I ratio. Provides a measurement of autophagic flux with the LC3B-II/LC3B-I ratio concomitantly increasing with autophagosome numbers.	WB
LC3 localization. Punctate spots visible by microscopy. Total intracellular levels may increase along with autophagosome numbers.	ICC, FC, transfection of LC3 reporter plasmid followed by fluorescent microscopy or FC
Quantitation of autophagy-associated gene expression levels, e.g., BECN-1.	qPCR
Quantitation of autophagy-associated protein levels, e.g., Beclin-1.	WB, ELISA
Silencing of autophagy-associated genes.	RNAi
Manipulation of autophagic flux.	Use of rapamycin, bafilomycin A1, and 3-methyladenine

Western blot (WB), flow cytometry (FC), immunocytochemistry (ICC), quantitative PCR (qPCR), RNA interference (RNAi)

2.1.5 AUTOPHAGY AND HIV

Autophagy is the first innate immune barrier against invading pathogens, trying to clear them and also triggering the immune response. However, some pathogens have developed strategies to block or use autophagy to their own benefit[51]. HIV-1 has developed multiple mechanisms to ensure its survival long enough to guarantee productive infection[52]. Thus, viral replication can be either favored or blocked by autophagy. It has been previously reported that more than 35 genes are involved in autophagy, and 10 of these autophagy-associated genes have been linked to HIV-1 replication[50]. A complex link exists between HIV-1 and autophagy and discordant results have been reported in different *in vitro* models regarding the way HIV and autophagy modulate each other[50, 51]. Different effects of HIV-1 on autophagy have been described depending on the cell type and on the infectious status of the target cell type, i.e., if the target cell is productively infected or not.

- ***In vitro* effects on T cells**

*S*ome reports claim that HIV induces autophagy in Jurkat and $CD4^+$ T cells during infection by detecting increased levels of Beclin-1 in western blot and autophagosome formation by electron microscopy[53]. In contrast, other reports assure that HIV infection down-regulates autophagy by reducing Beclin-1 protein levels and the autophagosome formation in infected $CD4^+$ T cells in confocal microscopy and western blot, respectively[54].

Furthermore, when looking into the productively infected or bystander cells, differences have been observed. In $CD4^+$ T cells productively infected by R5 or X4 HIV-1 strains autophagy reduction has been reported[55]. However, autophagy is induced in uninfected, bystander CD4 T cells after interaction of their CXCR4 or CCR5 co-receptor with HIV-1-infected cells that express the envelope glycoprotein (Env) on their surface, specifically due to gp41. The fusogenic function of gp41 triggers autophagy induction in uninfected $CD4^+$ T cells after contact with infected cells[56].

- ***In vitro* effects on macrophages and dendritic cells**

Macrophages are another important cellular reservoir of HIV-1. Several groups have reported that HIV infection of monocytes-derived macrophages (MDM) is associated with an initial increase in the number of autophagosomes and a late blockage of the maturation stages of autophagy[55]. All these data suggest that in MDM HIV needs autophagy for productive infection. These results were reinforced by the fact that autophagy inhibition resulted in a reduction of infection[55]. However, in the monocytic cell line U937, HIV infection was associated with autophagy inhibition[54], pointing out that the effects of HIV-1 on autophagy in monocytic cell lines can differ from those found in MDM. Regarding autophagy in bystander cells, and in contrasts to the effects on $CD4^+$ T cells, HIV do not trigger uninfected human monocytic THP-1 cells, MDM or U937 to undergo autophagy[55]. However, other reports claim an effect of HIV on bystander autophagy, since HIV infected macrophages blocked rapamycin-induced response in non-infected macrophages, suggesting that HIV can impair autophagy in non-infected cells[57].

During HIV-1 infection, dendritic cells (DCs) might be the first cells to encounter the virus in the course of sexual transmission. Despite low rates of infection, DCs constitute one of the main sources of HIV transmission, being able to efficiently capture HIV-1 and mediate a potent viral transmission, by migrating from mucosal sites to lymph nodes, promoting viral spread through bystander $CD4^+$ T cells[58, 59]. When DCs are exposed to HIV, autophagy is downregulated independently of infection. Based on that, one group showed that when DCs were exposed to HIV Env, but without becoming infected themselves, autophagy was downregulated through mTOR activation to protect the virus from autophagy degradation, and thus, increase viral transmission to $CD4^+$ T cells[59].

- ***In vivo* effects in HIV-1 infected individuals**

To date, relatively few studies have investigated the interplay of HIV and autophagy *in vivo* during HIV infection. Long-term non-progressors (LTNP) and elite controllers (EC), which are infected individuals that naturally control viral replication in the absence of ART treatment, have

shown increased levels of autophagic activity in PBMCs compared to normal progressors (NP)[60]. Another report, in line with these results, has observed an impairment in the autophagy induced response in aviremic-treated individuals who fail to recover their $CD4^+$ T cells[61]. These results from HIV-1 infected patients suggest that autophagy could play a role in HIV infection and thus, disease progression. In other studies, cardiac and brain tissue from HIV-1 infected patients and animal models showed autophagy dysregulation due to HIV infection, suggesting a connection between increased risk to acquire HIV-related comorbidities and autophagy dysfunction[62, 63].

2.2 CELL DEATH MECHANISMS: APOPTOSIS AND PYROPTOSIS

Cell death is a conserved cellular process across prokaryotic and eukaryotic cells, that takes place when the cell stops to carry out its functions. Cell death could be the result of a natural process of old dying cells, or due to injury or diseases[64]. Based on morphological examinations and the DNA fragmentation status of dead cells, cell death was initially classified as 'programmed' apoptosis and 'accidental' necrosis in mammalian cells. However, decades of research in the field have conceptually advanced our understanding of cell death as regulated processes[65]. Among all the proposed forms of programmed cell death (PCD), pyroptosis, apoptosis and necroptosis are the most well-defined, with molecular machineries responsible for the initiation, transduction and execution of cell death[64, 65].

2.2.1 CASPASES

Caspases are from a structurally related family of cysteine-aspartic proteases widely known for their essential role in programmed cell death. There are two groups of caspases, inflammatory caspases (caspase-1, -4, -5, -11 and -12) and apoptotic caspases, divided into initiator caspases (caspase-2, -8, -9 and -10) and executioner caspases (caspase-3, -6 and -7)[66].

2.2.2 APOPTOTIC PATHWAY

Apoptosis is a non-inflammatory form of programmed cell death which is a highly regulated and controlled process, also called cellular suicide. Apoptosis is an essential process for normal development and tissue homeostasis, and perturbations in its regulation contribute to numerous pathological conditions, including cancer, autoimmune and degenerative diseases. Cells initiate intracellular apoptotic signaling in response to stress. There are two different apoptotic pathways described[67]:

- **Extrinsic pathway** → The cell kills itself because of signals coming from other cells, also called death receptor pathway. Extrinsic apoptosis is triggered through activation of cell-

surface-expressed death receptors, such as CD95 (Fas) and tumor necrosis factor receptor (TNF), leading to the activation of caspase-8 and its downstream effector caspases.

- **Intrinsic pathway** → The cell kills itself because it senses intracellular stimuli, such as oxidative stress, hypoxia and nutrient deprivation leading to permeabilization of the mitochondrial outer membrane, also called mitochondrial pathway. It is regulated primarily by the Bcl-2 family of proteins.

Both pathways activate initiator caspases (caspase-2, caspase-8, caspase-9 and caspase-10) which then activate executioner caspases (caspase-3, caspase-6 and caspase-7), which then kill the cell by degrading proteins indiscriminately.

2.2.2.1 INTRINSIC OR MITOCHONDRIAL APOPTOTIC PATHWAY

Mitochondria are essential for organisms to exist, without them, a cell ceases to do aerobic respiration and dies[68]. This apoptotic process is initiated in response to different stress signals, and a complex interaction between Bcl-2 proteins, which transmit this signal to the mitochondrial outer membrane (MOM) to start Bax and Bak activation, oligomerization and MOM damage, resulting in pore formation and mitochondrial outer membrane permeabilization (MOMP)[69, 70]. MOMP takes place after pore formation, causing mitochondrial inner membrane permeabilization (MIMP) and subsequently, the release of mitochondrial proteins and pro-apoptotic factors, such as cytochrome C or mitochondrial DNA (mtDNA)[69, 71]. Once cytochrome C is released into the cytosol, activates the caspase cascade forming the protein complex known as apoptosome. The apoptosome activates caspase-9, which in return activates caspase-3, -6 and -7, which causes the induction of apoptosis[69, 72].

2.2.3 PYROPTOSIS

Pyroptosis comes from the Greek and means fire/fever (pyro) and falling (ptosis). Pyroptosis is a caspase-dependent and pro-inflammatory form of programmed cell death, usually caused by microbial infection[73]. Pyroptosis is morphologically and mechanistically distinct from other forms of cell death. Caspase-1 dependence is a defining feature of pyroptosis, and is the enzyme that mediates this cell death process[74, 75]. Pyroptosis is initiated by the formation of a large supramolecular complex called inflammasome, activated upon intracellular danger signals produced by pathogen-associated molecular patterns (PAMPs), which are involved in inducing an inflammatory response. Once formed, inflammasomes activate inflammatory caspases, which contribute to the maturation and activation of several pro-inflammatory cytokines, like

IL-1β and IL-18, and produce pore formation on the cellular membrane. Caspase-1-dependent plasma membrane pores dissipate cellular ionic gradients, producing a net increased osmotic pressure, water influx, cell swelling and, eventually, osmotic lysis and release of inflammatory intracellular contents[76] (**Figure 6**). This release of cytokines and damage-associated molecular patterns (DAMPs) recruit more immune cells and further perpetuate the inflammatory cascade in the tissue. Importantly, caspase-1 is not involved in apoptosis, and caspase-1-deficient mice have no defects in apoptosis and develop normally[77, 78]. At the same time, apoptotic caspases, including caspase-3, caspase-6 and caspase-8, are not involved in pyroptosis[79-82]. Furthermore, loss of mitochondrial integrity and release of cytochrome C, which can activate apoptotic caspases, do not occur during pyroptosis[82, 83].

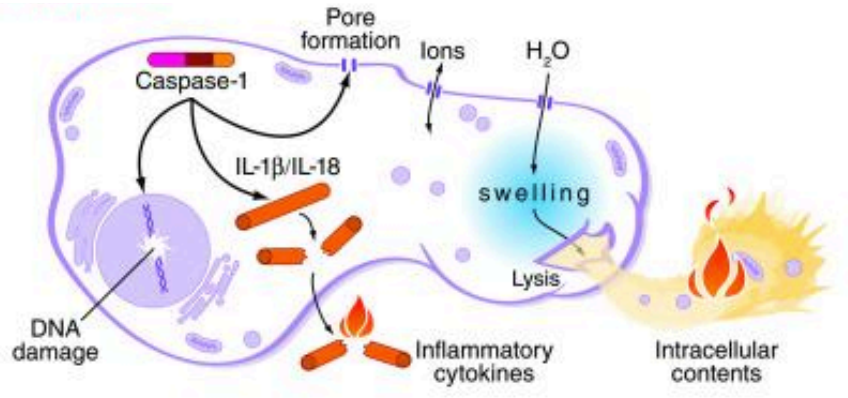

Figure 6. Cell death mediated by pyroptosis. Pyroptosis mechanism, when induced, activates caspase-1, and thus, the release of inflammatory cytokines (IL-1β and IL-18), pore formation, swelling and release of intracellular content upon cell membrane lysis. Image from David W. Ehlert and Brad Cookson, University of Washington.

2.2.4 CELL DEATH AND HIV

Although the replicative life cycle of HIV within $CD4^+$ T cells is understood in molecular detail, less is known about how this human retrovirus promotes the massive loss of CD4 T lymphocytes. The hallmark of AIDS pathogenesis is a progressive depletion of $CD4^+$ T cell population. Massive $CD4^+$ memory T cell destruction is known to occur early in infection[11, 84]. In most individuals, this initial destruction is counteracted by $CD4^+$ memory T cell regeneration that preserves $CD4^+$ T cell counts and functions above the threshold associated with immunodeficiency[85]. This regeneration, however, does not restore all functionally important $CD4^+$ T cell population and is not stable over time[85]. Ultimately, $CD4^+$ memory T cell homeostasis fails and critical effector

populations of cells decline below the level necessary to prevent the appearance of opportunistic infections[85]. Initially, depletion was thought to reflect a viral cytopathic effect occurring in productively infected $CD4^+$ T cells[86]. This notion found support in studies involving immortalized T cell lines or activated cultures of peripheral blood cells. Infection of these cells with laboratory-adapted strains of HIV resulted in productive infection and ultimately apoptotic death of the virus-producing cells. However, the frequency of these activated $CD4^+$ T cells appeared too limited to explain the massive loss of $CD4^+$ T cells observed *in vivo*[87]. As mentioned above, not all $CD4^+$-expressing cells are rapidly depleted by HIV. For example, monocyte-derived macrophages do not die quickly; instead, they produce virus over a period of weeks[88]. This suggests that viral infection and replication are not inherently linked with cell death. Therefore, other features of HIV and its interaction with the host must be responsible for the massive $CD4^+$ T cell loss in AIDS.

2.2.4.1 HIV-MEDIATED BYSTANDER APOPTOSIS

Multiple studies have reported increased levels of apoptosis in PBMCs from HIV infected individuals, that correlates with $CD4^+$ decline[89]. However, the number of HIV infected cells in patients is relatively low, and cannot account for the loss of $CD4^+$ T cells *in vivo*. It is believed that the loss of $CD4^+$ T cells during HIV infection is due to bystander apoptosis induction[90, 91]. So, the majority of cells undergoing apoptosis during HIV infection are not infected, but in close proximity to infected cells. Thus, bystander apoptosis is believed to be one of the major causes of $CD4^+$ T cell loss leading to AIDS[92].

Various mechanisms have been proposed to contribute to bystander cell death, including the action of host factors (e.g., tumor necrosis factor-α, Fas ligand, and TRAIL)[93], and various viral factors (e.g., HIV-1 Tat, Vpr, and Nef) released from infected cells[94]. Considerable interest was focused on the role of gp120 Env protein in bystander killing, suggesting death signals involve gp120 binding to its chemokine receptor or occur through subsequent gp41-mediated hemifusion events[95, 96].

Chronic immune activation is another mechanism that can promote this apoptotic cell death during HIV infection, which is a key immunopathological feature of HIV infection, that corresponds with a $CD4^+$ T cell decline[97]. Activation of both $CD4^+$ and $CD8^+$ T cells have been associated with HIV disease, and it was hypothesized that immune activation can induce apoptosis in cells via the process of activation-induced cell death (AICD)[92].

2.2.4.2 HIV-MEDIATED BYSTANDER PYROPTOSIS

Levels of immune activation are high in untreated HIV-1 infection, perhaps reflecting the translocation of microbial products across a compromised gastrointestinal barrier[98-101], and it is commonly assumed that this immune activation is responsible for $CD4^+$ T cell loss. The best evidence for this, comes from studies of infections with simian immunodeficiency virus where there are high levels of virus replication, but little immune activation or $CD4^+$ T cell depletion[102]. However, the link between immune activation and $CD4^+$ T cell depletion remains unknown. A possible explanation was postulated by Doitsh and colleagues, who suggested that the link could be in the manner of cell death. They used cultures of isolated human cells from spleen or tonsils (HLACs), where they demonstrated that more than 95% of $CD4^+$ T cells that die following HIV-1 infection were quiescent cells that undergo pyroptosis[103]. Only a small proportion of dying $CD4^+$ T cells were activated and productively infected, and thus, undergoing apoptosis[20]. They suggested that cell death by pyroptosis was due to the accumulation of incomplete reverse transcription products inside the cell, like DNA, as a result of cell-to-cell HIV-1 transmission, resulting in an abortive infection process. These findings indicate that reverse transcripts generated during DNA chain elongation, are detected by the IFI16 DNA sensor[104], and induce a pro-inflammatory innate immune response involving caspase-1 activation in quiescent T cells. Caspase-1 activation leads to pro-inflammatory IL-1β cytokines release, resulting in a state of chronic inflammation[105] (**Figure 7**). This mechanism does not clear virus infection, but in contrast, creates an endless loop of inflammation by bringing new permissive cells to the site of infection[92]. This trafficking of new activated target cells increase cell-to-cell viral transmission from infected to uninfected cells, which is more efficient than by free viral particles, and consequently, could rise the infection levels.

However, there is a lot of controversy in this matter, other authors do not consider pyroptosis as the main mechanism of massive cell death in bystander CD4 T cells, since they failed to detect caspase-1 activation in infected humanized mice, and instead detected apoptosis and caspase-3 activation[106].

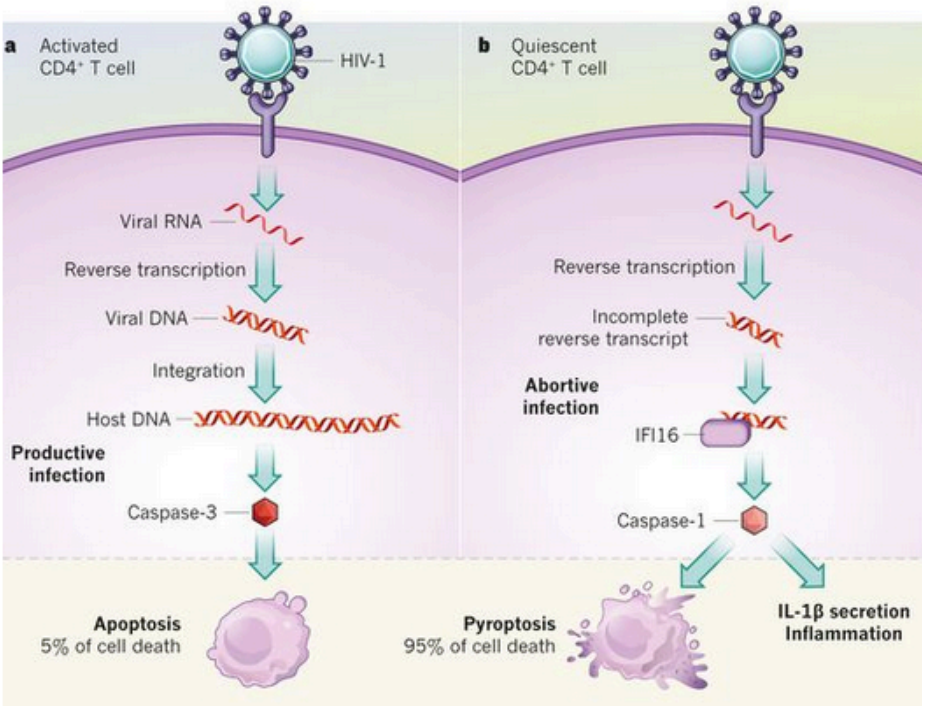

Figure 7. CD4⁺ T cell death during HIV infection. **a)** Productive HIV-1 infection of a CD4⁺ T cell, where viral RNA enters the cells, is reverse transcribed to DNA and integrated into the host genome. Finally, the infected cell dies through apoptosis-mediated caspase-3 activation (this represents 5% of cells). **b)** Non-activated quiescent CD4⁺ T cells undergo abortive infection by accumulating incomplete viral DNA transcripts which remain in the cell. Transcripts are sensed by cellular DNA sensor IFI16, activating caspase-1 and resulting in cell death activation by pyroptosis and cytokine release. From Cox, A. L. et al., 2014[107].

This highlights that CD4 T cell depletion is not due to a single mechanism of cell death, but instead it is a combination of different mechanisms that all together produce this massive depletion.

3. CASPASES BEYOND CELL DEATH

Besides their role in cell death, increasing evidence suggests that caspases have other functions and participate in different processes. Some of these processes are proliferation of immune cells (caspase-8), cell differentiation (caspase-8 and caspase-3), regulation of cell migration (caspase-2, caspase-8 and caspase-11), tissue regeneration (caspase-3 and caspase-7), tumorigenesis (caspase-1, -2, -3, -6, -7, -8, -10 and -14), aging (caspase-2, caspase-6, caspase-7 and caspase-9), neural development (caspase-2, caspase-3, caspase-6 and caspase-9) and innate immunity (caspase-1, -4, -5, -3, -7 and -9)[66, 108].

3.1 cGAS-STING PATHWAY AS AN ANTIVIRAL RESPONSE

cGAS (cyclic GMP-AMP (cGAMP) synthase) is a cytoplasmic DNA sensor that activates innate immune responses to fight microorganisms[109]. cGAS is also a key sensor for DNA viruses and retroviruses, including HIV-1 and HIV-2[110]. After HIV viral capsids enter macrophages and dendritic cells, released reverse transcriptase converts the viral RNA into cDNA, which is injected directly into the nucleus and is integrated into the host genome. So, if viral cDNA is detected in the cytosol before its entrance to the nucleus, cGAS is able to create an immune response to fight it[110]. It has been also described that mtDNA released from damaged mitochondria activates DNA sensors[111] and facilitates its recognition by cGAS[71], activating the cGAS-STING signaling pathway and triggering a caspase-independent immune response[112].

Once cGAS enzyme is activated, triggers the cGAMP production. cGAMP, at the same time, functions as a second messenger to activate STING (stimulator of IFN genes), located at the endoplasmic reticulum. In parallel, RNA polymerase III also recognizes cDNA and produces the transcription into dsRNA, thus stimulating RIG-I-MAVS pathway[113]. RIG-I is a cytosolic pattern recognition receptor (PRR) responsible for the type-I IFN response, meanwhile, MAVS is a mitochondrial antiviral signaling protein used to activate the signaling pathway for type-I IFN[114]. Activation of these receptors (STING and RIG-I-MAVS) lead to the activation of IKK and TBK1 (TANK-binding kinase 1), which have essential roles in innate immunity through signal-induced activation of NF-κβ, IRF-3 and IRF-7, respectively[115]. TBK1 phosphorylates STING, which in return recruits IRF-3 or IRF-7 (Interferon regulatory factors) for phosphorylation by TBK1. Phosphorylated IRF-3 dimerizes and then enters the nucleus, where it functions with NF-kβ to turn on the expression of various cytokines like type-I IFNs and other immunomodulatory molecules, in order to decrease virus infection (**Figure 8.**)[110] . IFNs play an important role in innate resistance to viruses, acting on virus-infected cells and surrounding cells to produce an antiviral state characterized by the expression and antiviral activity of IFN-stimulated genes (ISGs)[116].

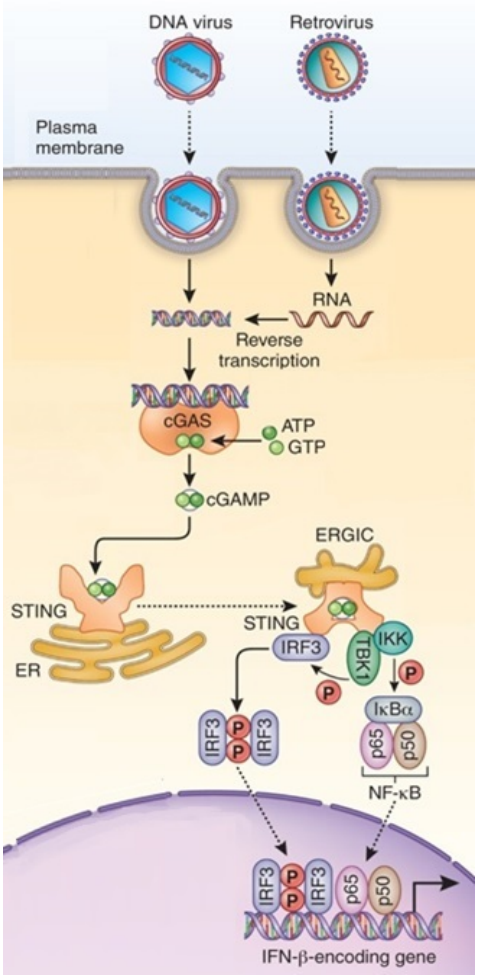

Figure 8. The cGAS-STING pathway of cytosolic DNA sensing. cDNA from reverse transcribed retroviruses RNA or DNA from DNA viruses, bind to and activates cGAS, which catalyzes the synthesis of cGAMP from ATP and GTP. cGAMP binds to the ER adaptor STING, which will activate IKK to induce NF-kβ production, and TBK1 to activate IRF-3 or IRF-7. IRF-3 with NF-kβ will translocate to the nucleus and there, turn on the expression of type-I IFN expression and other ISGs to induce an immune response. Adapted from Chen, Qi et al., 2016[110].

3.2 REGULATION OF cGAS-STING PATHWAY BY APOPTOTIC CASPASES

Viral infections, including HIV-1, causes cell stress, which leads to mitochondrial damage and inflammasome formation and cytochrome C and mtDNA release[117]. Once mtDNA is released to the cytosol, triggers the activation of a robust cGAS-STING pathway response, which results in the production of a potent antiviral type-I interferon response in order to control and stop viral infection (**Figure 9**)[70, 71]. An excessive innate immune activation would be detrimental to the host; therefore, cells have evolved varieties of mechanisms for self-limiting the response. In this regard, caspases have been postulated to play a fundamental role by fine-tuning the level of innate immune response. Two studies have showed that apoptotic caspases-3, -7 and -9 negatively regulate the induction of type-1 interferon by blocking the cGAS-STING pathway

through cGAS cleavage[118, 119]. In addition to the apoptotic caspases, inflammatory caspases were also found to negatively regulate cGAS-STING pathway by cGAS cleavage[113].

Viruses have developed efficient strategies to evade or prevent the immune surveillance and the subsequent responses. HIV infection, as we have already explained above, activate both pyroptosis (caspase-1 activation) and apoptosis (caspase-3 activation). The activation of these caspases will result in cGAS destruction, blocking type-I IFN production and thus, preventing the activation of a protective immune response (**Figure 9**). Therefore, one of the roles that HIV-induced apoptosis and pyroptosis are playing in viral pathogenesis is to keep the infection immunologically silent[120].

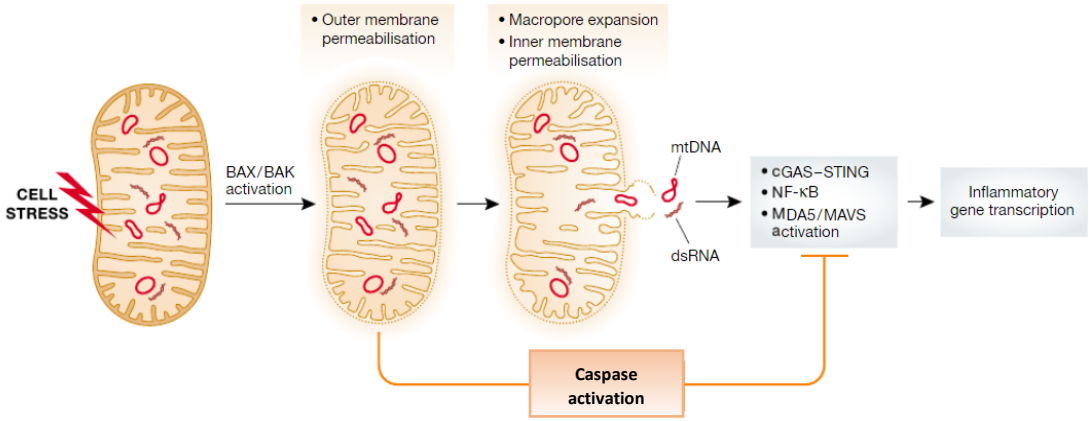

Figure 9. Bax-Bak pore formation releases mtDNA which activates the cGAS-STING antiviral pathway. Cell stress activates Bax and Bak, leading to mitochondrial outer and inner membrane permeabilization and pore formation releasing mtDNA and cytochrome C to the cytosol. Once cytochrome C is released, it activates apoptotic caspases. When mtDNA is released, it activates cGAS-STING pathway activating the transcription of type-I IFN. IFN production can be inhibited upon apoptotic caspase activation. Adapted from Riley, J. S. et al., 2020[117].

3.3 CASPASE INHIBITORS

Increased apoptosis and caspase activity are associated with a number of disorders including hepatic and transplant injuries, myocardial infarction and neurodegenerative diseases. While pro-inflammatory caspases are implicated in rheumatoid arthritis or psoriasis[121, 122]. For nonalcoholic steatohepatitis, pharmacological inhibition of caspases represents a possible therapeutic approach, as proved in animal models and phase II clinical trials[123, 124].

Caspase inhibitors are characterized for their unique ability to recognize specific short peptide sequences and to cleave their substrates at an aspartic acid residue, which is a distinctive residue among mammalian proteases. The first caspase inhibitor was the Cowpox virus product CrmA,

for its ability to prevent cell death by targeting caspase-1. From here, several caspase inhibitors of biological origin targeting a single caspase were determined, like PI-9 and IAPs among others. Subsequently, synthetic caspase inhibitors were developed based upon the substrate cleavage site. However, caspase inhibitors with effects over several caspases simultaneously would be more useful[125, 126]. First generations of pan-caspase inhibitors were originated in the 1990s. The development of cell-permeable peptide-based caspase inhibitors, provide valuable tools for *in vivo* and *in vitro* studies of apoptosis[127]. In recent years, several inhibitors that prevent caspase activation and apoptosis have emerged. Several types of caspase inhibitors are commercially available, including Boc-D-fmk and Z-VAD-fmk, which are the most used cell-permeable broad-spectrum inhibitors, that work by inhibiting the activation of some, but not all, initiator or effector caspases[128]. The concern with these types of inhibitors is that they require high doses to be effective, and at these high doses, they produce cytotoxic effects on cells. As alternative, Q-VD-OPh (Quinoline-Val-Asp-Difluoro phenoxymethylketone) is a potent pan-caspase inhibitor that is very effective at preventing apoptosis, even more potent than Z-VAD-fmk. Also, Q-VD-OPh has shown not to be cytotoxic to cells even at extremely high concentrations (1mM), and is able to cross the blood-brain barrier[129]. Q-VD-OPh has been tested in pre-clinical studies with rodent models to treat several human-related diseases. In all cases, the goal was to decrease cell death produced in damaged tissues after an ischemic stroke, spinal cord injury or cardiac dysfunction. Treatment with Q-VD-OPh resulted in protective effects over the damaged tissue in all these pre-clinical models. Similar results were observed in rodents with neuropathies, like Alzheimer's or Huntington's disease, when they were treated with this pan-caspase inhibitor[128].

Another pan-caspase inhibitor described is Emricasan (IDN-6556). This drug, a potent pan-caspase inhibitor with anti-apoptotic and anti-inflammatory effects, has been used in clinical studies to treat liver diseases[130]. In fact, Emricasan has been tested in several phase II clinical trials for liver cirrhosis treatment proving to be more effective in improving liver function than placebo group[131-134]. Besides, its effect has also been tested in another clinical trial on patients with chronic hepatitis c, showing reduced levels of aminotransferase activity and no adverse effects after 14 days of treatment[135].

HYPOTHESES AND OBJECTIVES

HIV infection is known to cause progressive and massive depletion of bystander $CD4^+$ T cells, especially in lymphoid tissue. Although current direct-acting antiviral therapies are highly effective in suppressing HIV-1 replication, combination antiretroviral therapy (cART) is not curative. Nowadays, treated HIV-1 infected-patients still suffer from severe comorbidities due to persistent inflammation and residual viral replication in cellular reservoirs. In addition, the emergence of multidrug-resistant viruses has become an increasing concern in recent decades. Host-directed strategies are an emerging therapeutic approach to improve treatment outcomes in infectious diseases. The strategy behind this therapy is to interfere with host cell factors that are required by pathogens for their own replication, and to enhance protective immune responses against them. Novel strategies aimed at the functional cure of persistent viral infections and the development of broad-spectrum antivirals against emerging viruses seem to be crucial.

Autophagy has been postulated to play an important role in HIV infection and disease progression. However, discordant results have been reported in different *in vitro* models regarding how HIV and autophagy modulate each other, depending on the cell type and the infectious status of the target cell type. To date, relatively few studies have investigated the interplay of HIV and autophagy *in vivo* during HIV infection. In HIV-1 infected-patients and animal models, autophagy dysregulation by HIV has been observed in cardiac tissue and brain. However, and surprisingly, the effect of HIV on autophagy in lymphoid tissue is almost unknown. Human lymphoid aggregate cultures (HLACs) prepared from tonsillar tissue closely replicate the conditions encountered by HIV *in vivo*, by forming an attractive and biologically relevant system that have shed light on key pathogenic properties of HIV. HLACs are permissive for HIV-1 infection independent of exogenous stimulation, and thus, preserve the endogenous cytokine milieu and cellular heterogeneity. Consequently, given the interplay of HIV and autophagy and the central role that lymphoid tissue plays in HIV pathogenesis; this study was designed to investigate both the effect that the virus has on autophagy and the effect that autophagy modulation has on the virus in *ex vivo* lymphoid tissue culture.

OBJECTIVE 1. Determine the use of HLACs as a model to study autophagy in lymphoid tissue: characterization of basal autophagy and the functionality of the autophagic pathway in HLACs.

OBJECTIVE 2. Determine the effect of HIV on autophagy in lymphoid tissue, and evaluate the effects that HIV infection exerts on the functionality of the autophagic pathway.

OBJECTIVE 3. Establish the impact of modulation of the autophagic pathway on HIV replication and transmission in lymphoid tissue cultured *ex vivo*.

The pathways causing $CD4^+$ T cell death in HIV-infected hosts remain poorly understood, although apoptosis of uninfected bystander cells was postulated as a key mechanism of cell depletion. On HLACs from human tonsils, it has been proposed that most of the quiescent CD4 T cells die by caspase-1-mediated pyroptosis triggered by abortive viral infection, even though this mechanism of cell death in lymphoid tissue has not been confirmed yet. Regardless of the contribution of apoptosis or pyroptosis, after HIV infection, most cells die by HIV-induced caspase-dependent cell death. Therefore, caspase inhibition could emerge as a therapeutic strategy to ameliorate or prevent $CD4^+$ T cell loss after HIV infection.

OBJECTIVE 4. Evaluate the HIV-induced mechanism of cell death in lymphoid tissue cultured *ex vivo*.

OBJECTIVE 5. Determine the effect of a pan-caspase inhibitor on HIV pathogenesis.

OBJECTIVE 6. Characterize the mechanism of action of a pan-caspase inhibition in HIV restriction.

CHAPTER 1.

Modulation of the autophagic pathway to prevent HIV infection in human lymphoid tissue

MATERIALS AND METHODS

Reagents

Rapamycin, 3-methyladenine, chloroquine, bafilomycin, mefloquine, quinacrine, JM-2987 and azidothymidine (AZT) were purchased from Sigma-Aldrich (Spain).

Autophagy modulation in HeLa cells

For western blot analysis, HeLa cells were cultured in a 12-well plate and $0.2 \cdot 10^6$ cells/well were added in a final volume of 1ml of DMEM (Dulbecco's Modified Eagle Medium) with 10% Heat-inactivated Fetal Bovine Serum (FBS, Gibco), and incubated overnight at 37°C. Where indicated, cells were treated with rapamycin (100nM) in fresh medium for 24 hours at 37°C. Chloroquine (30µM) was added for the last 3 hours of culture, where specified. After incubation, drugs were washed out with Phosphate buffered saline (PBS, Gibco) and cells were detached with lysis buffer. Cell lysates were stored at -80°C until western blot analysis.

For fluorescence microscopy, $0.7 \cdot 10^5$ cells/well were cultured in Millicell EZ 8-well slides (Millipore) in a final volume of 500µl of DMEM with 10% FBS and incubated overnight at 37°C. Cells were washed with PBS, and where indicated, treated with rapamycin (100nM) and/or chloroquine (30µM) for 4 hours in a final volume of 200µl/well at 37°C.

Tonsil cells acquisition and generation of Human Lymphoid Aggregate Cultures (HLACs)

Tonsil tissues were collected from non-identifiable healthy donors in routine tonsillectomies. All individuals provided written informed consent, and the study was approved by the Ethics committee at Hospital Germans Trias i Pujol. Tissues were processed within 1 hour after surgery and HLACs were prepared and cultured as previously described[20, 136]. Briefly, tonsils were dissected and minced into ~1cm^2 pieces and filtered through a 40µm cell strainer (Greiner) to create a single-cell suspension. Cells were cultured in U-bottomed 96-well plates and 10^6 cells were seeded in a final volume of 200µl/well of culture media (CM). CM contained RPMI 1640 (Roswell Park Memorial Institute) supplemented with 15% FBS, 50µg/ml gentamycin (Merck), 1mM sodium pyruvate (Invitrogen), 0.1mM non-essential amino acids 100x (Invitrogen), 2.5µg/ml fungizone (Thermo Fisher), 100U/ml penicillin and 100µg/ml streptomycin (Thermo Fisher). HLACs were cultured at 37°C and 5% CO_2 in a water-saturated incubator. Each figure legend provides details on how many individual donors were analyzed in the given experiment.

Autophagy modulation in tonsil cells

For western blot analysis, $2 \cdot 10^6$ tonsil cells/well were cultured in a final volume of 1ml in 24-well plates. Cells were pre-treated with or without 3-methyladenine (10mM) for 2 hours and then incubated with rapamycin (100nM) or medium, and cultured for 24 hours at 37°C. Bafilomycin

(25nM) and chloroquine (30µM) were added to the culture for the last 3 hours of incubation. For autophagy modulation with mefloquine (15µM, 10µM, 7.5µM and 5µM) and quinacrine (10µM, 5µM, 2.5µM and 1µM), cells were treated with drugs for 24 hours at 37°C. After the incubation time, cells were washed with PBS, and dry pellets were stored at -80°C until western blot analysis.

For fluorescence microscopy, $2 \cdot 10^6$ tonsil cells/well in a final volume of 200 µl were cultured in U-bottomed 96-well plates. Cells were treated with rapamycin (100nM) and/or chloroquine (50 µM) for 24 hours at 37°C. After incubation, cells were washed with PBS, resuspended in 200µl of PBS containing 20% FBS and processed for fluorescence microscopy immediately.

Western blot analysis

Dry pellets were lysed on ice in 1X RIPA buffer (Werfen) supplemented with halt protease inhibitor cocktail (Invitrogen) and 1mM phenylmethylsulfonyl fluoride (PMSF) (Werfen). Concentration of solubilized protein was determined by Bradford assay (Thermo Fisher) and between 20µg to 30µg of protein were used for polyacrylamide gel electrophoresis (PAGE) analysis. Briefly, protein samples were loaded in 12% Sodium Dodecyl Sulfate (SDS) - PAGE gels (Thermo Fisher), run in a vertical electrophoresis cell and subsequently transferred to 0.2µm PVDF membranes (Bio-Rad Laboratories). Membranes were blocked with 5% non-fat milk in PBS + 0.05% Tween-20 (PBST) for 1 hour at room temperature and incubated overnight at 4°C with the following primary antibodies: anti-LC3 rabbit antibody 1:1000 (NB100-2331, Novus Biologicals) and anti-GAPDH mouse antibody 1:5000 (MA5-15738, Thermo fisher). After washing with PBST, membranes were incubated for 1 hour at room temperature with the following Horseradish Peroxidase (HRP)-conjugated secondary antibodies: donkey anti-rabbit IgG at 1:5000 dilution (711-036-152, Jackson ImmunoResearch) or goat anti-mouse IgG at 1:10000 dilution (115-036-071, Jackson ImmunoResearch), respectively. Signal from labeled protein bands was developed with SuperSignal West Pico Chemiluminescent Substrate (Thermo Fisher) and imaged through a ChemiDoc Imaging system (Bio-Rad). Density of protein bands, corresponding to LC3I (16kDa) and LC3II (14kDa) forms of the LC3 protein, were quantified with Image Lab software and LC3II/LC3I ratio was calculated as a quantitative measurement of autophagic activity.

Fluorescence microscopy

Treated tonsil cells were attached (100 µl cells/channel) onto Shandon EZ Double Cytofunnel (Thermo Fisher) glass slides by cytospin centrifugation at 650rpm for 5 minutes at low acceleration force. Cells were washed with PBS and fixed in 4% paraformaldehyde (Sigma-

Aldrich) for 15 minutes at room temperature. After fixation, cells were washed with cold PBS, permeabilized with absolute methanol for 10 minutes at -20°C, washed with PBS and then blocked for 1 hour at 4°C with 1% Bovine Serum Albumin (BSA). Immunodetection of LC3 and CD4 receptor in tonsil cells was performed with rabbit anti-LC3 (1:800 dilution in 1% BSA; NB100-2331, NovusBio) and mouse anti-CD4 (1:40 dilution in 1% BSA; ab67007, Abcam) antibodies with an overnight incubation at 4°C in a moist and humid chamber. Slides were next washed with PBS and incubated with secondary antibodies goat anti-rabbit Alexa Fluor 488 (1:500 dilution in 1% BSA) and goat anti-mouse Alexa Fluor 568 (1:600 dilution in 1% BSA) for 1 hour at room temperature. Finally, slides were washed with PBS, incubated with Hoechst (1:200 dilution in PBS, ImmunoChemistry Technologies) for 10 minutes at room temperature and coverslips were mounted. Slides were examined using a Zeiss AxioObserver Z1 inverted fluorescence microscope using a 63x oil immersion objective. Images were analyzed with the ZEN blue software (Carl Zeiss Microscopy GmbH).

Cell viability assay

HLACs were treated with serial dilutions of rapamycin (400nM, 200nM, 100nM, 50nM, 25nM), 3-methyladenine (20mM, 10mM, 5mM, 2.5mM, 1.25mM), chloroquine (120μM, 60μM, 30μM, 15μM, 7.5μM), bafilomycin (100nM, 50nM, 25nM, 12.5nM, 6.25nM), mefloquine (30μM, 15μM, 7.5μM, 3.7μM and 1.8μM) and quinacrine (10μM, 5μM, 4μM, 3μM, 2μM), and incubated for 3 days at 37°C. Serial dilutions of the HIV-1 entry inhibitor JM-2987 (10μg/ml, 5μg/ml, 2.5μg/ml, 1.25μg/ml, 0.625μg/ml) and DMSO (1:10, 1:20, 1:40, 1:80, 1:160 dilutions from absolute DMSO, Sigma-Aldrich) were used as positive and negative controls for viability, respectively. After 3 days, cell viability was monitored for rapamycin, 3-methyladenine, chloroquine, bafilomycin and mefloquine by flow cytometry using a Live/Dead fixable Aqua cell staining kit (Invitrogen) (1:1500 dilution in PBS and incubated 30 minutes at 4°C). Then, anti-CD3 APC-Cy7 (Biolegend) staining for 15 minutes at room temperature was also performed. To determine cell viability for quinacrine treatment, Perfect-Count™ Microspheres (Beads) (CYT-PCM-50, Cytognos) were added for absolute counts of cells and compared to the untreated control. Data was acquired in a LSRII cytometer (BD Biosciences) and analyzed with FlowJo software. Results were expressed as percentage relative to the untreated control.

Virus stock production

HIV-1 strain pBR-NL43-GFP virus (CXCR4 tropic virus) production was performed by infecting $10 \cdot 10^6$ MT-4 cells on exponential growth with 500μl of pBR-NL4-3 viral stock ($16.5 \cdot 10^6$ $TCID_{50}$)

and incubated for 2 hours at 37°C (shaking every 30 minutes). Cells were washed with PBS to remove unbound virus, resuspended with 40ml RPMI + 10% FBS and incubated for 2 days at 37°C in a T75 culture flask (Falcon). Culture supernatant was spun down, aliquoted and stored at -80°C until further use.

Autophagy analysis in HLACs after HIV infection

HLACs were infected one day after cell preparation by spinoculation at 1200g for 2 hours at 4°C with 80ng of Gag p24 of a X4-tropic strain of a HIV-1 virus. After spinoculation cells were maintained 1 or 2 hours at 37°C without disturbing the pellet (**Figure 1**). Three hours post-infection, virus was removed and cells were cultured for 24 hours with rapamycin or 3 days with medium and then 24 hours with rapamycin. At the end of the incubation time, chloroquine was added to the cultures for the last 3 hours of incubation. Uninfected HLACs were also treated in parallel with the infected ones and used as controls. Three replicates were performed for each condition and after the incubation time, replicates were pooled together. Cells were washed with PBS and dry pellets were stored at -80°C until western blot analysis.

Effect of autophagy modulation in HIV infection

HLACs were treated for 2 hours with rapamycin (100nM), 3-methyladenine (10mM), chloroquine (30µM), bafilomycin (25nM), mefloquine (15µM, 10µM, 7.5µM, 5µM, 2.5µM), quinacrine (10µM, 5µM, 4µM, 3µM, 2µM) and the entry inhibitor JM-2987 (1µg/ml). Then, cultures were infected by spinoculation as explained before. After incubation, the virus was washed out and fresh drugs were added. Cell cultures were maintained for 3 days at 37°C. Then, cells were collected and dry pellets were performed and stored at -80°C until total HIV DNA analysis by quantitative real time PCR.

To evaluate the effect on HIV replication, HLACs were treated with drugs and infected for 2 hours at 37°C without the spinoculation step. Then, the virus was washed out and fresh drugs were added. After 3 days of culture, cells were washed with PBS and fresh medium without drugs was added. Cultures were maintained for 7 days at 37°C. Supernatants were collected at days 3, 5 and 7 post-infection and the amount of HIV-1 Gag p24 capsid antigen was measured by HIV-1 p24 AlphaLISA immunoassay (PerkinElmer).

Quantification of total HIV DNA

DNA was isolated using QIAamp DNA Blood kit (51106, Qiagen) according to the manufacturer's instructions. A standard curve was generated by ten-fold serial dilutions (10^6 to 10^1) of a recombinant plasmid expressing the HIV-1 *gag* gene. The cellular equivalents of DNA in each

sample were determined using the same serial dilutions of a plasmid carrying the human C-C chemokine receptor type 5 (CCR5) gene. Quantitative real-time PCR was performed using a TaqMan Universal Master Mix (Applied Biosystems) and the following primers and probes: 688F (5'-GAC GCA GGA CTC GGC TTG-3'); 809R (5'-ACT GAC GCT CTC GCA CCC-3') and F480PRO (5'-FAM-ACA GAG ACA CTT CCC GCC CCC G-TAMRA-3') to detect HIV-1 gag and CCR5-576F (5'-TCA TTA CAC CTG CAG CTC TCA TTT-3'); CCR5-726R (5'-ACA CCG AAG CAG AGT TTT TAG GAT-3') and CCR5-661T (5'-VIC-CTG GTC CTG CCG CTG CTT GTC A-TAMRA-3') for human CCR5 detection. Absolute HIV DNA copies per million cells were calculated with the HIV-1 gag and human CCR5 copy numbers obtained from the standard curves for each sample. Fold changes relative to the infected control without drug were determined. All real-time PCR reactions were performed on an ABI Prism 7000 (Applied Biosystems).

HIV-1 pseudovirus production

Pseudotyped luciferase reporter viruses were produced in HEK293T cells by co-transfection of pNL4-3luc.R-E- vector and the VSV-G envelope-expressing vector by using the X-tremeGENE HP DNA Transfection Reagent (Sigma-Aldrich). Transfected cells were incubated for 48h at 37°C. Supernatant was harvested and treated with 100U/ml of DNAse I (Invitrogen) for 1h at 37°C. Aliquots were stored at -80°C until use.

Single-cycle infectivity assay

HLACs were incubated for 2 hours at 37°C with serial dilutions of rapamycin (100nM, 50nM, 25nM, 12.5nM, 6.25nM, 3.125nM, 1.56nM, 0.78nM, 0.39nM , 0.195nM, 0.097nM and 0.048nM), 3-methyladenine (10mM, 5mM , 2.5mM , 1.25mM , 0.625mM , 0.312mM, 0.156mM and 0.078mM), chloroquine (30µM, 15µM, 7.5µM, 3.75µM) and bafilomycin (25nM, 12.5nM, 6.25nM, 3.125nM, 1.56nM, 0.78nM, 0.39nM, 0.195nM), and then infected with the (VSV-G)-NL4-3 luciferase reporter pseudovirus by spinoculation as described before. After washing out the virus, cells were cultured for 3 days in the presence of fresh drugs. The HIV-1 reverse-transcriptase inhibitor AZT (5µg/ml) was used as a control. Cells were lysed with Britelite plus Reporter Gene assay (PerkinElmer) and luciferase was measured using an EnSight multimode plate reader with the Kaleido software.

Analysis of cell-to-cell HIV transmission

HLACs were infected with a replicative X4-tropic virus by spinoculation as explained before. After 3 days, uninfected cells were labeled with CellTrace carboxyfluorescein succinimidyl ester (CFSE) (2µM, Invitrogen) for 5 minutes at room temperature. Excess of dye was washed out with PBS,

and $0.6 \cdot 10^6$ of uninfected-$CFSE^+$ cells were pre-treated for 2 hours at 37°C with or without autophagy modulators (3-methyladenine 10mM, chloroquine 30µM and bafilomycin 25nM). Then, $0.6 \cdot 10^6$ of infected or uninfected $CFSE^-$ cells were added to the treated $CFSE^+$ target cells in a ratio 1:1 and incubated in the presence or absence of drugs for 2 days at 37°C. After 2 days, cells were collected and analyzed by flow cytometry. Cells were stained with antibodies anti-CD3-APC-Cy7, anti-CD4-APC and anti-CD8-PerCP (BioLegend), fixed and permeabilized (FIX & PERM kit, Thermo Fisher) and stained with an anti-HIV-1 p24 antibody (KC57-PE, Coulter). To calculate CD4 T cell depletion, total live lymphocytes were first gated according to forward and side scatter, and then $CD3^+$ population was determined. Next, $CFSE^+$ cells were selected, and CD4+ and CD8+ T cells were gated to calculate the $CD4^+/CD8^+$ ratio. Cell depletion was calculated as a percentage compared to the uninfected control as previously described[25]. To analyze intracellular p24 levels, $CD3^+$ $CFSE^+$ cells were gated and CD8-negative cells were selected to include both CD4-positive and CD4-negative cells. Data was acquired in a LSRII cytometer and analyzed with FlowJo software.

Statistical analysis

Statistical analysis and data visualization were performed with GraphPad Prism (version 9). One sample t-test and two-tailed unpaired Student's t test were used. Differences were considered significant at *P<0.05, **P<0.01, ***P<0.001 and ****P < 0.0001.

RESULTS

Autophagy modulation in HeLa cells

Several studies have already described that autophagy can be modulated by either inducers or inhibitors that interfere with several steps of the autophagic machinery in different cell lines. In HeLa cells, one of the cell lines most commonly used to test autophagy[137, 138], treatment for 24 hours with the inducer rapamycin (100nM) resulted in a slight increase in the LC3II/LC3I ratio analyzed by western blot (**Fig. 1a**). To corroborate our results, LC3 puncta was also analyzed by fluorescence microscopy, which did not show any increase compared to the untreated control (**Fig. 1b**). Moreover, when HeLa cells were treated with the inhibitor chloroquine (30µM) for 3 hours, an increase in LC3II was detected by western blot (**Fig. 1a upper panel**) resulting in a significant increase in the LC3II/LC3I ratio compared to the untreated control (**Fig. 1a lower panel**), and an increase in the number of LC3 puncta per cell (**Fig. 1b**). The highest LC3II/LC3I ratio and number of LC3 puncta per cell was observed after 24 hours of treatment with rapamycin and when the autophagic flux was blocked with chloroquine for the last 3 hours (**Fig. 1a and Fig 1b**).

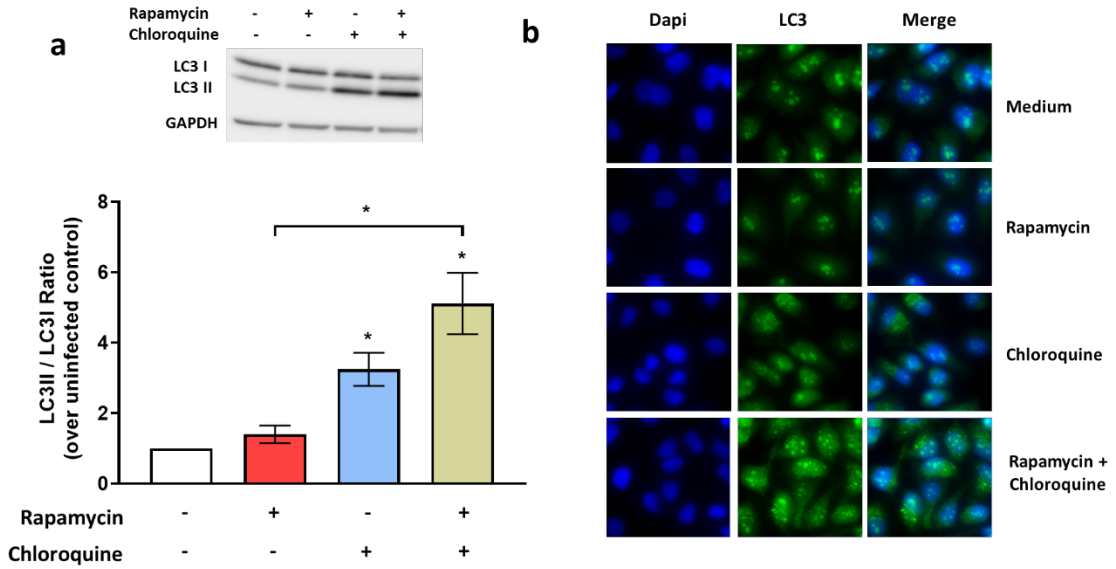

Figure 1. Basal autophagy and autophagy modulation in HeLa cells. a) HeLa cells were treated for 24 hours with rapamycin (100nM) or medium, and where indicated, chloroquine (30µM) was added for the last 3 hours. Cell were lyzed, and the expression levels of LC3I, LC3II and GAPDH, used as loading control, were measured by western blot. **Upper panel**: A representative western blot image from a single experiment is shown. **Lower panel**: LC3II/LC3I ratios were calculated and levels relative to the control with no drugs are represented as bars (mean ±SEM of 3 donors). Differences between the untreated control and treated samples were analyzed by one sample t-test (*P < 0.05). **b)** Images from fluorescence microscopy are represented, showing Dapi (blue), LC3 (green) and the merge of both stainings in HeLa cells treated for 4 hours with medium, rapamycin (100nM), chloroquine (50µM) or both drugs.

Autophagy modulation on human lymphoid aggregate cultures

Basal autophagy and autophagy modulation in HLACs were first analyzed using various chemical compounds commonly used for that purpose. In this tissue-like-culture, a significant autophagy induction was observed after 24 hours of rapamycin treatment (100nM), which resulted in an increase in LC3I and LC3II by western blot (**Fig. 2a upper panel**), and a higher LC3II/LC3I ratio compared to the untreated control (**Fig. 2a lower panel**). As previously described with HeLa cells, when we visually tracked the autophagic response to rapamycin using fluorescence microscopy, no changes in the redistribution of the LC3 protein was observed in comparison with non-treated HLACs, with no apparent cells displaying LC3 puncta (**Fig. 2b**). A significant decrease in basal autophagy or in the rapamycin-induced autophagy was observed in HLACs cultured for 26 hours with 3-methyladenine (10mM) (**Fig. 2a**). After chloroquine treatment, an increase in the LC3II/LC3I ratio was observed after 3 hours (**Fig. 2a**), reflecting the increase in the number of autophagosomes and measured as an increase in the number of LC3 puncta by cell (**Fig. 2b**). We also detected and increase in the LC3II/LC3I ratio after 3 hours of bafilomycin treatment (**Fig. 2a**), similar to that observed with chloroquine. Moreover, the LC3II/LC3I ratio and the number of cells displaying LC3 puncta was higher in cultures co-treated with rapamycin and chloroquine, indicative of the autophagic flux functionality in HLACs (**Fig. 2a and 2b**).

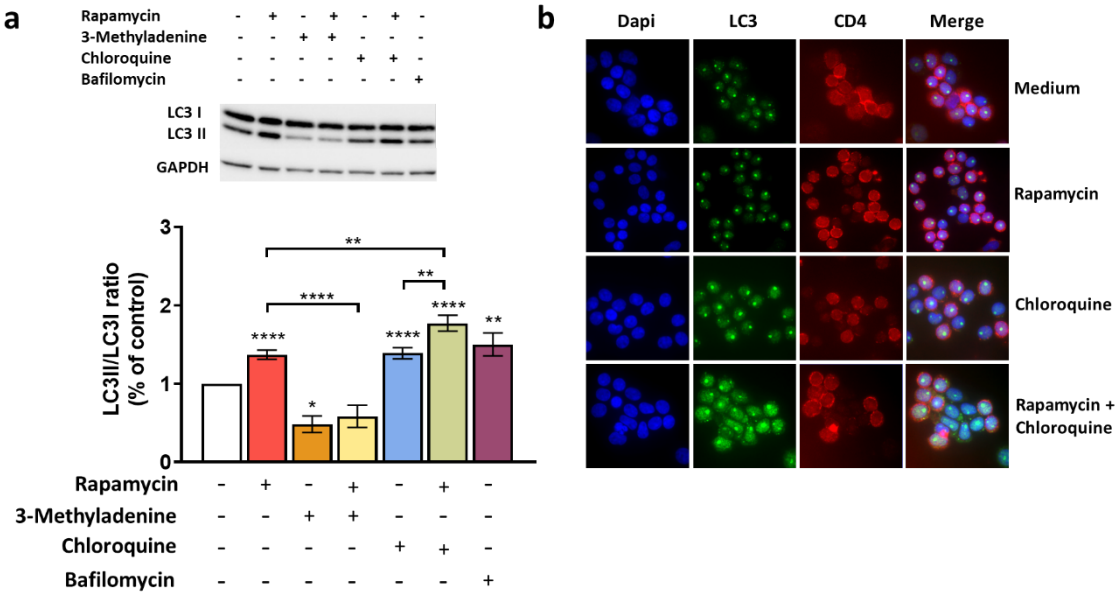

Figure 2. Basal autophagy and autophagy modulation in HLACs. a) Isolated tonsil cells were treated for 24 hours with medium or rapamycin (100nM) and where indicated, 2 hours of pre-incubation with 3-methyladenine (10mM) was done. Autophagic flux was analyzed by treating cells cultured with medium or rapamycin during 24 hours with chloroquine (30µM) for the last 3 hours. Cells cultured in medium were treated with bafilomycin (25nM) for 3 hours. The expression levels of LC3I, LC3II and GAPDH as loading control were measured by western blot. **Upper panel:** Western blot image of a representative experiment. **Lower panel:** LC3II/LC3I ratios are shown (mean ±SEM; n=27 donors; for rapamycin + 3-methyladenine and 3-methyladenine n=4 donors). Fold increase is relative to the untreated cells. Differences to the untreated control were tested by using one sample t-test. Differences between conditions were tested by t-test. *P < 0.05; ***P < 0.001; ****P < 0.0001. **b)** Representative immunofluorescence images showing DAPI (blue), LC3 (green) and CD4 (red) stainings of untreated tonsil cells or treated with rapamycin (100nM) and/or chloroquine (50µM) for 24 hours. All images are merged at the right panel.

It has been previously described, that autophagy modulators can be toxic to cells at relatively low concentrations[139]. Although in treated HLACs we observed by microscopy an increase in autophagic markers in the absence of visible changes that would be associated with cell toxicity (**Fig. 2b**), cytotoxicity was further analyzed using flow cytometry. HLAC were treated for 3 days with different concentrations of rapamycin, 3-methyladenine, chloroquine and bafilomycin and the percentage of viable cells was determined using a live/dead staining (**Fig. 3a**). No significant decrease in cell viability was observed after 3 days of exposure with the drug concentrations that were used to modulate autophagy (**bars highlighted in bold in Fig. 3b**) or in any of the different concentrations tested of rapamycin, 3-methyladenine or bafilomycin. Chloroquine became cytotoxic at 60µM and 120µM but not at lower concentrations. The entry inhibitor JM-2987 was used at different concentrations as a non-toxic control, while DMSO was used as a positive control and we observed a dose-dependent decrease in cell viability. Therefore, since these concentrations were non-toxic and able to modulate autophagy in HLACs, we next evaluated their effect on HIV replication.

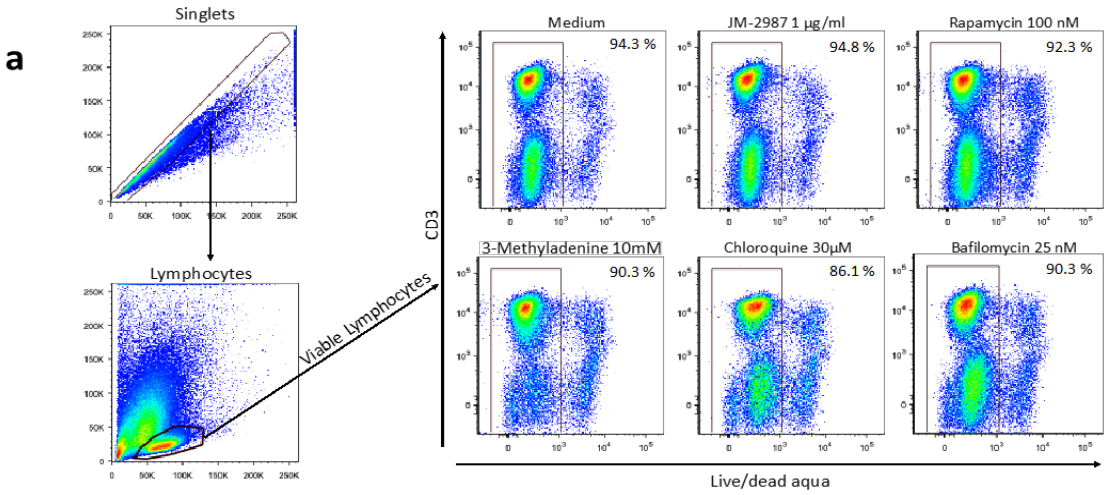

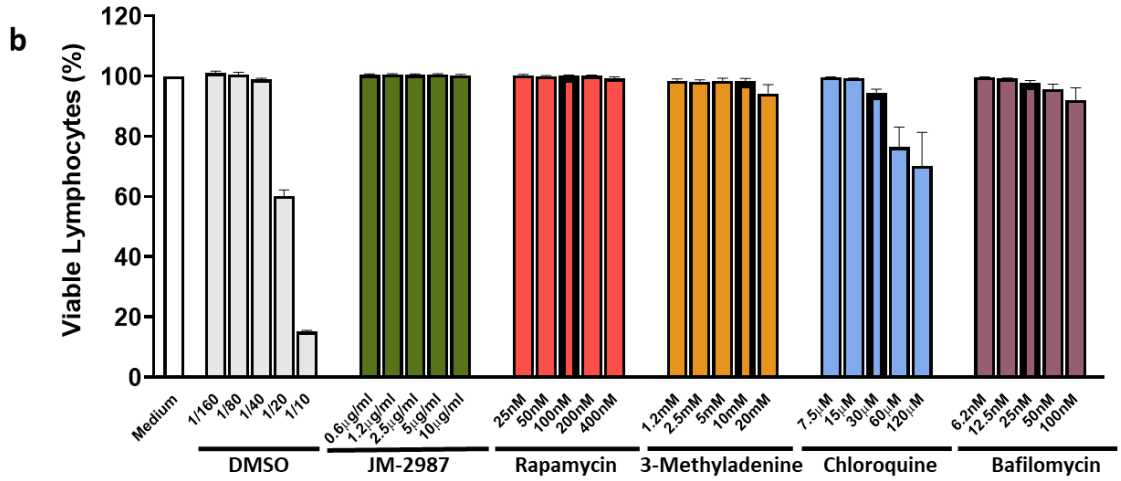

Figure 3. Autophagy modulators are not cytotoxic in HLACs. Tonsil cells were treated with serial dilutions of rapamycin, 3-methyladenine, chloroquine, bafilomycin or medium for 3 days. The entry HIV inhibitor JM-2987 and DMSO were used as controls. Cell viability was measured by flow cytometry using a live/dead staining. **a)** Gating strategy used. Doublets were excluded and lymphocytes were gated by forward and side scatter and live lymphocytes were selected. Representative flow cytometry plots are shown. **b)** Proportion of viable lymphocytes following treatment with concentration ranges of different drugs (mean ±SEM; n=4 donors, 2 of them measured in duplicate). Concentrations used in all study experiments are highlighted in bold in the graph: 100nM rapamycin, 10mM 3-methyladenine, 30µM chloroquine and 25nM bafilomycin.

HIV infection induce autophagy in HLACs without an impairment in the response to autophagic modulators

Prior studies have reported both, induction and inhibition of autophagy during HIV-1 infection[53, 54]. In order to investigate whether HIV-1 infection was able to modulate autophagy in lymphoid tissue, HLACs were infected and autophagy levels were analyzed 24 hours and 4 days post-infection by western blot (**Fig. 4a**). LC3II/LC3I ratio was significantly higher in HIV-infected HLACs (grey bars) than in uninfected cultures (white bars), both at 24 hours and 4 days post-infection (**Fig. 4b**). Since *in vivo* HIV-1 infection has been associated with an impairment in the autophagic response[57, 60, 61], we next evaluated the functionality of this response in infected HLACs. Rapamycin (red bars) and chloroquine (blue bars) treatment led to an increase in the LC3II/LC3I ratio compared with infected HLACs without drugs (grey bars) (**Fig. 4b**), both 24 hours and 4 days after infection. The autophagic modulation in uninfected HLACs cultured in parallel are shown for comparison with the infected ones. In infected HLACs, treatment with rapamycin plus chloroquine (green bars) resulted in a higher LC3II/LC3I ratio (**Fig. 4b**), which indicates that

infected cells have a functional autophagic flux. To ensure comparable conditions, infected and uninfected cells were treated identically at each step, including the culture media change.

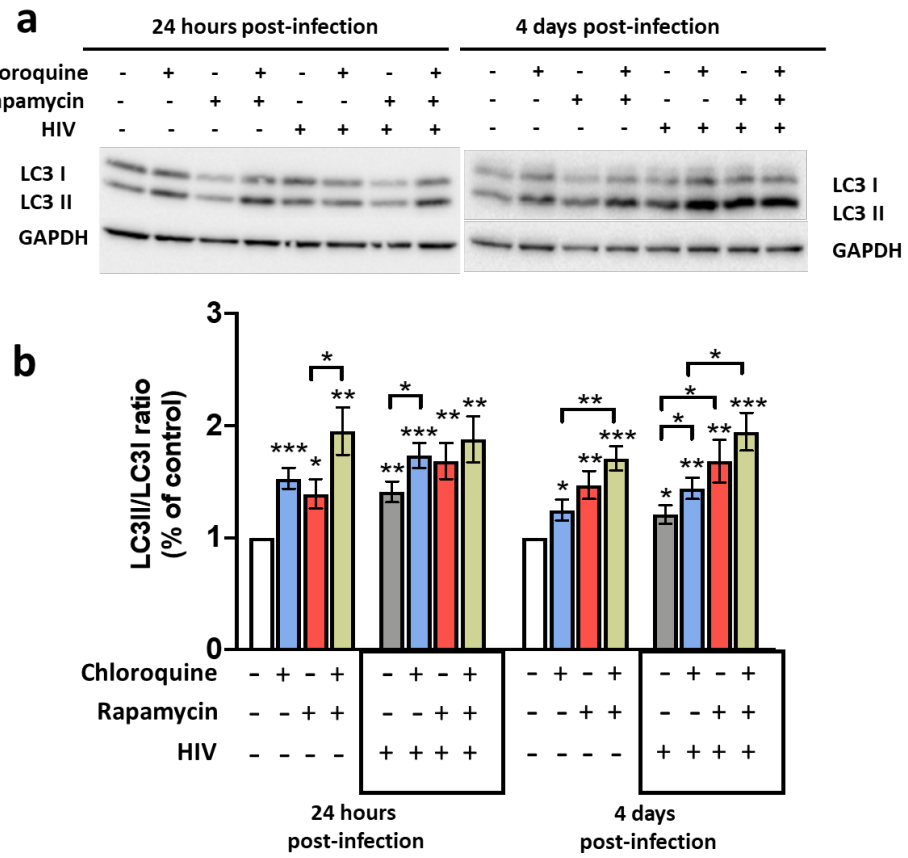

Figure 4. HIV-1 induces autophagy in HLACs without impairment in the response to autophagic modulators. Tonsil cells were infected by spinoculation with a X4 strain of HIV-1. Three hours or 3 days after infection, and where indicated, cells were cultured for 24 hours in the presence of rapamycin and/or chloroquine for the last 3 hours. Cells were harvested and lysates were immunoblotted to quantify LC3I, LC3II and GAPDH. **a)** Western blot images of a representative experiment 24 hours post-infection (3 hours of infection + 24 hours with rapamycin) and 4 days post-infection (3 days of infection + 24 hours with rapamycin) are shown. Autophagic flux was analyzed in both conditions by treating cells with chloroquine for the last 3 hours of culture. **b)** LC3I and LC3II levels were quantified and LC3II/LC3I ratios are represented (mean ±SEM; n=9 donors). Fold increases are relative to the untreated uninfected controls. Differences to the control samples were tested by using one sample t-test. Differences between samples were tested by t-test. *P < 0.05; **P < 0.01; ***P < 0.001.

Autophagy modulation inhibits HIV-1 infection

The effect that the autophagy modulation has on HIV-1 replication has shown conflicting results, with an outcome that seems to be dependent on the cell type and/or the viral strain used[50, 55]. To evaluate the effect of autophagy modulation on HIV-1 infection in HLACs, cultures were

treated for 2 hours with drugs, infected and then cultured in their presence for 3 days. Autophagy induction with rapamycin led to a significant decrease in total HIV DNA levels compared with the untreated infected control (**Fig. 5a**). Autophagy inhibition at the initial steps, using 3-methyladenine, or blocking the autophagic flux, with chloroquine or bafilomycin, resulted also in a strong and significant decrease in the levels of total HIV DNA. JM-2987, added as a control, inhibited completely HIV DNA levels. To further investigate the effect, HLACs were infected and viral replication was monitored by measuring the amount of p24 protein released in the culture supernatant after 7 days post-infection by ELISA. After infection, a progressive increase over time in the p24 levels were observed in the infected control without drug (**Fig. 5b**). In concordance with the decrease in the levels of HIV DNA after autophagy modulation, we observed an almost total inhibition in p24 production with all tested drugs.

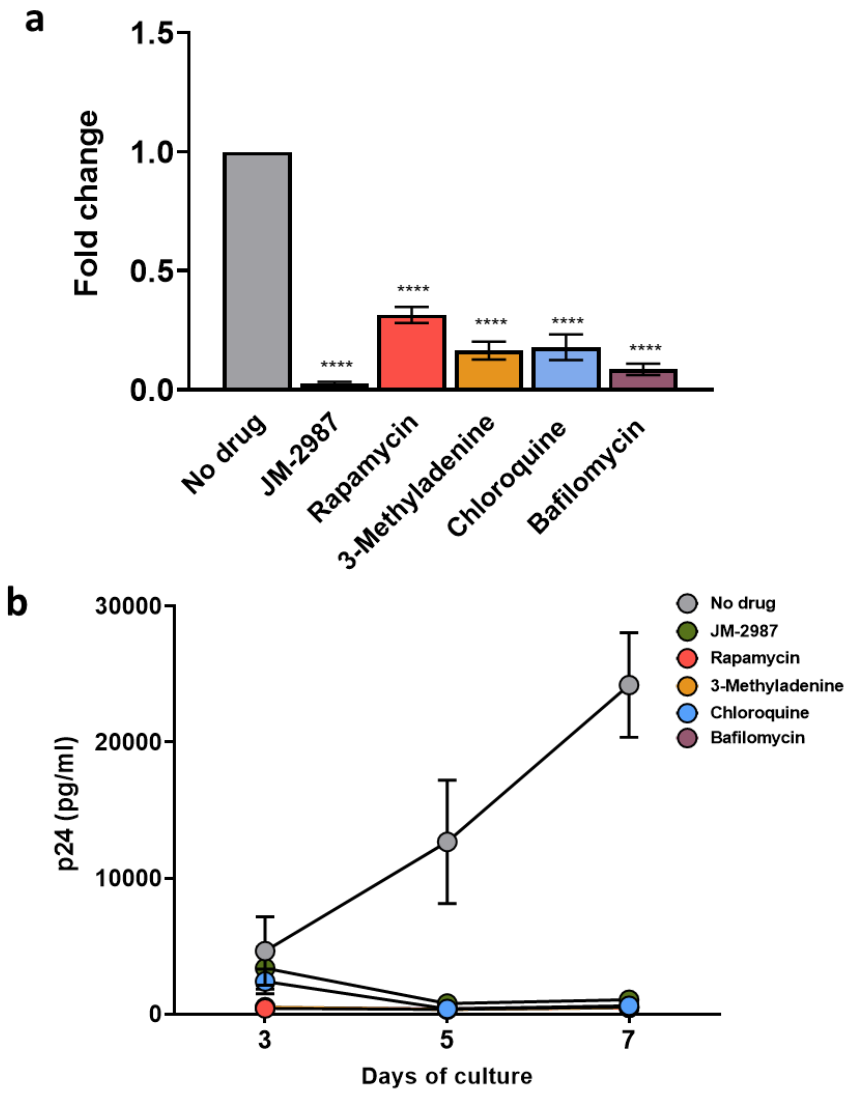

Figure 5. Autophagic modulation prevents HIV infection. a) Tonsil cells were pre-incubated for 2 hours with rapamycin, 3-methyladenine, chloroquine and bafilomycin before infection by spinoculation with a X4 HIV-1 virus. Entry inhibitor JM-2987 was used as a control. Infections were maintained for 3 days and levels of total HIV DNA were measured by qPCR. Results are expressed as fold changes relative to the untreated infected control. Data represents mean ±SEM of 6-12 donors. Differences to the infected control were tested by using one sample t-test. ****P < 0.0001. **b)** Cells were pre-incubated for 2 hours with rapamycin, 3-methyladenine, chloroquine and bafilomycin before infection with a X4 HIV-1 virus without spinoculation and kept in culture for 3 days. After 3 days, drugs were washed out, and medium was added to the culture for 4 more days. HIV p24 protein production was measured in the supernatant by ELISA at days 3, 5 and 7 post-infection. Entry inhibitor JM-2987 was used as a control. Shown are the mean values ±SEM (n=3).

HIV-1 inhibition by autophagy modulation is envelope independent

We further sought to investigate the effect that autophagy modulation has over HIV-1 infection using a single-cycle assay. In order to fulfill this, HLACs were treated with serial dilutions (1:2) of different autophagy modulators for 2 hours, infected with a single-cycle HIV-1 NL4-3 luciferase reporter pseudotyped virus with the heterologous Env vesicular stomatitis glycoprotein (VSV)-G and then incubated for 3 days. Reverse transcriptase inhibitor AZT was used as a control. A significant decrease on luciferase activity was observed within a very wide range of rapamycin concentrations (from 100nM to 0.1nM), compared to the untreated control (**Fig 6**). A similar pattern was found with 3-methyladenine, where a significant reduction of infection was measured at different concentrations (from 10mM to 0.3mM). With chloroquine and bafilomycin treatment, a significant decrease on luciferase activity was also detected, although the reduction was only significant at the highest concentrations (30µM and 15µM with chloroquine, and from 25nM to 3.1nM with bafilomycin) (**Fig. 6**). A total inhibition was detected in HLACs cultured with AZT. These results indicate that autophagy modulation is able to inhibit viral replication in an envelope-independent manner and therefore, would be able to inhibit both, X4 and R5 HIV-1 strains.

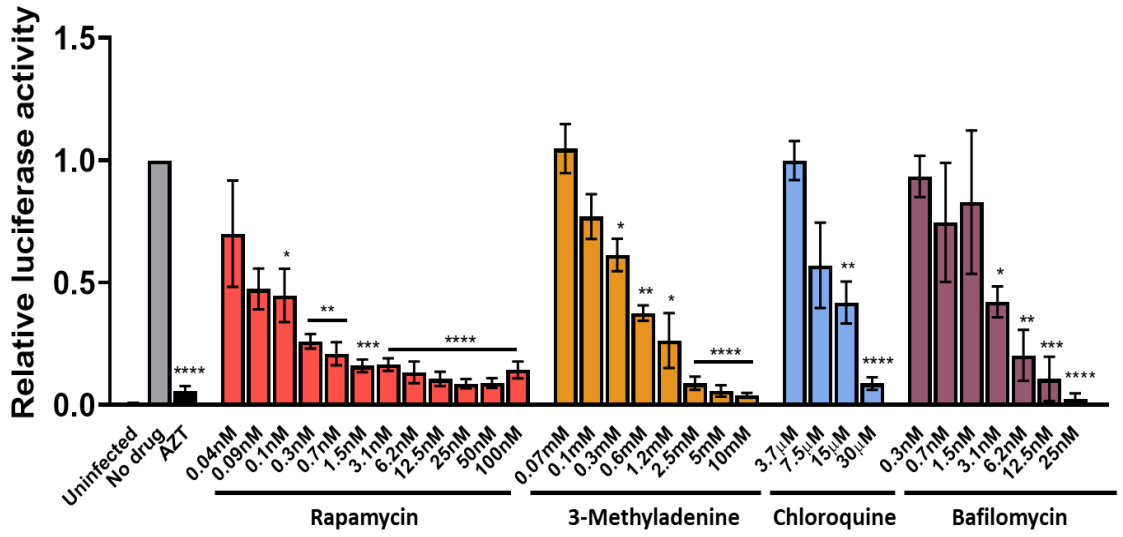

Figure 6. HIV envelope-independent inhibition after autophagy modulation. Cells were pre-incubated for 2 hours with serial dilutions of rapamycin (100-0.049nM), 3-methyladenine (10-0.078mM), chloroquine (30-3.75µM) and bafilomycin (25-0.39nM) before infection. Cells were infected by spinoculation with a (VSV-G)-NL4-3luc.R-E- HIV pseudovirus, and luciferase activity was measured 72 hours after infection. Transcriptase inhibitor AZT (5µg/ml) was used as a control. Results were expressed as luciferase activity relative to the infected control without drug. Data represents mean ±SEM of 4-6 donors, each performed in duplicate. Differences to the control sample were tested by using one sample t-test. *P < 0.05; **P < 0.01; ***P < 0.001; ****P < 0.0001.

Autophagy modulation inhibits cell-to-cell HIV-1 transmission

In vivo, in lymphoid tissue, HIV may be predominantly transmitted between cells by cell-to-cell contacts[104]. Thus, antiretroviral therapies must remain effective against the high MOI observed during cell-to-cell transmission to inhibit both viral replication and pathogenesis associated with HIV infection. Therefore, we employed a co-culture approach in which HLACs productively infected with HIV-1 were co-cultured for 2 days with autologous CFSE-labeled target tonsil cells pre-treated with 3-methyladenine (10mM), chloroquine (30µM) and bafilomycin (25nM), to test their effect in cell-to-cell transmission (**Fig. 7**). Autophagic drugs were kept during the 2 days of co-culture. Under these conditions, as expected, $CFSE^+$-target tonsil CD4 T cells were massively depleted when co-cultured with productively infected cells without drugs (**Fig. 7a**). However, cell depletion was significantly prevented after autophagy inhibition. The impact on HIV replication levels was evaluated measuring cell-associated p24 antigen by flow cytometry (**Fig. 7b**). After infection, and in the absence of drugs, a significant increase in p24 levels was observed in $CD8^-$ $CFSE^+$ T cells compared to the uninfected control. $CD8^-$ cells were analyzed to include $CD4^+$ and $CD4^-$ cells, which are the one that are productively infected. In co-cultures, the presence of autophagic modulators resulted in a significant decrease in the intracellular p24

content in the CFSE$^+$-target cells. A significant decrease in p24 levels was also observed with the control inhibitor JM-2987. Altogether, these results indicate that autophagy modulation represents a strategy that may be relevant to prevent HIV-1 transmission.

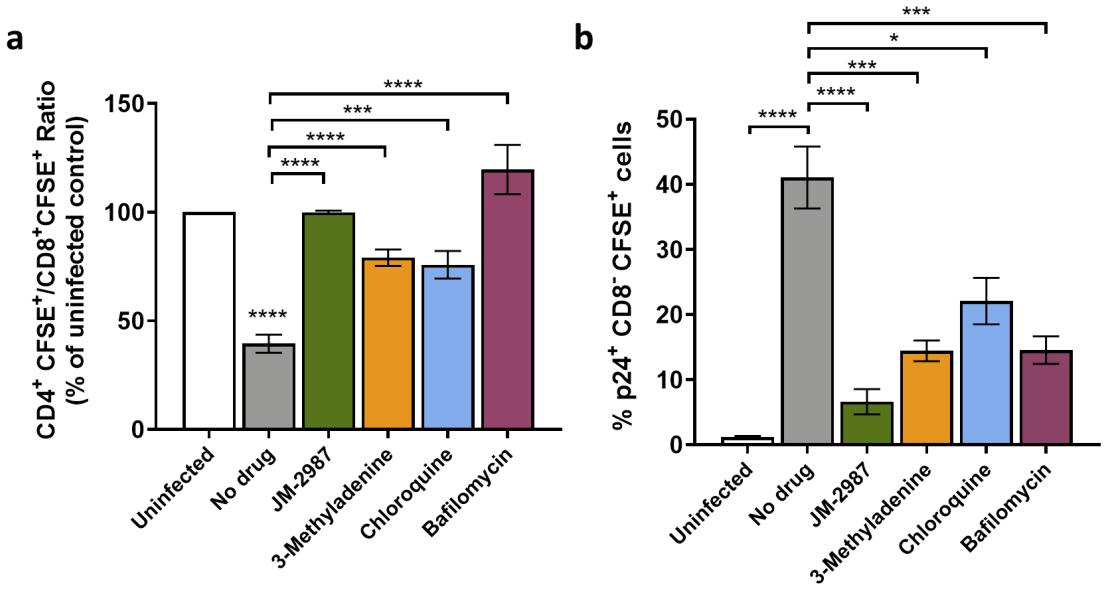

Figure 7. Inhibition of cell-to-cell transmission of HIV-1 by autophagy inhibitors. HLACs were infected for 3 days by spinoculation with a X4 HIV-1 virus, and then cocultured with uninfected CFSE$^+$-HLACs pre-treated for 2 hours with 3-methyladenine, chloroquine and bafilomycin. **a)** CD4$^+$ T cell depletion results are represented as ratios of CD4$^+$CFSE$^+$/CD8$^+$CFSE$^+$ T cells in untreated infected cultures or treated with different drugs compared to the uninfected control from the same donor (mean ±SEM; n=6). **b)** Frequency of intracellular p24 levels in CD8$^-$ CFSE$^+$ cells. The percentage of p24$^+$ cells was plotted and compared between uninfected cultures, untreated infected cultures and treated infected cultures with different autophagy modulators (mean ±SEM; n=6).

HIV-1 inhibition by mefloquine and quinacrine

We next evaluated two other drugs currently used in the clinic: mefloquine and quinacrine. In agreement with previous publications[140-143], both drugs were able to modulate autophagy in HLACs, and a dose-dependent increase in LC3II expression was observed by western blot (**Fig. 8a**). To evaluate their effect on HIV replication, HLACs were exposed to different drug concentrations for 2 hours, infected with a HIV-1 replicative virus and total HIV DNA levels were quantified after 3 days of infection. A significant HIV-1 inhibition was observed, measured as a dose-dependent decrease in HIV DNA levels with both tested drugs (**Fig. 8b**). No cytotoxicity was observed at concentrations with anti-HIV-1 activity (**Fig. 8c**).

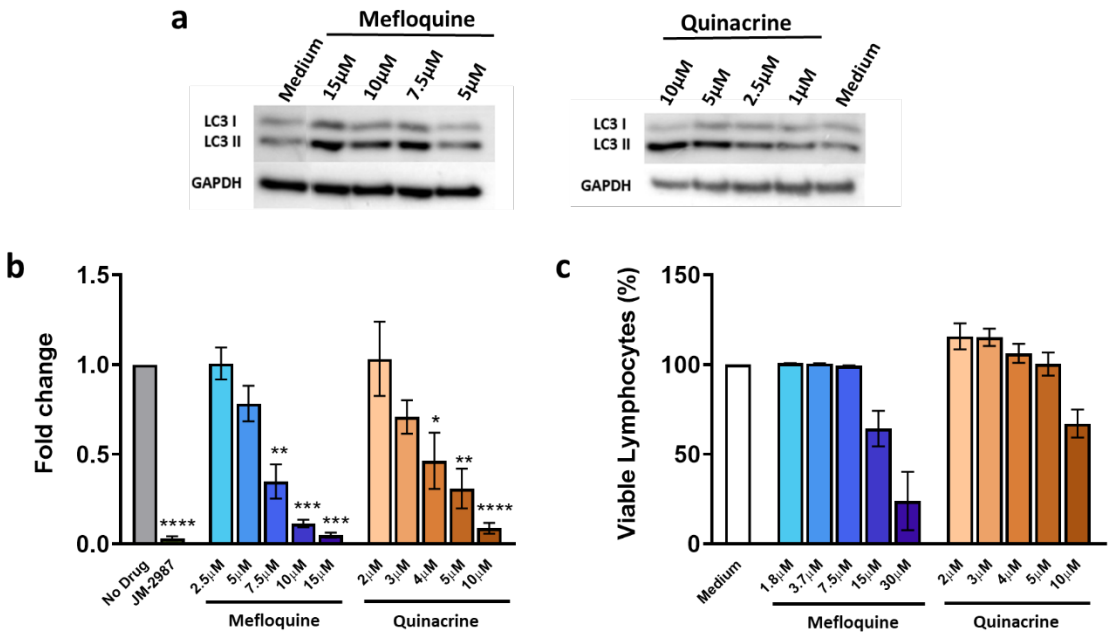

Figure 8. Autophagy modulation and HIV inhibition by mefloquine and quinacrine. a) Isolated tonsil cells were treated for 24 hours with different concentrations of mefloquine, quinacrine or medium. Cells were harvested and lysates were immunoblotted to quantify LC3I, LC3II and GAPDH. Western blot images of one donor for each drug are represented. **b)** Cells were pre-incubated for 2 hours with medium or with different concentrations of mefloquine and quinacrine before infection. Cells were infected by spinoculation with a X4 HIV-1 virus and incubated for 3 days. Levels of total HIV DNA were measured by qPCR. Entry inhibitor JM-2987 was used as a control. Data represents means ±SEM of 3 donors. Differences to the infected control without drug were tested by using one sample t-test. *P < 0.05; **P < 0.01; ***P < 0.001; ****P < 0.0001. **c)** Tonsil cells were treated with medium or different concentrations of mefloquine and quinacrine for 3 days. Cell viability for mefloquine was measured using a live/dead staining; and for quinacrine, absolute counts were obtained with beads, both by flow cytometry. Doublets were excluded and lymphocytes were gated by forward and side scatter and live lymphocytes were selected. Proportion of viable lymphocytes following treatment (mean ± SEM; n=2) are shown.

CHAPTER 2.

Modulation of cell death pathways to enhance innate immune response

MATERIALS AND METHODS

Reagents

7-aminoactinomycin D (7-AAD), pyronin Y, saponin, phytohemagglutinin (PHA), valinomycin, azidothymidine (AZT) and pan-caspase Q-VD-OPh were purchased from Sigma-Aldrich. Human inerleukin-2 (Il-2) was obtained from Roche. JC-10 Mitochondria Membrane Potential assay kit was purchased from Abcam. The pNL4-3luc.R-E-, JM-2987, Raltegravir (RAL) and TAK-779 were obtained through the AIDS Research and Reference Reagent Program, Division of AIDS, NIAID, NIH. Q-VE-OPh was purchased from AdipoGen. FAM-FLICA-1 and FAM-FLICA-3 caspase assay kits were obtained from ImmunoChemistry Technologies (Bloomington, MN). CFSE was purchased from Thermo Fisher. Human Type-I IFN Neutralizing Antibody Mixture, was obtained from PBL Assay Science. The Vaccinia Virus B18R Recombinant Protein (eBioscience, was kindly provided by Nuria Izquierdo-Useros).

Preparation of human lymphoid aggregate cultures (HLAC) and human lymphoid histocultures (HLH) from tonsils

Human tonsils were collected from non-identifiable healthy donors in routine tonsillectomies. All individuals provided written informed consent and the study was approved by the Ethics committee at Hospital Germans Trias i Pujol. Tissues were processed within 1 hour after surgery and HLACs were prepared and cultured as previously described[20, 136].

To prepare HLACs, tonsils were dissected and minced into ~1 cm^2 pieces and filtered through a 40µm cell strainer to create a single-cell suspension. Cells were cultured in U-bottomed 96-well plates ($1x10^6$ cell/well in a final volume of 200µl per well) in culture medium (CM). CM contained RPMI 1640 medium supplemented with 15% FBS, 50µg/ml gentamicin (Merck), 1mM sodium pyruvate (Invitrogen), 0.1mM minimal essential medium with non-essential amino acids 100x (Invitrogen), 2.5µg/ml fungizone, 100U/ml penicillin and 100µg/ml streptomycin. To prepare HLH, tonsils were processed as previously described[136, 144]. Briefly, tissue was dissected into ~2-3 mm^3 blocks and cultured in medium on top of pre-soaked collagen sponges (Gel Foam; Pfizer) at the medium-air interface. Nine individual blocks were placed on the gel foam per well of a six-well plate. HLH and HLACs were cultured at 37°C in a 5% CO_2 water-saturated incubator.

Infection of HLAC, HLH and activated peripheral blood mononuclear cells (PBMCs) with a replicative-competent HIV-1

HLACs were infected one day after cell preparation with HIV-1 in 96-well U-bottom plates by spinoculation of 80ng p24 Gag of HIV particles of the X4-tropic virus NL4-3 in a final volume of

150µl per well. Virions and cells were subjected to high-speed centrifugation (1200g) for 2 hours at 4°C and, subsequently, cells were cultured for 2 hours at 37°C in a 5% CO_2 incubator. Where indicated, cultures were pre-treated for 2 hours before infection with JM-2987 (1µg/mL), RAL (1µg/mL) and Q-VD-OPh (40µM). After incubation, viral input was washed out, specified drugs were added and the infected culture was maintained for 3-5 days at 37°C. Cells were collected and analyzed by flow cytometry. Cell pellets were also stored at -80°C for further analysis.

In some experiments, to analyze viral replication, cells were infected without spinoculation. Cells were infected for 2 hours at 37°C and, where indicated, cultures were pre-treated with Q-VD-OPh and washed out at different time points before and during the infection course. Cultures were maintained for 7 days, and supernatants from different time points were collected.

HLHs were left uninfected or infected with 5µl of HIV-1 (2ng of HIV-1 Gag p24 from the X4-tropic virus NL4-3) for each tissue block. Cultures were pre-treated for 2 hours before infection with JM-2987 (1µg/mL), RAL (1µg/mL) and Q-VD-OPh (40µM). Fresh drugs were added at every medium change. In some experiments, HLHs were infected and subsequently treated at different time-points after infection with JM-2987 and Q-VD-OPh. Culture medium was harvested every 3–4 days, centrifuged and frozen at -80°C until use. Thirteen days after infection, cells were mechanically isolated from uninfected and infected tissue blocks and analyzed by flow cytometry. Cell pellets were also stored at -80°C for further analysis. Each experimental condition was composed of two wells whose culture media and tissue blocks were pooled together. Cells egressed to the medium were also analyzed including those cells obtained by gentle squeezing of the collagen sponge.

Blood samples from de-identified HIV-1 seronegative blood donors were purchase to the Banc de Sang i Teixits (BST), and informed consents were obtained. Peripheral blood mononuclear cells (PBMCs) were purified by ficoll density gradient and activated with PHA (5µg/ml) and IL-2 (20U/ml) for 4 days and infected without spinoculation. Q-VD-OPh was added and washed out at different time points before and during the infection course. After 3 days of culture, medium was collected, centrifuged and frozen at -80°C until use.

To analyze viral replication, the amount of HIV-1 p24 capsid antigen present in culture supernatants, INNOTEST® HIV Antigen mAb immunoassay (Fujirebio) was performed according to the manufacturer's protocol.

Flow cytometry analysis and gating strategy

CD4 T cell depletion and intracellular p24 protein detection:

HLACs and isolated tissue cells from HLH were stained with cell surface antibodies anti-CD3-APC-Cy7, anti-CD4-APC and anti-CD8-PerCP (BioLegend). Then, cells were permeabilized (FIX & PERM Cell permeabilization kit, ThermoFisher) and stained with an anti-p24 antibody (KC57-PE, Coulter). To calculate CD4 T cell depletion, total live lymphocytes were gated according to forward and side scatter morphology and then $CD3^+$ population was selected. Next, $CD4^+$ and $CD8^+$ T cells were gated and $CD4^+/CD8^+$ ratio was determined. Cell depletion was calculated as percentages compared to the uninfected control of the same donor, as previously described[25]. For the analysis of intracellular p24 levels, $CD3^+$ gated cells were further identified and CD8-negative cells were gated to include both CD4-positive and CD4-negative cells. The level of $p24^+$ cells was assessed in both populations: $p24^+$ CD4-positive cells and $p24^+$ CD4-negative cells (productively infected cells). Data was acquired on a LSRII cytometer and analyzed with FlowJo software.

Active caspase detection:

The activation of caspase-1 and caspase-3/7 in HLAC and HLH cells was determined using a fluorescent inhibitor probe (FAM-FLICA Assay Kit, ImmunoChemistry). Cells were also stained with cell surface markers anti-CD3-APC-Cy7, anti-CD4-APC and anti-CD8-V500 (Biolegend). The presence of active caspases was determined by gating live and dead cells with forward and side scatter, followed by gating on $CD3^+$ and then on CD8-negative T cells. A LSRII cytometer was used to acquire the data, which was analyzed with FlowJo software.

Immunophenotypic characterization of HLACs cells:

HLACs were prepared as explained above and cultured for 3 days in the presence of Q-VD-OPh (40µM). At the end of the incubation time, cells were immunophenotyped using monoclonal antibodies against the following surface antigens: CD3, CD4, CD8, CD25, CCR5, CCR7, CD27, CD69, CD45RA, HLADR and CD38 (Biolegend). Cells were permeabilized (Fixation/ Permeabilization Solution Kit, BD) and stained with the intracellular antigen Ki-67. Multicolor analysis was performed with a Fortessa flow cytometer (Becton Dickinson). Data was analyzed with FlowJo software.

Single-cycle infectivity assay

Pseudovirus production:

HIV-Luc Reporter viruses were produced from HEK293T cells by transfecting VSV-G, X4 (NL4-3) and R5 (JRFL)-envelope and pNL4-3luc.R-E- expression vectors by using the X-tremeGENE™ HP DNA Transfection Reagent (Merck). Envelope expression vector was constructed previously in our laboratory[96]. Transfection was incubated for 48 hours at 37°C, then supernatants were harvested. EnvX4 and EnvR5 pseudoviruses were concentrated with the Lenti-X™ Concentrator reagent (Clontech) according to the manufacturer's protocol.

Infectivity assay:

HLACs or PHA-activated PBMCs were infected with VSV-G-, HIV-1 X4- or R5-envelope HIV-1 pNL4-3luc.R-E- luciferase reporter pseudoviruses. Cells were pre-incubated with AZT (5µg/ml), Q-VD-OPh (40µM), Q-VE-OPh (40µM), JM-2987 (1µg/ml) and TAK-779 (5µg/ml) (2 hours for HLACs and 24 hours for PBMCs) and then infected by spinoculation (1200g for 2 hours at 4°C, and then 1 hour incubation at 37°C). After washing out non-infectious input virus, cells were cultured for 48 hours in complete media or fresh drugs where indicated. Infection levels were determined by measuring luciferase luminescence with Britelite Plus Reporter Gene Assay System (Perkin-Elmer). Luciferase activity was normalized to the infected control without drug.

T cell proliferation

To monitor cell division and proliferation, tonsils cells were labeled with CFSE. Cells were cultured in the absence or presence of PHA (5µg/ml) and in the absence or presence of Q-VD-OPh (40µM). Briefly, cells were incubated with 1µM CFSE (Invitrogen) in PBS for 5 minutes at room temperature in the dark. Excess of labeling was stopped by washing cells with complete media and then, incubated for 20 minutes at 37°C, followed by further washes. CFSE staining was assessed every day for 4 days in total lymphocytes population by flow cytometry. Proliferation was reported as the percentage of $CFSE^{low}$ cells.

Cell cycle analysis

Isolated tonsil cells were pre-incubated with or without Q-VD-OPh (40µM) for 2 hours at 37ºC and then cultured in the presence or absence of PHA (5µg/ml). After 3 days, cells were resuspended in PBS containing 0.03% saponin (Sigma-Aldrich), and then incubated with the DNA dye 7-AAD (20µM) for 30 minutes at room temperature in the dark, followed by 5 minutes at

4°C. Then, for RNA staining Pyronin Y was added at a final concentration of 5µM and incubated at 4°C for 10 minutes. To distinguish between lymphocyte population in G_0-G_1 phase, S phase and G_2/M phase, cells were acquired in a CANTO flow cytometer (BD Biosciences). Data was analyzed using FlowJo software (BD Biosciences). Cell population in dot plots of 7-AAD fluorescence versus Pyronin Y fluorescence were gated. Debris was excluded by forward and side scatter, and doublets were discriminated by width versus area. G_0-G_1 cells were identified as cells with the lowest RNA values, while G_2/M cells had the highest RNA and DNA values, being S cells in the middle phase.

Total and Integrated HIV-1 DNA detection

Total HIV-1 DNA quantification:

Total HIV DNA was evaluated by quantitative real time PCR (qPCR). DNA from HLACs and isolated cells from HLH was obtained using QIAamp DNA Blood kit (Qiagen) according to the manufacturer's instructions. Quantitative real-time PCR was performed using a TaqMan Universal Master Mix (Applied Biosystems) and the following primers and probes: CCR5-576F (5'-TCA TTA CAC CTG CAG CTC TCA TTT-3'); CCR5-726R (5'- ACA CCG AAG CAG AGT TTT TAG GAT-3') and CCR5-661T (5'-VIC-CTG GTC CTG CCG CTG CTT GTC A-TAMRA-3') for human CCR5 detection, and DNA PROVIRAL-688F (5'-GAC GCA GGA CTC GGC TTG-3'), DNA PROVIRAL-809R (5'-ACT GAC GCT CTC GCA CCC- 3') and F480PRO (5'-FAM-ACA GAG ACA CTT CCC GCC CCC G-TAMRA-3') to detect HIV-1 gag.

Integrated HIV-1 provirus DNA quantification. Alu-gag qPCR:

For integrated HIV-DNA quantification, an Alu-gag pre-amplification was performed to assure amplification of integrated HIV-1 only using the following primers: Alu-forward 5'-GCC TCC CAA AGT GCT GGG ATT ACA G-3', and gag-reverse 5'AGG GTT CCT TTG GTC CTT GT-3 followed by gag amplification using the primers and probes used to the amplification of the Total HIV DNA. Human CCR5 was also amplified as a control.

Ct values for total and integrated HIV DNA were normalized using CCR5 as housekeeping gene by the ΔΔCt method. Infections were normalized to the untreated control. All real-time PCR reactions were performed on an ABI Prism 7000 (Applied Biosystems).

Gene expression analysis

HLACs were cultured in the presence or absence of Q-VD-OPh (40µM) at different time points (3, 24 and 72 hours). For relative mRNA quantification, RNA was extracted using the NucleoSpin RNA II kit (Macherey-Nagel) as recommended by the manufacturer, including the DNase I treatment step. mRNA levels of all genes were measured by two-step quantitative RT-PCR. Reverse transcription was performed using the PrimeScript™ RT-PCR Kit (Takara) following manufacturer instructions and quantitative PCR was carried out using TaqMan™ Universal PCR Mastermix (Life Technologies). mRNA levels were normalized to GAPDH mRNA expression using the ΔΔCt method. Primers and probes were TaqMan Gene expression assays from Life Technologies (TaqMan *IFNB1A* Hs01077958, TaqMan *ISG15* Hs01921425, TaqMan *IFNA1* Hs00855471, TaqMan *CXCL10* Hs00171042, TaqMan *MX2* Hs01550808, TaqMan *MX1* Hs00895608, TaqMan *Trim22* Hs01001179, TaqMan *Trim23* Hs01106625, TaqMan *IFITM1* Hs00705137, TaqMan *IFITM3* Hs03057129, Taqman *IRF1* Hs00971965, TaqMan *Trim5α* Hs01552558, TaqMan *BST2* Hs00171632, TaqMan *IFNAR1* Hs01066118, TaqMan *IFNAR2* Hs01022060 and TaqMan *GAPDH* Hs02786624).

Gene expression in sorted cells:

HLACs were cultured in the presence or absence of Q-VD-OPh (40µM) for 24 hours. After culture, cells were labeled with anti-CD3-APC-Cy7, anti-CD4-APC, anti-CD8-PerCP and anti-active-caspase-3-V450 (BD) antibodies and acquired using an LSRII cytometer (BD). In parallel, additional cells were stained with anti-CD3-APC-Cy7 antibody, resuspended in PBS containing 1% FBS, and $CD3^-$ and $CD3^+$ populations were sorted in a FACS Aria II cell sorter (BD). Dry pellets from sorted and unsorted (control) cells were kept at -80°C until RNA extraction and subsequent *Ifnb1* and *Gapdh* gene expression quantification by real-time PCR as stated above.

Mitochondrial membrane potential measurement

HLACs were cultured with medium alone or with increasing concentrations of Q-VD-OPh (0.31µM, 0.62µM, 1.25µM, 2.5µM, 5µM, 10µM, 20µM and 40µM) and incubated for 3 days at 37°C in a 5% CO_2 incubator. Where indicated, cells were incubated in the same experimental condition with Q-VE-OPh (40µM). Cells were collected at different time points (24, 48, 72 and 96 hours), and the mitochondrial membrane potential was measured using the JC-10 Mitochondrial Membrane Potential assay kit by flow cytometry according to the manufacturer's instructions. Briefly, cells were stained with anti-CD3-APC-Cy7, anti-CD4-APC and JC-10 dye, and

incubated for 15 minutes at 37°C. Fluorescence was monitored using a LSRII cytometer. Data was analyzed with FlowJo software. Lymphocytes were gated according to forward and side scatter and then $CD3^+$ cells were selected. A gate with the green fluorescent monomeric signal and the red fluorescent aggregated signal was stablished. In polarized cells, JC-10 dye concentrates in the mitochondrial matrix where forms red fluorescent aggregates; while in depolarized cells, JC-10 changes to a monomeric form and stains cells with green fluorescence. To define the depolarized gate and make compensation corrections, valinomycin (100nM) was used as a control. Percentages of cells with polarized and depolarized mitochondria were quantified in all cultured conditions. In some experiments, depolarization was measured on $CD4^+$ and $CD8^+$ T cells. Lymphocyte viability was established in the absence or presence of Q-VD-OPh (40µM) in HLACs incubated for 3 days at 37°C and 5% CO_2. After incubation, Perfect Count™ Microspheres (Cytognos) were added to the culture, acquired with a LSRII flow cytometer and analyzed with FlowJo software. Total number of cells were quantified and percentages were calculated relative to untreated control. Where indicated, the compound Q-VE-OPh (40µM) was used as a negative control.

Effects of anti-IFN type-I agents on viral infection and gene expression

Effects on HIV-1 replication:

HLACs were pre-incubated for 2 hours with the IFN-blocking recombinant receptor B18R (2µg/mL) or anti-IFN type-I antibody mixture (1:50) in the presence or absence of Q-VD-OPh (40µM). AZT (5µg/ml) was used as a control. After incubation, cells were infected with a VSV-G-pseudotyped HIV-1 reporter virus by spinoculation. After washing the excess of viral input, cells were cultured for 48 hours with fresh compounds. Replication was measured by luciferase luminescence quantification.

Effect on type-I IFN gene expression:

HLACs were treated with anti-IFN type-I antibody mixture (1:50), in the presence or absence of Q-VD-OPh (40µM). After 3 days of culture, RNA was isolated and expression levels of IFNβ, ISG15 and MX1 were measured by quantitative RT-PCR as explained above. Ct values obtained were normalized using GAPDH as housekeeping gene by the ΔΔCt method, as stated above. Results were normalized to the untreated control. All real-time PCR reactions were performed on an ABI Prism 7000 (Applied Biosystems, Spain).

Statistical analysis

For statistical analysis, data were analyzed by using GraphPad Prism 7.0. Two-tailed unpaired Student's *t* test and non-parametric Mann–Whitney U-test were used according to the type of experiments (*$P < 0.05$; **$P < 0.01$; ***$P < 0.001$; ****$P < 0.0001$).

RESULTS

Caspase 1 and caspase 3 activation after HIV infection in tonsil cultures

Prior studies have reported the role of caspase-3 (apoptosis) and caspase-1 (pyroptosis) activation in HIV pathogenesis[98, 145]. Here we tested the role of the pan caspase inhibitor Q-VD-OPh in HIV-1 infection by using *ex vivo* cultures of human lymphoid tissue. Fresh human tonsils were homogenized, and human lymphoid aggregate cultures (HLACs) were stablished and infected with HIV-1 as previously reported[18, 20] (**Fig. 1a**). Cell suspensions were pre-incubated in the presence or absence of the pan-caspase inhibitor Q-VD-OPh and antiretroviral drugs, namely JM-2987, a synthetic antagonist of the chemokine receptor CXCR4 (required for the X-tropic virus entry), and raltegravir (RAL), an inhibitor that blocks HIV integration. After drug incubation, cultures were infected by spinoculation with the X4-tropic HIV-1 virus NL4-3, and incubated in the presence of drugs. The expression of active caspase-3 and caspase-1 was analyzed by flow cytometry 5 days post-infection using specific FLICA probes. The percentage of $CD3^+CD8^-$ T cells (which include CD4-positive cells and productively infected CD4-negative cells) expressing active caspase-1 and caspase-3 was significantly increased after infection compared to uninfected cells (**Fig. 1b**). This indicated that HIV-1 infection led to both caspase-3-driven apoptosis and caspase-1-driven pyroptosis in HLACs. Moreover, the increase in active caspases 1 and 3 was significantly prevented when viral replication was inhibited using antiretroviral drugs. Also, and as expected, the pan-caspase inhibitor Q-VD-OPh abrogated the activation of both caspases (**Fig. 1b**). Using a three-dimensional human lymphoid histoculture (HLH), a much more in *vivo*-like model of infection (**Fig. 1c**), HIV-1 infections were performed as previously reported[146]. In HLHs, we observed that the percentage of cells expressing active caspase-1 and -3 was also significantly higher in infected tissues than in the uninfected controls (**Fig. 1d**). However, while all three drugs significantly reduced active caspase-1 in HLH, the decrease in the level of active caspase-3 in the presence of the entry inhibitor JM-2987 or Q-VD-OPh did not reach a statistical significance. These results confirmed the activation of both pyroptotic and apoptotic pathways in lymphoid tissue after HIV infection.

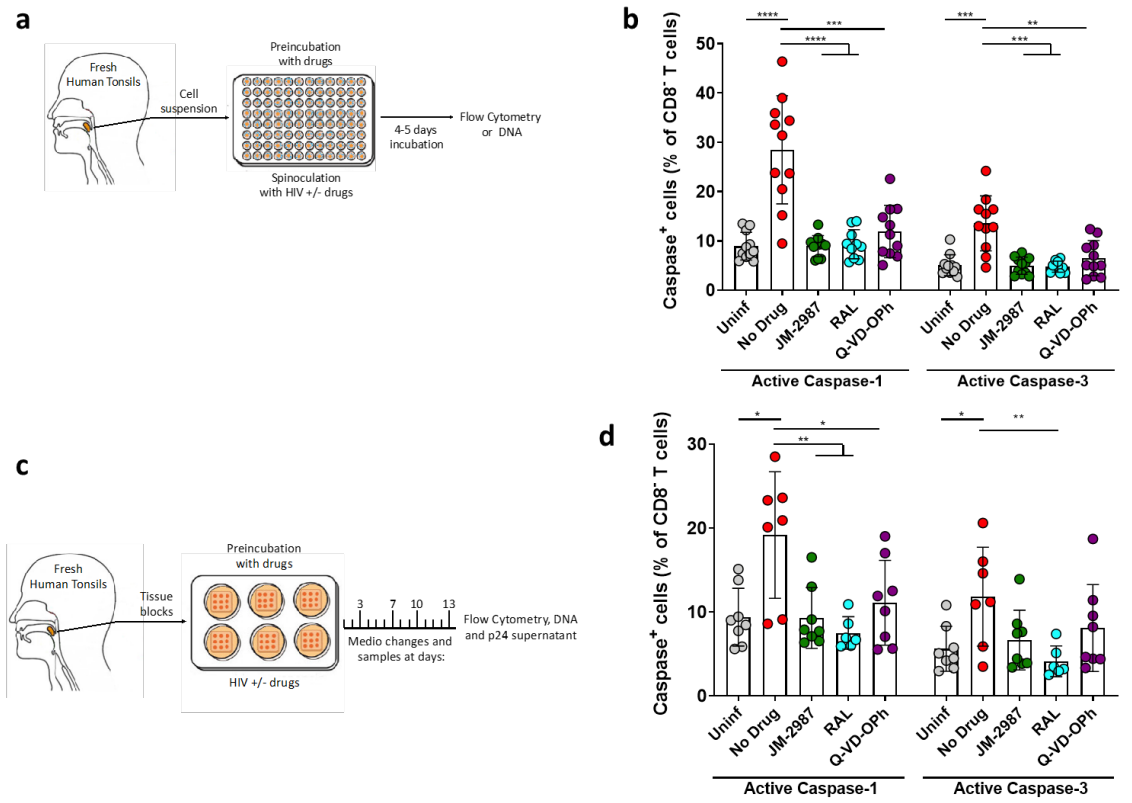

Figure 1. HIV infection induces active caspase-1 and active caspase-3 in HLACs and HLH. **a)** Schematic representation of the experimental procedure. Fresh human tonsils from healthy donors were collected, dissected, filtered, and plated as previously described. After overnight resting, HLACs were pre-incubated for 2 hours with the entry inhibitor JM-2987 (1µg/mL), the integrase inhibitor raltegravir (RAL, 1µg/mL), and the pan-caspase inhibitor Q-VD-OPh (40µM) and spinoculated without virus (uninfected) or with a X4 strain of HIV-1 (NL4-3). After 5 days of incubation with or without drugs, cells were collected and analyzed by flow cytometry. **b)** The percentage of $CD3^+CD8^-$ T cells expressing active caspase-1 and caspase-3 was measured in uninfected HLAC cultures (Uninf) and in HIV-infected cultures without drug, JM-2987, RAL or Q-VD-OPh (n=11 different donors). Caspase activity was determined using specific FLICA probes in $CD3^+CD8^-$ T cells to include productively infected cells (which presents down-regulation of CD4 expression). **c)** Schematic representation of the experimental setup used. Fresh human tonsils from healthy donors were dissected into small blocks (2-3 mm^2), and nine individual blocks were placed at the medium-air interface on collagen rafts in six-well plates as previously described (REF). HLHs were pre-incubated for 2 hours with medium (no drug), the entry inhibitor JM-2987 (1µg/mL), the integrase inhibitor raltegravir (RAL; 1µg/mL) and the pan-caspase Q-VD-OPh (35µM). After incubation, tissue was infected with a X4 strain of HIV-1 (NL4-3). Culture medium bathing the tissue blocks was changed every 3–4 days and analyzed for p24 production. After 13 days, cells were mechanically isolated, collected and analyzed by flow cytometry. **d)** Frequency of $CD3^+CD8^-$ T cells expressing active caspase-1 and caspase-3 in cells from HLH. Isolated cells from uninfected HLH, HIV-infected treated with no drug, JM-2987, RAL or Q-VD-OPh (n=7) were labeled with specific FLICA probes and analyzed by flow cytometry. Data represent mean values (bars) and ±SD (error bars). Differences were tested using Mann-Whitney U nonparametric test or by unpaired Student's t-test when comparing fold changes (*P < 0.05; **P < 0.01; ***P < 0.001; ****P < 0.0001).

Pan-caspase inhibitor Q-VD-OPh prevents HIV-induced $CD4^+$ T cell depletion and viral infection in tonsil cultures

Since Q-VD-OPh reduced apoptosis and pyroptosis, two mechanisms of cell death, we further evaluated whether caspase inhibition was able to prevent the HIV-induced $CD4^+$ T cell depletion observed after lymphoid tissue infection. A significant protection of $CD4^+$ HIV-induced depletion was observed with Q-VD-OPh treatment in both HLAC and HLH, thus suggesting that caspase inhibition could be able to prevent HIV-induced $CD4^+$ T cell depletion *in vivo* (**Fig. 2a and Fig. 2f in HLAC and HLH, respectively**).

The impact of Q-VD-OPh treatment on the levels of HIV replication was evaluated measuring the cell-associated p24 antigen by flow cytometry. After infection, a significant increase in p24 levels was observed in $CD8^-CD4^+$ and $CD8^-CD4^-$ T cells (productive infection) compared to the uninfected control, both in HLAC and HLH (**Fig. 2b and Fig. 2g, respectively**). In HLAC, the frequency of $CD4^+$ T cells $p24^+$ was poorly inhibited when treated with JM-2987 and the inhibition was non-significant with RAL (**Fig. 2b**). However, in HLHs where the viral input is lower, the replication is detected after a longer period of time and spinoculation is not used, a significant decrease in the intracellular p24 content was observed with the two antiretroviral drugs (**Fig. 2g**). This could be explained by the fact that spinoculation dramatically enhances HIV-1 viral adsorption to T cells[147, 148]. In contrast, among productively infected cells, T cells with a down-regulated CD4 expression, intracellular-associated p24 was almost completely inhibited by antiretroviral drugs in both HLAC and HLH (**Fig. 2b and Fig. 2g, respectively**). Surprisingly, Q-VD-OPh treatment significantly prevented HIV infection in total $CD4^+$ T cells in HLH, and in productively infected cells in both HLAC and HLH. Consistent with the decrease in cell-associated p24 levels, the presence of Q-VD-OPh led to a strong and significant decrease in total HIV DNA levels (**Fig. 2c and Fig. 2h, HLAC and HLH, respectively)** and integrated HIV DNA levels (**Fig. 2e in HLAC)** and with an even greater inhibition when no spinoculation was used (**Fig. 2c**). Total HIV DNA levels were also significantly reduced when a R5-tropic virus was used (**Fig. 2d**), suggesting that the ability of Q-VD-OPh to prevent HIV infection is envelope-independent.

Overall, these findings show that in lymphoid tissue, the inhibition of caspase activation by Q-VD-OPh was able to prevent not only HIV-induced $CD4^+$ T cell depletion but also HIV replication and decrease both total and integrated HIV DNA.

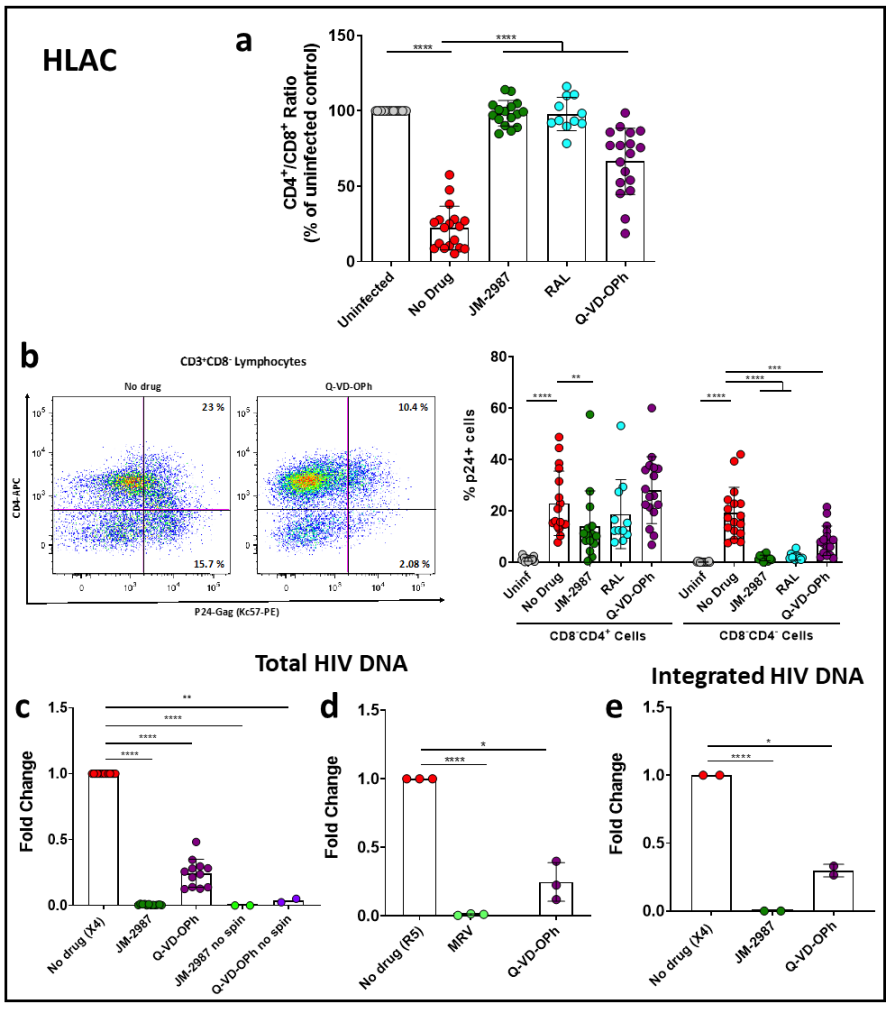
HLAC
a
CD4+/CD8+ Ratio (% of uninfected control)
Uninfected
No Drug
JM-2987
RAL
Q-VD-OPh
b
CD3+CD8- Lymphocytes
No drug
Q-VD-OPh
23 %
15.7 %
10.4 %
2.08 %
CD4-APC
P24-Gag (Kc57-PE)
% p24+ cells
CD8-CD4+ Cells
CD8-CD4- Cells
Total HIV DNA
Integrated HIV DNA
c
Fold Change
No drug (X4)
JM-2987
Q-VD-OPh
JM-2987 no spin
Q-VD-OPh no spin
d
No drug (R5)
MRV
Q-VD-OPh
e
No drug (X4)
JM-2987
Q-VD-OPh

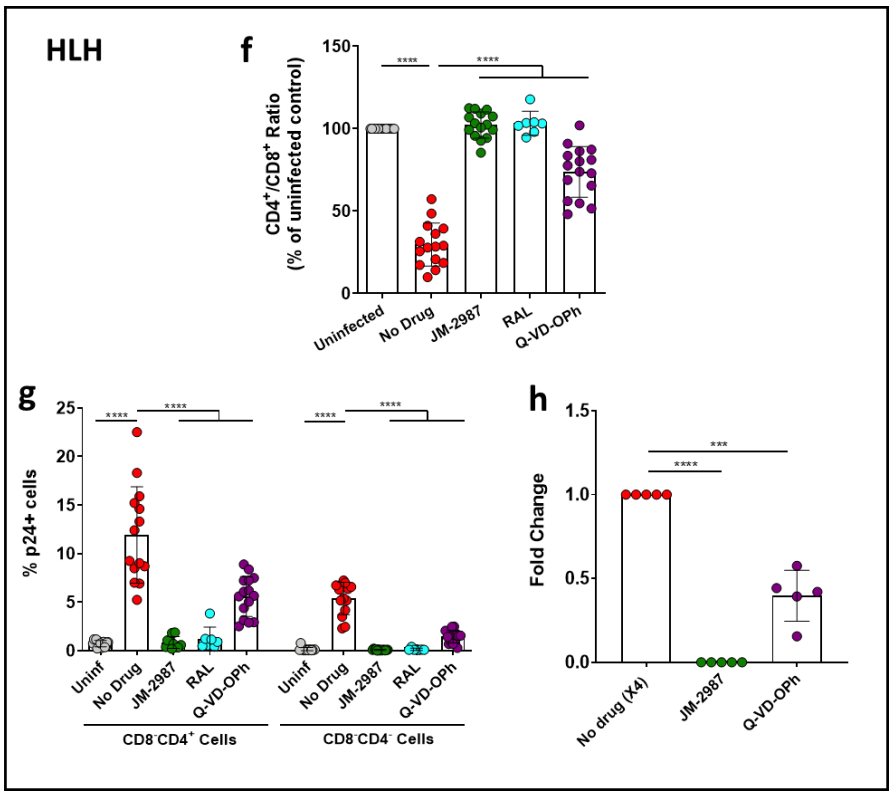
HLH
f
CD4+/CD8+ Ratio (% of uninfected control)
Uninfected
No Drug
JM-2987
RAL
Q-VD-OPh
g
% p24+ cells
Uninf
No Drug
JM-2987
RAL
Q-VD-OPh
CD8-CD4+ Cells
CD8-CD4- Cells
h
Fold Change
No drug (X4)
JM-2987
Q-VD-OPh

Figure 2. **Pan caspase inhibitor Q-VD-OPh inhibits HIV *ex vivo* infection in HLACs and HLH. HLAC:** HLACs were pre-incubated for 2 hours with JM-2987 (1µg/mL), RAL (1µg/mL) and Q-VD-OPh (40µM) and spinoculated with a X4 HIV-1 virus. After 3-5 days of incubation with or without drugs, cells were collected and analyzed by flow cytometry and quantitative real-time-PCR (qPCR). **a)** $CD4^+$ T cell depletion results are represented as ratios of $CD4^+/CD8^+$ T cells in infected cultures untreated or treated with different drugs compared to the uninfected control from the same donor (n=18). **b)** Frequency of intracellular HIV p24 levels in CD4-positive and CD4-negative T cells. A representative flow cytometry image shows CD4-positive infected T cells and CD4-negative infected T cells (productively infected cells) in cultures treated without drug or treated with Q-VD-OPh (upper panel). The percentage of $p24^+$ cells were plotted and compared among uninfected cultures, HIV-infected cultures treated without drug, JM-2987, RAL, or Q-VD-OPh (n=16) (lower panel). **c)** Changes in total HIV DNA levels after infection with a X4-tropic virus by spinoculation (n=16) or without spinoculation (n=2), and **d)** after infection with a R5-tropic virus by spinoculation (n=3). Total HIV DNA was quantified by qPCR. Fold changes were calculated in infected cultures treated with JM-2987 (X4-tropic), maraviroc (MRV; R5-tropic) and Q-VD-OPh compared to the untreated-infected culture. **e)** Changes in the amount of integrated proviral HIV DNA (quantified by an Alu-based nested qPCR). Fold changes calculated between non-treated HIV-infected cultures and HIV-infected cultures treated with JM-2987 or Q-VD-OPh (n=2). **HLH:** HLHs were pre-incubated for 2 hours without drug or with JM-2987 (1µg/mL), RAL (1µg/mL) and Q-VD-OPh (35µM). After incubation, tissue was infected with a X4 HIV-1 virus. After 13 days of infection, cells were mechanically isolated, collected and analyzed by flow cytometry and quantitative real-time-PCR (qPCR). **f)** $CD4^+$ T cell depletion was presented as ratios of CD4+/CD8+ T cells in each HIV-infected or uninfected culture. Results are expressed as a percentage relative to the uninfected control from the same donor (n=15; RAL n=7). **g)** Percentage of p24-positive cells in CD4-positive and CD4-negative T cells (productively infected cells). The percentage of $p24^+$ cells was compared among uninfected cultures, HIV-infected cultures treated with no drug, JM-2987, RAL or Q-VD-OPh (n=14). **h)** Fold change in total HIV DNA content measured by qPCR in cultures infected in the presence of no drug, JM-2987 and Q-VD-OPh (n=5). Results are presented as mean (bars) and ±SD (error bars). Differences were tested using Mann-Whitney U nonparametric test or by unpaired Student's t-test when comparing fold changes (*P < 0.05; **P < 0.01; ***P < 0.001; ****P < 0.0001).

Q-VD-OPh pre-incubation render cells less suitable to HIV infection

To further investigate the effects of Q-VD-OPh on HIV replication, HLACs were infected and viral replication was monitored by measuring the levels of p24 released in the culture supernatant after 7 days post-infection by ELISA. First, the efficacy of Q-VD-OPh was tested by pre-incubating cells with the drug at different times (24 hours, 2 hours, 30 minutes or with no pre-incubation) before infection. In addition, the durability of the anti-HIV effects after drug washout was also evaluated (**Fig. 3a**). There were no significant changes between the different pre-incubation times if the drug was present during the 7 days of infection, and an almost total inhibition of p24 production in all conditions was observed. When Q-VD-OPh was washout after 3 days post-infection, the viral replication was also significantly inhibited regardless the preincubation time. The inhibitory effect of Q-VD-OPh was diminished but still significant if a pre-incubation step before infection was not realized. Finally, if the drug was removed at the time of infection, there was still a significant decrease in p24 levels in cultures pre-incubated with Q-VD-OPh for 24

hours; with only a partial and non-significant inhibition when the preincubation time was shorter (i.e., 2 hours or 30 minutes) (**Fig. 3a**). JM-2987, added as a control, inhibited completely the p24 release. To better understand the effect of Q-VD-OPh on HIV-1 infection under highly permissive conditions, we examined the role of this drug in activated peripheral blood mononuclear cells (PBMCs). A similar pre-incubation time-dependent and wash out effect on HIV viral replication was noticed, although the inhibitory potency was lower (**Fig. 3b**).

These observations suggest that Q-VD-OPh acts on the cell rather than affecting the virus itself, since pre-incubating cells with the drug is enough to condition the cell to become less susceptible to be infected or to impair viral production.

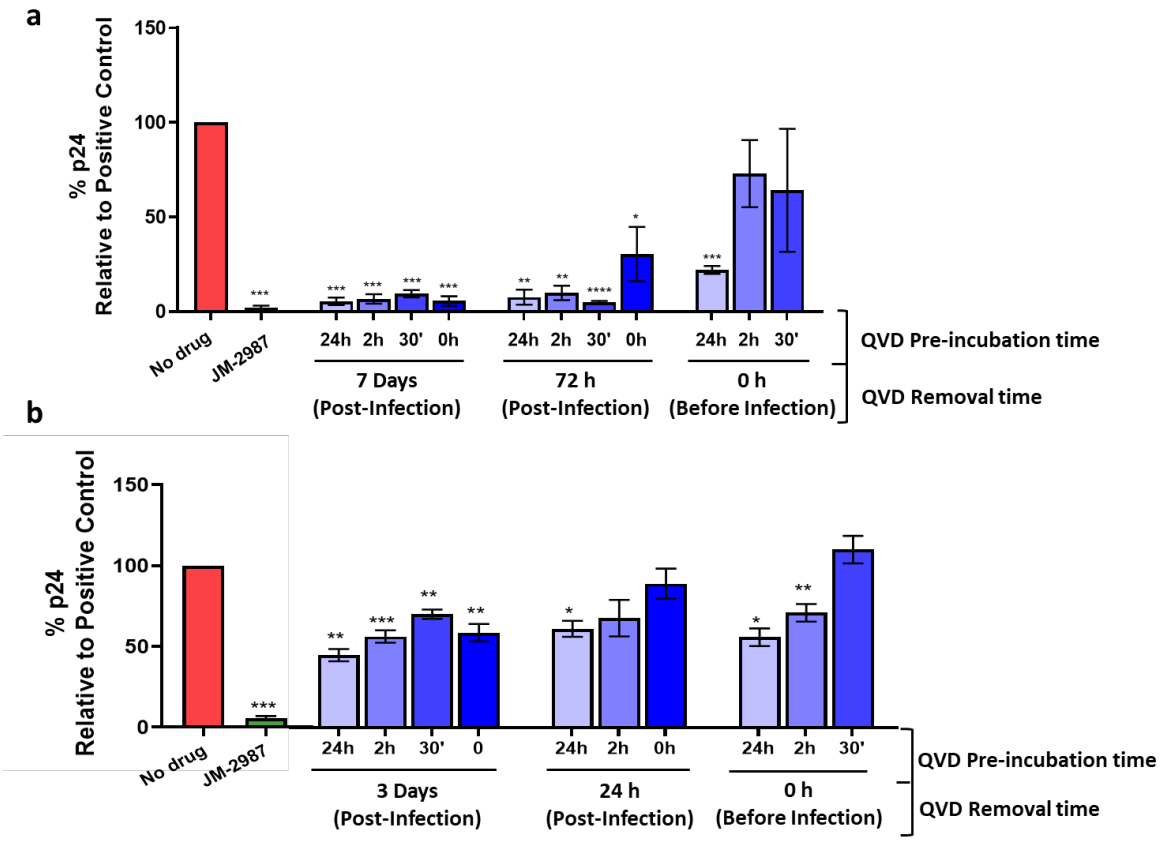

Figure 3. Effect of the pan-caspase inhibitor Q-VD-OPh in p24 production in HLACs and activated PBMCs. Effect of pre-incubation and wash out at different time points. **a)** HLACs were pre-incubated with JM-2987 (1µg/mL) and Q-VD-OPh (40µM) at the indicated time points up to 24 hours. Then, Q-VD-OPh was wash out just before infection or at day 3 post-infection, and fresh medium was added. Supernatants were collected after 7 days of infection, and the p24 antigen concentration was measured by ELISA. Values are represented as percentages relative to the infected control with no drug. Shown are mean values ±SEM (n=3). **b)** Activated peripheral blood mononuclear cells (PBMCs) were pre-incubated with Q-VD-OPh at the indicated time-points up to 24 hours, the drug was removed just before infection or the day after HIV infection, and fresh medium was added. Supernatants were collected after 3 days, and p24 antigen concentration was measured by ELISA. Values are represented as percentages relative to those of the infected control with no drug. Shown are mean values ±SEM (n=3). Differences were tested using a t-test (*P < 0.05; **P < 0.01; ***P < 0.001; ****P < 0.0001).

Q-VD-OPh maintains a durable effect against HIV replication in tissue culture even after infection is established

Next, we aimed to determine Q-VD-OPh treatment efficacy after infection is established. In HLH, HIV infection in the absence of drug revealed the typical kinetics previously described[25, 149]. Viral replication, measured as p24 released into the supernatant, was detectable at day 7 post-infection and continued to increase until day 13. JM-2987 and Q-VD-OPh added just before infection (Day 0) strongly inhibited viral replication (**Fig. 4a and Fig. 4b**). In histocultures the potent inhibition elicited by JM-2987 and Q-VD-OPh persisted even though drugs were added 4 days after infection. The inhibitory potency declined when drugs were added 6 days after infection. No statistical significance was detected at this time point compared to the untreated controls (**Fig. 4a and Fig. 4b**). Similar results were observed for CD4+ T cell depletion levels, where a significant reduction of T cell depletion is observed when JM-2987 and Q-VD-OPh were added just before infection, keeping the significant levels for JM-2987 when added 4 days after infection (**Fig. 4c**). Protection is also observed when cells are treated with Q-VD-OPh 4 days post-infection, however, it did not reach significance possibly due to the low number of donors tested. However, no significant protection was observed when neither JM-2987 nor Q-VD-OP-h were added 6 days post-infection, but a rise is observed compared to the untreated control (**Fig. 4c**).

Overall, these findings demonstrate that the inhibitory effect elicited by Q-VD-OPh is robust, even if the drug is washed out from the culture or added after the infection is established.

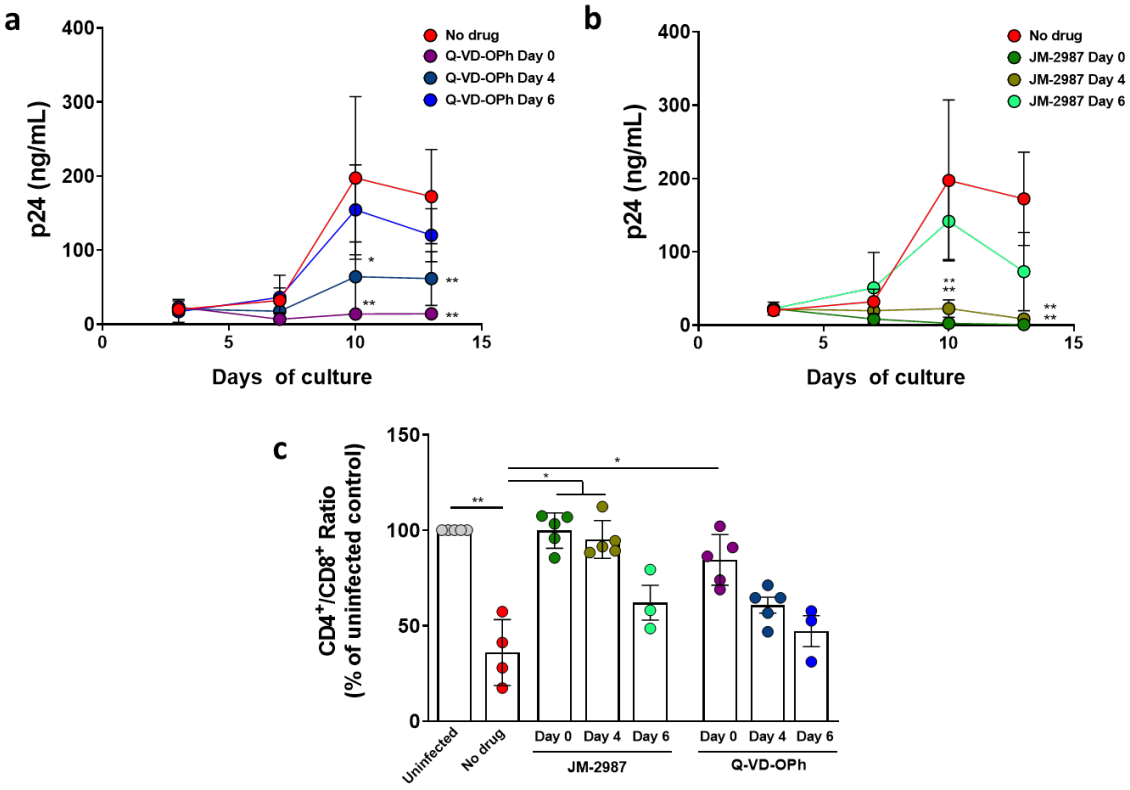

Figure 4. Effect of the pan-caspase inhibitor Q-VD-OPh added at different times post-infection in HLH. Efficacy of delayed treatment with Q-VD-OPh. Kinetic analysis of HIV-1 replication in HLH. Histocultures were infected with NL-43 and **a)** Q-VD-OPh or **b)** JM-2987 were added at different time points: at the same time of infection, or 4 and 6 days after infection, and kept in culture for 13 days. Culture medium was sampled at the indicated times, and p24 released was measured by ELISA. Results are presented as mean values and ±SD (error bars) (n=5). **c)** CD4 T cell depletion was measured by $CD4^+/CD8^+$ ratio at day 13 post-infection and analyzed by flow cytometry. Results are expressed over the infected control untreated, and presented as mean values and ±SD (error bars) (n=3 to 5 donors). Differences were tested using Mann-Whitney U nonparametric test (*P < 0.05; **P < 0.01).

Caspase-dependent, envelope glycoprotein-independent effect of Q-VD-OPh in a single-cycle infectivity assay

We further sought to test whether Q-VD-OPh had a different effect using a single-cycle assay, than the one observed in a spreading infection using a replicative-competent virus. Thus, HLACs were infected with a single-cycle HIV-1 NL4-3 luciferase reporter pseudotyped virus with the heterologous Env vesicular stomatitis glycoprotein (VSV)-G (**Fig. 5a**). The presence of the reverse transcription inhibitor AZT and Q-VD-OPh resulted in a significant decrease in the luciferase production, while the treatment with Q-VE-OPh (a cognate negative control to Q-VD-OPh)[150] showed no significant effect. This indicated that the inhibition observed by the pan-caspase

inhibitor Q-VD-OPh is independent of the HIV-1 envelope protein and requires caspase activity, since Q-VE-OPh is unable to inhibit caspases or viral replication (**Fig. 5a**).

In activated PBMCs, which are more susceptible to infection, Q-VD-OPh significantly inhibited luciferase activity in cultures infected with single-cycle VSV, X4-tropic and R5-tropic pseudoviruses (**Fig. 5b**). AZT, JM-2987 and TAK-779, used as positive controls, inhibited VSV, X4- and R5-pseudoviruses respectively. Neither TAK-779 reduce the luciferase activity after the exposure of a X4-tropic pseudovirus, nor JM-2987 the activity of a R5-tropic pseudovirus (**Fig. 5b**).

In summary, these experiments showed that the ability of Q-VD-OPh to block viral infection, in a single-round infectivity assay, on both tonsils and activated PBMCs, is caspase-dependent and envelope-independent.

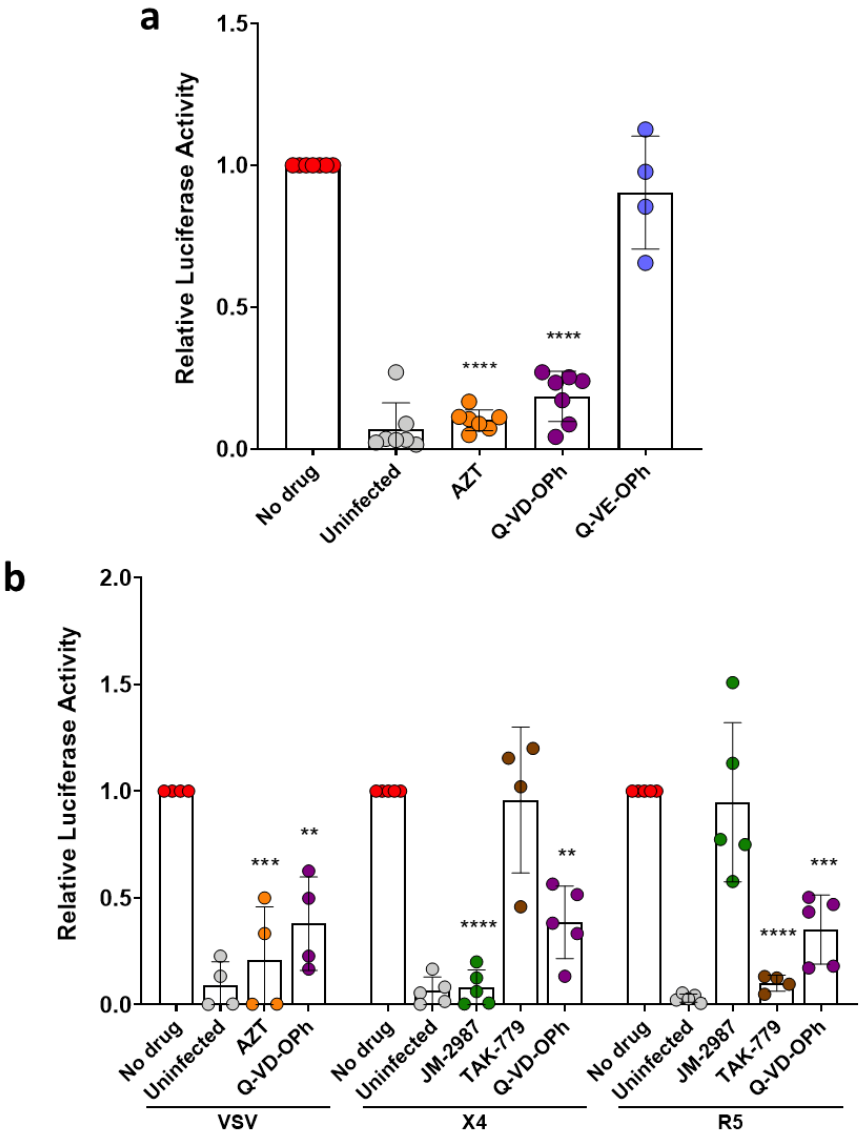

Figure 5. Q-VD-OPh blocks HIV infection in a single-round infection assay. a) HLAC were pre-incubated for 2 hours in the presence of no drug (n=7), AZT (n=7), Q-VD-OPh (n=7) and Q-VE-OPh (40μM; n=4). After incubation, cells were infected by spinoculation with a (VSV-G)-NL4-3luc.R-E- pseudovirus, and luciferase activity was measured 72 hours post-infection. **b)** Activated PBMCs were pre-incubated for 24 hours in the presence of no drug, AZT and Q-VD-OPh, infected with (VSV)-G (n=4), HIV-1 X4-envelope (n=5) or HIV-1 R5-envelope (n=5) NL4-3luc.R-E- pseudoviruses, and luciferase activity was measured 48 hours post-infection. JM-2987 was used as a control in cells infected with the X4-tropic pseudovirus and the entry inhibitor TAK-779 was used as a control in cells infected with the R5-tropic pseudovirus. Relative luciferase activity was calculated as a ratio of luciferase activity in cells infected without drug over infected cells with different drugs. The results are presented as the relative mean (bars) and ±SEM (error bars). Differences were tested by unpaired Student's t-test (**P < 0.01; ***P < 0.001; ****P < 0.0001).

Changes in the cellular activation profile by Q-VD-OPh

To unravel the mechanism of action of Q-VD-OPh, we first tested whether it was affecting the phenotype of the cell, since our results indicated that it was acting on the host cell rather than on the virus. Many retroviruses efficiently replicate only in activated cells and in HIV it is well established that the activation status of $CD4^+$ cells determine the susceptibility to the infection [151, 152]. In fact, it has been reported that in cultured human lymphoid tissue, viral infection is supported predominantly by activated T cells expressing either CD25 or HLA-DR or both, but not other activation markers [153]. In HLAC, Q-VD-OPh treatment resulted in a statistically significant decrease in the expression of CCR5, CD25 and Ki67 in $CD4^+$ and $CD8^+$ T cells (although the decrease of CD25 was not significant in $CD8^+$ T cells) in comparison with HLACs cultured only in medium (**Fig. 6a**). *However, significant changes were not observed in the expression of other T cell activation markers such as CD38, HLA-DR or CD69, nor in markers associated with cell maturation or CD4 or CD8 expression (***Fig. 6b***). These results provided evidence that Q-VD-OPh induces changes in the pattern of cellular activation. These changes could render $CD4^+$ T cells less permissive to productive HIV-1 infection.*

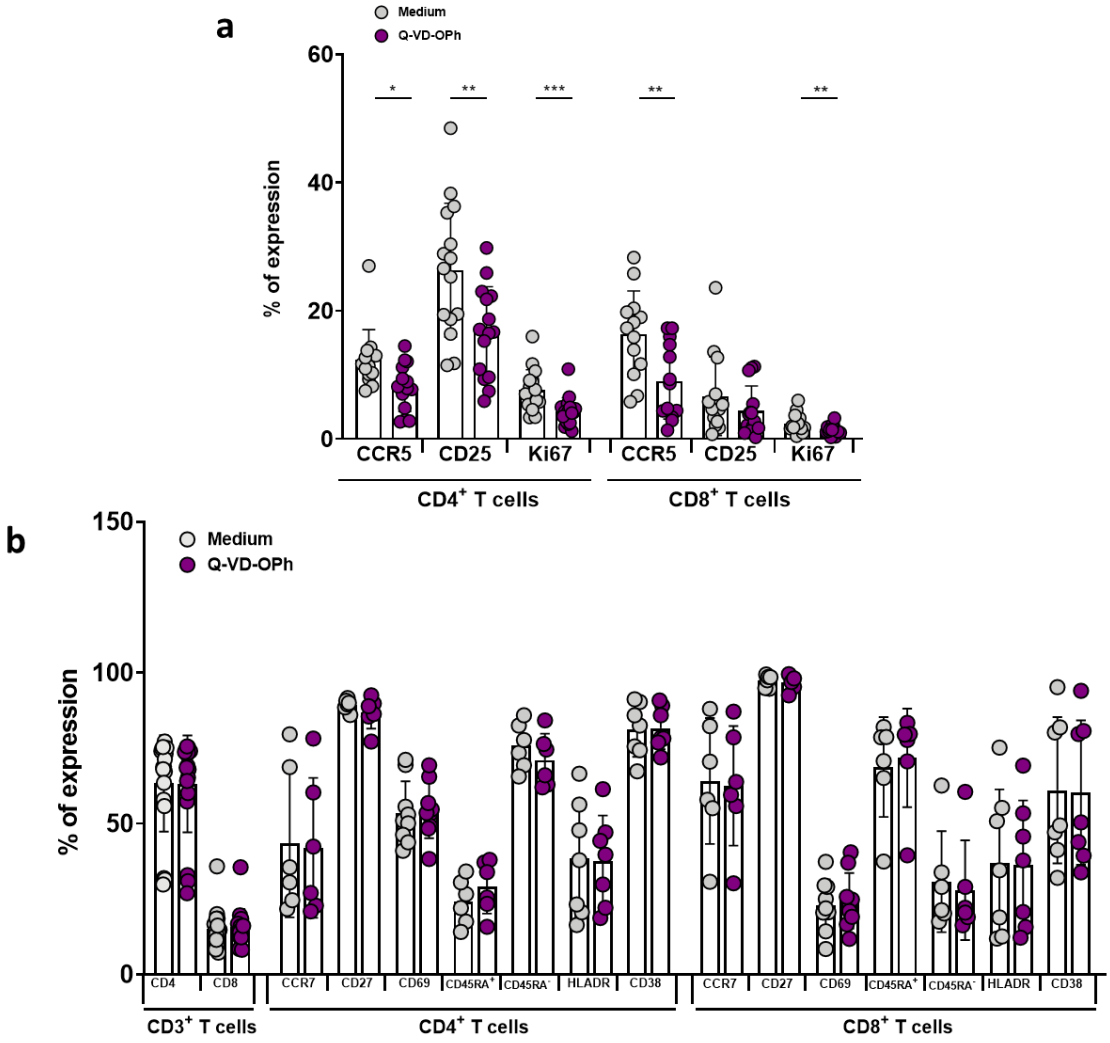

Figure 6. Q-VD-OPh decreases the expression of T cell markers correlated with activation in tonsil cells. HLACs were cultured for 3 days in the presence or absence of Q-VD-OPh. **a)** The surface expression of CCR5 and CD25, and the intracellular expression of Ki67 in T cells (n=15 and n=13, in $CD4^+$ and $CD8^+$ respectively) was evaluated by flow cytometry. **b)** Immunophenotypic characterization of $CD4^+$ and $CD8^+$ T cells was carried out by flow cytometry (n=6 or 12 donors). The results are presented as the mean value (bars) and ±SD (error bars). Differences were tested using Mann-Whitney U nonparametric test (*P < 0.05; **P < 0.01; ***P < 0.001).

Caspase inhibition by *Q-VD-OPh* induces cell cycle arrest

Caspase inhibitors have been reported to inhibit cell line proliferation[154], therefore we next tested whether Q-VD-OPh would reduce the basal or PHA-induced proliferation of lymphoid cells using a CFSE proliferation assay. In non-stimulated tonsil cells, no proliferation was observed in the presence or absence of Q-VD-OPh (**Fig. 7a**). Cell incubation with PHA resulted in a continuous increase in the proliferation along time (measured as increase in the percentage

of $CFSE^{low}$ cells). No changes were observed when PHA-stimulated cells were cultured in the presence of Q-VD-OPh.

Besides proliferation, caspases have also been reported to be involved in cell cycle progression[155], thus, the effect of their inhibition by Q-VD-OPh was analyzed by dual DNA/RNA co-staining (7AAD/Pyronin Y, respectively) in our model. No changes in cell cycle were observed after Q-VD-OPh treatment in unstimulated cells, where the vast majority of cells were in G_0/G_1 phases (**Fig. 7b**). After stimulation with PHA, the proportion of cells in G_0/G_1 phase significantly decreased at the expense of an increase in cells entering S and G_2/M phases, which is consistent with an increase in PHA-driven cell proliferation (**Fig. 7b**). A similar pattern was observed when caspases were inhibited with Q-VD-OPh. However, the pan-caspase inhibitor significantly increased the proportion of cells into both the S and G_2/M phases of the cell cycle and decreased in cells in G_0/G_1.

Taken together, the increase in the proportion of cells in $S/G_2/M$ phases and the lack of effect on proliferation suggest that Q-VD-OPh induces cell cycle arrest.

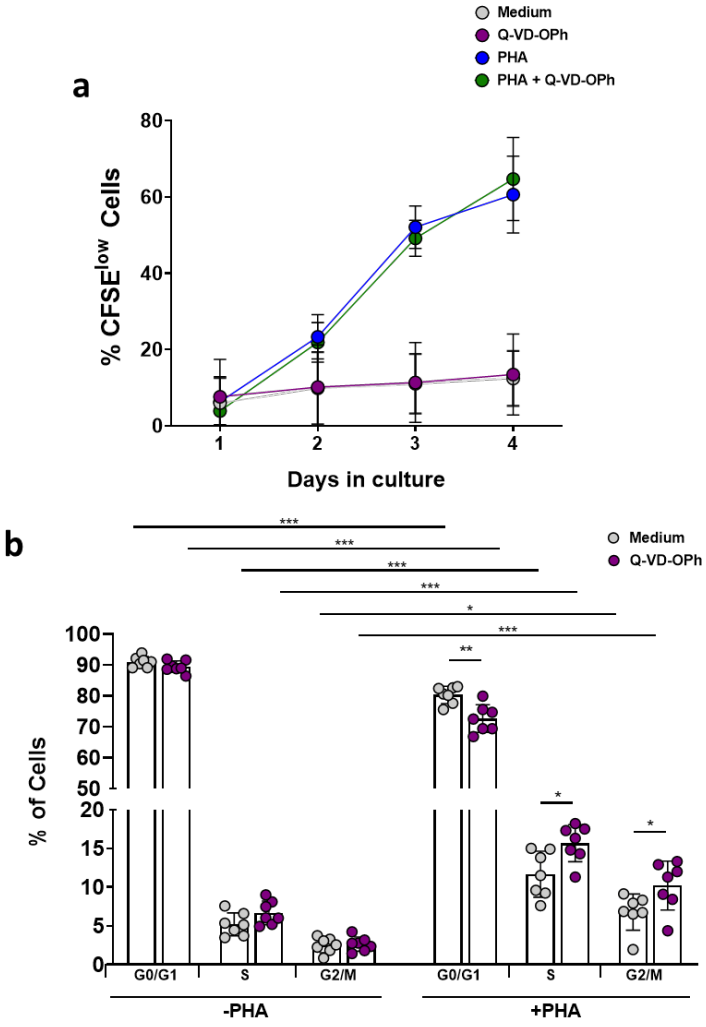

Figure 7. Proliferation and cell cycle in tonsil cells after caspase inhibition. a) CFSE proliferation assay. Tonsil cells (n=4) were labeled with CFSE and cultured in the absence or presence of PHA and in the absence or presence of Q-VD-OPH. The proliferative capacity was analyzed by flow cytometry at days 1, 2, 3 and 4. Proliferation is reported as the percentage of $CFSE^{low}$ lymphocytes**. b)** Cell cycle analysis. Tonsil cells (n=7) were incubated for 3 days in the absence or presence of PHA and in the absence or presence of Q-VD-OPH, and the cell cycle was evaluated by DNA (7-AAD) and RNA (Pyronin Y) staining by flow cytometry. The histogram shows the percentage of cells in each phase, in cultures with or without PHA stimulation and in the presence or absence of *Q-VD-OPh*. Results are presented as mean values (bars) and ±SD (error bars). Differences were tested using a Mann-Whitney U nonparametric test (*P < 0.05; **P < 0.01; ***P < 0.001).

Modulation of type I IFN pathway by Q-VD-Oph

Caspases control innate immunity by modulating the type-I IFN response[156]. Therefore, we aimed to determine whether Q-VD-OPh was affecting the type-I IFN pathway. The addition of the pan-caspase inhibitor led to an increase in IFNβ expression in tonsil cells (**Fig. 8a**). This increase was already observed after 3 hours of incubation, becoming significant after 24 and 72 hours of incubation. In addition to IFNβ, the expression of IFNα was also up-regulated, although the difference was not statistically significant (**Fig. 8b**). The expression of several IFN-stimulated genes (ISG) was also increased in a time-dependent manner even though significant differences were only observed in ISG15 (**Fig. 8b**). The low number of different donors used (between 2 and 6), could explain the lack of significance in some of these genes. To further elucidate the phenotype of the cells that are upregulating the IFN response, we first corroborated the presence of active caspase-3 and their down-regulation by Q-VD-OPh in different subpopulations of cells. Flow cytometry analysis showed that caspase-3 activity was present in both $CD3^-$ and $CD3^+$ cells, and within the $CD3^+$ lineage, present in both $CD4^+$ and $CD8^+$ subpopulations. Q-VD-OPh incubation resulted in a significant decrease in caspase-3 activity in all subpopulations (**Fig. 8c**). After cell sorting, we observed that caspase inhibition resulted in a similar gene expression increase of IFNβ in both isolated $CD3^-$ and $CD3^+$ (**Fig. 8d**), suggesting that this inhibitor is able to modulate type-I IFN pathway in both T cells and non-T cells.

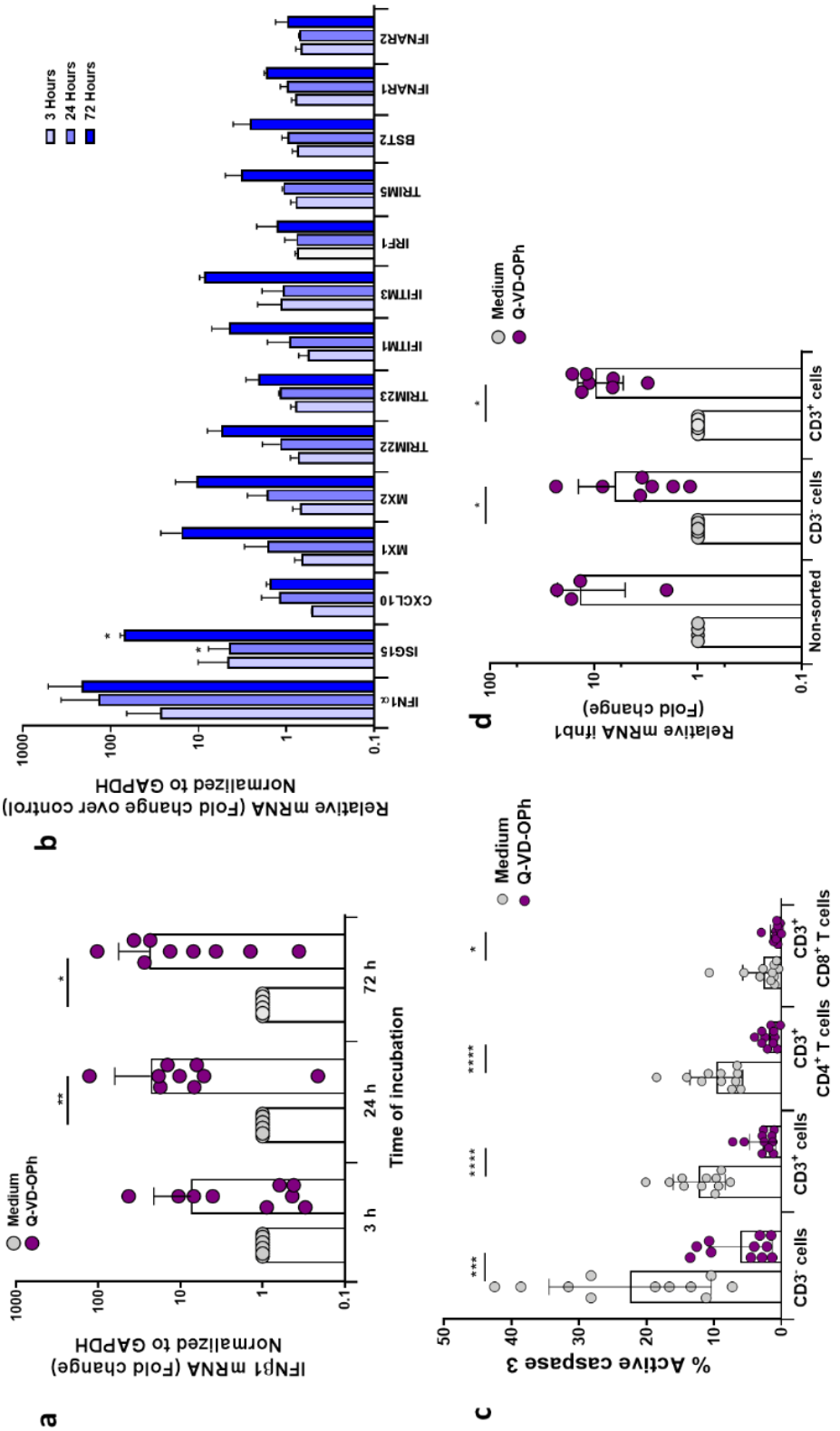
a
IFNβ1 mRNA (Fold change)
Normalized to GAPDH
Medium
Q-VD-OPh
3 h
24 h
72 h
Time of incubation
b
Relative mRNA (Fold change over control)
Normalized to GAPDH
3 Hours
24 Hours
72 Hours
IFNα
ISG15
CXCL10
MX1
MX2
TRIM22
TRIM23
IFITM1
IFITM3
IRF-1
TRIM5
BST2
IFNAR1
IFNAR2
c
% Active caspase 3
CD3- cells
CD3+ cells
CD4+ T cells
CD3+
CD8+ T cells
CD3+
d
Relative mRNA ifnb1
(Fold change)
Non-sorted
CD3- cells
CD3+ cells

Figure 8. Caspase inhibition induce upregulation of the type-I interferon pathway. HLACs were incubated with or without Q-VD-OPh and after 3, 24 or 72 hours RNA was extracted and mRNA levels of **a)** IFNβ and **b)** IFNα, ISG15, CXCL10, MX1, MX2, TRIM22, TRIM23, IFITM1, IFITM3, IRF1, TRIMS5, BST2, IFNAR1 and IFNAR2 were measured by quantitative RT-PCR. Data are normalized to the expression of the house-keeping gene GAPDH. **c)** The expression of active caspase-3 was evaluated by flow cytometry in $CD3^+$, $CD3^-$, $CD4^+$ and $CD8^+$ T cells from tonsils incubated for 24 hours in the presence or absence of Q-VD-OPh. The active caspase-3 was detected using an antibody specific for the active (cleaved) form. **d)** Tonsil cells were incubated in the presence or absence of Q-VD-OPh, and after 24 hours, $CD3^+$ and $CD3^-$ populations were sorted, RNA was extracted and mRNA levels of IFNβ were measured by quantitative RT-PCR. Data are normalized to the expression of the house-keeping gene GAPDH. The results are presented as the relative mean (bars) and ±SEM (error bars). Differences were tested using Wilcoxon test (*P < 0.05; **P < 0.01; ***P < 0.001; ****P < 0.0001).

Q-VD-OPh induces dose- and time-dependent sublethal mitochondrial depolarization

A link has previously been established between caspases and the induction of type-I interferons by mitochondrial damage[157]. In the absence of active caspases, mitochondrial permeabilization resulted in the expression of type-I interferons. Therefore, we aimed to evaluate the mitochondrial activity in cells treated with different doses of Q-VD-OPh. To assess mitochondrial activity, we measured the mitochondrial membrane potential changes in HLACs treated for 3 days with different concentrations of Q-VD-OPh by flow cytometry using the fluorescent dye JC-10. We observed that the addition of Q-VD-OPh increased the proportion of cells with depolarized mitochondria along with a decrease in the proportion of cells with polarized mitochondria in a dose-dependent manner (**Fig. 9a and Fig. 9b**). In addition, its effect also increased over time in both $CD4^+$ and $CD8^+$ T cells, with a significant depolarization peak after 72 hours of drug exposure (**Fig. 9c**). The increase in the percentage of cells with depolarized mitochondria was not correlated with an increase in cell death, since no loss in the total number of lymphocytes was observed. Conversely, as a consequence of its antiapoptotic effect, the presence of Q-VD-OPh was associated with a significant increase in the number of total lymphocytes **(Fig. 9d**). Finally, we observed that cells treated with Q-VE-OPh presented the same number of depolarized mitochondria than cells cultured with medium, suggesting that the depolarization of mitochondria was dependent on caspase inhibition (**Fig. 9e**).

Taken together, these results indicated that Q-VD-OPh is able to induce a sublethal decrease in mitochondrial membrane potential and that this effect is dependent upon its ability to inhibit caspases.

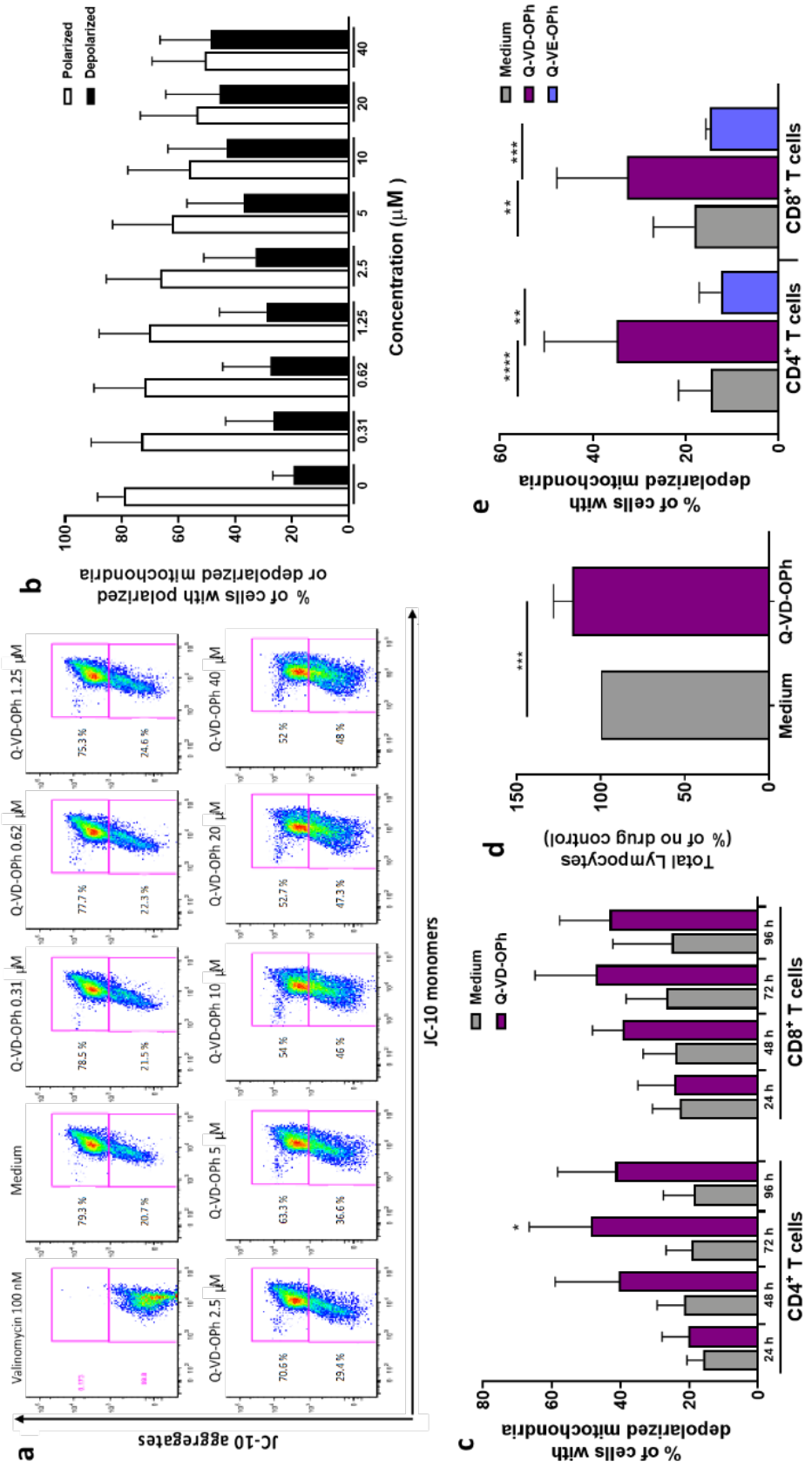
a
JC-10 aggregates
JC-10 monomers
Valinomycin 100 nM
Medium
Q-VD-OPh 0.31 µM
Q-VD-OPh 0.62 µM
Q-VD-OPh 1.25 µM
Q-VD-OPh 2.5 µM
Q-VD-OPh 5 µM
Q-VD-OPh 10 µM
Q-VD-OPh 20 µM
Q-VD-OPh 40 µM
79.3 %
20.7 %
78.5 %
21.5 %
77.7 %
22.3 %
75.3 %
24.6 %
70.6 %
29.4 %
63.3 %
36.6 %
54 %
46 %
52.7 %
47.3 %
52 %
48 %
b
% of cells with polarized or depolarized mitochondria
Polarized
Depolarized
Concentration (µM)
0
0.31
0.62
1.25
2.5
5
10
20
40
c
% of cells with depolarized mitochondria
Medium
Q-VD-OPh
CD4+ T cells
CD8+ T cells
24 h
48 h
72 h
96 h
d
Total Lymphocytes (% of no drug control)
Medium
Q-VD-OPh
e
% of cells with depolarized mitochondria
Medium
Q-VD-OPh
Q-VE-OPh
CD4+ T cells
CD8+ T cells

Figure 9. Changes in mitochondrial membrane potential induced by Q-VD-OPh. HLAC were cultured in the presence of Q-VD-OPh and stained with JC-10 dye and anti-CD3 and -CD4 antibodies. Changes in the mitochondrial potential were analyzed by flow cytometry. **a)** Gating strategy for the analysis of JC-10 staining in HLACs treated with increasing concentrations of Q-VD-OPh for 3 days. Lymphocytes were gated according to morphological parameters and JC-10 aggregates and monomers were analyzed in total $CD3^+$ T cells. Decrease in mitochondrial membrane potential was identified according to gates defined in valinomycin treated cells (observed as a decrease in JC-10 aggregate form and an increase in JC-10 monomeric form). **b)** Percentages of polarized or depolarized mitochondria with increasing concentrations of Q-VD-OPh after 3 days of culture. Means ±SD are presented for 4 donors. **c)** Time-dependent effect on mitochondria depolarization after Q-VD-OPh treatment in $CD4^+$ and $CD8^+$ T cells (n=4). Means ±SD are shown. **d)** Measurements of the effect of Q-VD-OPh (40µM) on lymphocytes viability. Total number of lymphocytes after 3 days of treatment were determined by flow cytometry. Viable lymphocytes were determined by forward and side scatter properties and the total number was quantified using beads. Percentages were obtained relative to the control without drug. Data represents means ±SD for 7 different donors **e)** Percentages of depolarization among $CD4^+$ and $CD8^+$ T cells in the presence or absence of Q-VD-OPh (n=12), or in the presence of the Q-VE-OPh control (n=4). The results are presented as means ±SD. Differences were tested using a Mann-Whitney U nonparametric test (**P < 0.01; ***P < 0.001; ****P <0.0001).

Type I IFN neutralization reverts caspase HIV inhibition and restores viral replication

To clarify the effect of type-I IFN on the HIV replication induced by Q-VD-OPh, we further investigated the blocking effect of B18R, a soluble recombinant receptor that has been shown to exhibit neutralizing activity to type-I interferon family members. As previously shown, Q-VD-OPh treatment before pseudovirus infection resulted in a significant decrease in luciferase production (**Fig. 10a and Fig. 10b**). This decrease was overcome when type-I IFN pathway was inhibited with BR18 (**Fig. 10a**). We also blocked the IFN pathway using a type-I IFN neutralizing antibody mixture directed against human type-I IFNs and type-I receptor subunit 2. The presence of these blocking antibodies in cultures also treated with Q-VD-OPh restored HIV infection to control levels, whereas blocking antibodies alone had no effect on the infection (**Fig. 10b**). Finally, the presence of type-I blocking antibodies in cells incubated with Q-VD-OPh was not able to inhibit the increased levels of IFNβ gene expression induced by Q-VD-OPh. However, a strong downregulation was observed in the expression of two IFN-stimulated genes, ISG15 and MX1, in cells co-treated with Q-VD-OPh and the mixture of antibodies (**Fig. 10c**). These results support the idea that Q-VD-OPh is inducing type-I IFN production.

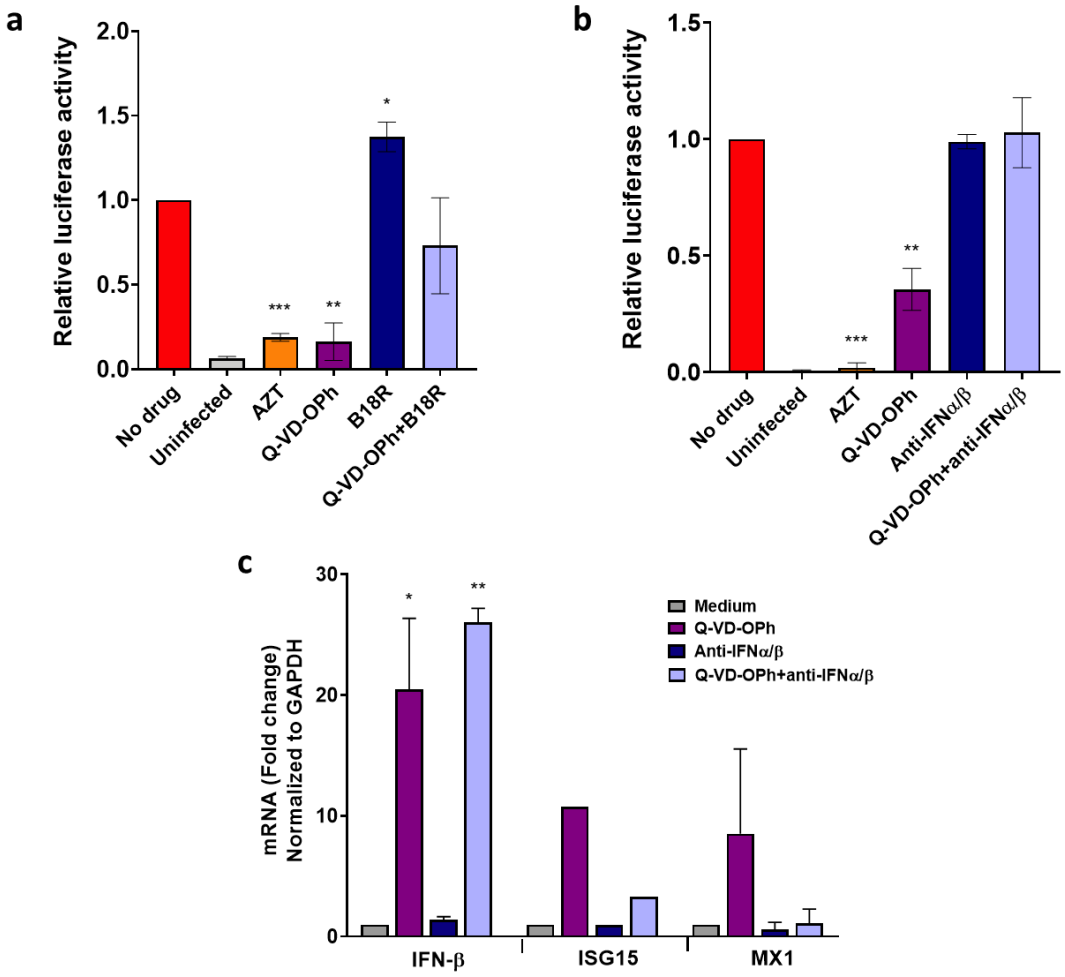

Figure 10. Type-I IFN neutralization reverts effects on HIV replication and type-I IFN pathway induced by Q-VD-OPh. HLACs were pre-incubated for 2 hours in the presence of no drug, AZT, Q-VD-OPh and **a)** the type-I interferon blocking receptor B18R alone or in combination with Q-VD-OPh or **b)** the mixture of type-I IFN neutralizing antibodies alone or in combination with Q-VD-OPh. After incubation, cells were infected by spinoculation with a (VSV-G)-NL4-3luc.R-E- pseudovirus and luciferase activity was measured 72 hours post-infection. Relative luciferase activity was calculated as a ratio of luciferase activity in infected cells without drug over infected cells treated with different drugs. **c)** HLACs were incubated with medium, Q-VD-OPh, type-I IFN neutralizing antibodies and the mixture Q-VD-OPh + anti-IFN antibodies for 3 days. RNA was extracted and mRNA levels of IFNβ and *IFN-stimulated genes (ISGs) ISG15 and MX1 were measured by qRT-PCR. Data are normalized to the expression of the house-keeping gene GAPDH.* Results are presented as means ±SD of two different donors, except the gene expression of ISG15 that is from one single donor. Differences were tested by an unpaired Student's t-test (*P < 0.05; **P < 0.01; ***P < 0.001).

DISCUSSION

HIV infection is characterized by high activation and inflammation levels, followed by a massive CD4+ T cell depletion, resulting in AIDS. Fortunately, ART treatment has increased life expectancy of HIV-infected patients and improved their quality of life by suppressing HIV-1 replication. However, ART's efficiency on controlling HIV is not the same to everyone, and side effects due to toxicity are still a problem to solve for many infected patients. Besides, one of the main challenges in the fight against HIV infection is the presence of integrated proviral DNA in latently infected reservoir cells[158]. Moreover, the emergence of resistant viruses to some commonly used antiretrovirals urge to find alternative treatments to fight HIV. This situation prompted us to investigate alternative therapeutic strategies directed to modulate host cell pathways to block HIV infection.

Accumulating evidence suggests that autophagy plays a role in both HIV-1 replication and disease progression[52, 59, 159]. However, the cross talk between the virus and autophagy has been demonstrated using immortalized cell lines or exogenously-activated primary cells. Nevertheless, none of these systems are completely representative of what is happening *in vivo* in infected individuals. Lymphoid organs are the primary sites of HIV replication and transmission, and are where the critical events of HIV disease progression occur[160, 161]. HLACs preserve the biology of human lymphoid tissue. In particular, cellular activation and proliferation, cell diversity, and HIV-1 infection, replication, and depletion within HLACs are nearly indistinguishable from what is observed *in vivo*, even in the absence of exogenous activation. In this study, HLACs displayed a fully functional autophagic activity; basal autophagy, induced response and autophagic flux were clearly observed. This model is unique since it permits concurrent analysis of multiple HIV-1 cellular targets. Thus, HLACs provide a suitable model to obtain further insights into HIV and its intricate relationship with autophagy, and hence to unlock the full therapeutic potential of autophagy modulators.

The effect of HIV on autophagy remains controversial. In HLACs, a significant induction of autophagy was shown 24 hours and 4 days after infection. HLACs are composed of a heterogeneous cell population, so the observed induction is the global effect exerted by the virus in different cell types, as well as in productively infected and uninfected bystander cells. In lymphoid tissue, a massive bystander cell depletion has been reported[20, 103]. Therefore, it could be suggested that the observed autophagy could derive from an Env-mediated autophagy induction in uninfected $CD4^+$ T cells, as previously published[55, 56]. These reports have also shown autophagy inhibition in productively infected $CD4^+$ T cells. In HLACs, we cannot rule out that there is induction in productively infected cells. In fact, the autophagic response could be different from the one observed in other *in vitro* infections, in which after PHA activation higher

levels of infection are reached. In addition, it is worth to mention that the use of PHA itself already modulates autophagy[162], which can complicate the interpretation of the effect of HIV in these *in vitro* systems. Importantly, our results are in agreement with *in vivo* data, where autophagy was up-regulated in axillary lymph nodes of HIV-1 infected individuals, compared to uninfected samples [60].

On the other hand, the effects that HIV infection exerts on the functionality of the autophagic pathway is barely known. In HLACs, we observed that both the autophagic response and the autophagic flux were preserved after infection. In contrast to our results, it has been previously reported that in macrophages from HIV-1 infected individuals the autophagic response to rapamycin and the autophagic killing of *Toxoplasma gondii* was impaired[57]. Regarding PBMCs, the autophagic effect could be associated with disease progression, since we have previously reported that in HIV-1 infected individuals a lower induced response and a lower autophagic flux was found compared to uninfected controls. Interestingly, the highest autophagy impairment was observed in individuals who failed to recover their $CD4^+$ T cells after ART treatment[61]. Furthermore, in PBMCs from HIV-1 infected LTNP, a higher rapamycin-induced response and autophagic flux have been shown compared to individuals with a normal progression [60].

The therapeutic potential of autophagy inhibition, as a possible strategy to control HIV replication is supported by the observation that downregulation of autophagy-related genes and autophagy inhibition leads to *in vitro* HIV inhibition, both in T cells[53, 163] and macrophages[55, 164]. In macrophages, it has been observed that HIV-1 infection might be assisted by autophagic proteins in early stages of infection, due to co-localization between Gag p55 viral protein and LC3-II protein, suggesting that autophagosome membranes might support viral replication[164, 165]. However, during late or degradative stages, HIV-1 down-regulates the expression of certain autophagic proteins to avoid its degradation, shown by the interaction of viral Nef with Beclin-1[54, 164, 166]. On the other hand, autophagy induction has been also associated with HIV-1 restriction *in vitro* in several experimental models[139, 167, 168], including a decrease in mucosal transmission between mucosal DCs and $CD4^+$ T cells[169]. However, reflecting the complex interaction between HIV and autophagy, it is important to note that *in vitro* autophagy induction has been associated with an increase in viral replication[164], and blocking autophagy with bafilomycin in macrophages resulted in an increase of infection[55].

The functional preservation of autophagy in lymphoid cells after HIV infection reinforces the idea that *in vivo* a modulating therapy of this pathway could be plausible. In lymphoid cells, we have shown that pre-treatment with autophagy modulators control HIV infection, even in an

envelope-independent manner. Notably, we observed that both, autophagy-enhancing or blocking drugs, were able to decrease HIV-DNA levels, HIV replication and cell-to-cell transmission. These data suggest that the virus fine-tune autophagic activity to maximize its replication levels. Therefore, the virus is not able to replicate whether the autophagic pathway is blocked or hyperactivated due to excessive induction.

We cannot rule out that the observed inhibition of HIV replication in HLACs with autophagy modulators is only due to their effect on autophagy. Lysosomal inhibitors like chloroquine and bafilomycin, not only impair the lysosomal function, but impede all other lysosomal pathways including the endo-lysosomal trafficking[44, 170]. In addition, chloroquine has been linked to different cellular effects, including inhibition of cytokine production and a decrease in DNA, RNA and protein synthesis (reviewed in[171]). 3-methyladenine also blocks all phosphatidylinositol 3-kinase–dependent signaling pathways thereby resulting in a plethora of side effects. Down-regulation of CCR5, inhibition of HIV-1 mRNA synthesis and increased levels of MIP-1 have been suggested as some of the mechanisms by which rapamycin, at low concentrations, is able to inhibit HIV-1 replication (Review in[172]).

Current direct-acting antiviral therapies are highly effective in suppressing HIV-1 replication. However, recent combination antiretroviral therapy (cART) is not curative, and treated HIV-1 patients still suffer from severe comorbidities due to persistent inflammation and residual viral replication in cellular reservoirs[173, 174]. Our data highlights the potential to modulate host autophagy to intervene in HIV-1 infections. Host-directed therapies are a promising emerging approach in addressing infectious diseases, and may have the potential to both interfere with host cell mechanisms hijacked by viruses for productive infection and boost innate immune defense mechanisms[175]. In addition, a major advantage of host-directed therapies is the reduced likelihood of emergence of drug-resistant variants.

Autophagy modulators are being clinically evaluated for treatment of several diseases as Huntington's disease, renal cell carcinoma, aging, and other autophagy-related disorders[35]. In HIV, the inhibition or hyperactivation of autophagy have been already used as an antiviral therapy. Rapamycin treatment at low concentrations was able to inhibit R5-tropic HIV replication in a mouse model, and show lower frequency of lymphocytes harboring HIV DNA in an HIV-infected kidney transplant recipient treatment[176, 177]. However, in these settings, the inhibition has been associated with a down-regulation of CCR5 and accumulation of anti-HIV beta-chemokine[168, 178]. Similarly, chloroquine was used to treat HIV-infected individuals early in the HIV pandemic and a reduction in HIV-1 RNA viral loads in plasma was reported, even though

the results were not reproduced in other studies (review in[179]). Very recently, the inhibition of autophagy during active HIV-1 infection has been considered as a potential supplementary treatment to effective ART for controlling HIV-1 infection[180]. Likewise, the induction of autophagy as a complement to a 'block and lock' approach, designed to induce a state of deep viral latency, has also been proposed as a new strategy to achieve a functional HIV-1 cure (review in[181]).

Drug repositioning is a rapid and feasible strategy to identify effective drugs for combating a disease. In recent decades, drugs used to treat malaria infection have been shown to be beneficial for many other diseases, including viral infections[179]. Our results have shown that mefloquine, widely tested as an antiviral; and quinacrine, used as an antimicrobial and as an anti-inflammatory treatment, were both able to modulate autophagy and inhibit HIV replication. In recent years, a large number of pharmacological agents targeting autophagy have been described[182]. Some of them are highly specific like the small molecule EACC, which inhibits the autophagic flux by selectively blocking autophagosome-lysosome fusion[183]. Further studies will be required to elucidate whether these compounds can play a role in the fight against HIV.

Autophagy operates as an innate antiviral mechanism to fight invading pathogens by autophagosome-lysosome degradation. Nevertheless, after infection, there are other cellular pathways that are activated to eliminate different pathogens. Infected cells have developed strategies to use cell death to fight pathogens. However, a massive HIV-induced caspase-dependent $CD4^+$ T cell death, by both apoptosis[92] and pyroptosis[184], is observed in HIV-1 infected individuals. Therefore, this massive cellular depletion could be avoided by using therapeutic strategies that include caspase inhibitors. Pan-caspase inhibitors act on one or more of the well-known caspases, and are pursued for their ability to treat diseases such as autoimmune disorders and cancer. Pan-caspase inhibitors can either be peptides, proteins or small molecule inhibitors. One of the most widely pan-caspase inhibitors used is Z-VAD-FMK, although, even at low doses it has been proved to be highly cytotoxic[129]. Q-VD-OPh is a very potent pan-caspase inhibitor that covalently binds and irreversibly blocks multiple caspases (from caspase-1, caspase-3, and caspase-7 to caspase-12). It is characterized for being a cell permeable compound that is not toxic to cells, even when tested at high concentrations (1mM) *in vitro* and *in vivo* in animal models (review in[128, 129]). Q-VD-OPh has been used to inhibit apoptosis in multiple pre-clinical models of non-infectious injuries and viral infections[128, 185-188] and can also inhibit or induce necroptosis associated with cerebral ischemia or hepatitis C viral infection,

respectively[187, 188]. In HIV infection, we have demonstrated that in lymphoid tissue, Q-VD-OPh was able to prevent HIV-induced $CD4^+$ T cell depletion and HIV replication, by decreasing both total and integrated HIV DNA. *In vitro*, Z-VAD-FMK treatment has been associated with the activation of HIV replication in chronically infected T cells[189]. However, in SIV-infected rhesus macaques Q-VD-OPh treatment was associated with a reduction of viral replication and a delayed progression to AIDS by decreasing $CD4^+$ T cell depletion[186].

In the elucidation of the mechanisms of action of Q-VD-OPh we observed a decreased expression of activation markers like CCR5, CD25, and Ki-67 on $CD4^+$ T cells, which are related with an increase of infection[190-192] . These results would suggest that one of the factors involved in the reduction in HIV infection by Q-VD-OPh, would be the decrease of activated target cells. We also observed a decrease in the levels of these activation markers within $CD8^+$ T cells, which has been also seen in PBMCs from SIV-infected macaques treated with this pan-caspase inhibitor. No decrease in the activation levels of $CD4^+$ T cells, either in periphery or in lymph nodes, was reported in this animal model[186].

Caspases have been suggested to regulate cell cycle in different cell lines. In HeLa and Jurkat cells, it has been observed a cell cycle arrest after caspase inhibition treatment or by knockdown of caspase-7, which appears to induce an arrest in mitosis progression in a human liver cancer cell line[155]. Other groups have also demonstrated a link between caspases and cell cycle, suggesting that an elevated number of caspases are involved in many different phases of the cell cycle, inducing the activation of cell cycle proteins, and concluding that caspase inhibitors suppress proper regulation of cell cycle-controlling proteins in PBMCs[193, 194]. In lymphoid tissue cultured *ex vivo*, Q-VD-OPh treatment has also been shown to have an impact on cell cycle, manifested with an increase percentage of cells on S and G_2/M phases, and without modulation in proliferation, suggesting that the drug induces cell cycle arrest.

Caspases have evolved from being considered solely as regulators of apoptosis or inflammation to having a wider range of functions within the cell. Regarding innate immunity, some studies have reported that inflammatory caspase-1 and apoptotic caspases-3 and -9 suppress type-I interferon production by inhibiting either cGAS-STING or RIG-I-MAVS pathways, and showing that, caspase-deficient cells produced elevated levels of type-I IFN creating a potent state of antiviral resistance[113, 118, 157]. In this regard, we demonstrated that in HLACs, pan-caspase inhibition was able to modulate the type-I IFN pathway, in both T cells and non-T cells. An increase was observed in both, IFN production and modulation of several IFN-stimulated genes (ISG), which are related to the host antiviral response[195].

The main molecules that activate the cGAS-STING innate immune pathway are actually viral genomic DNA and cDNA generated from genomic retroviral RNA [109, 110]. However, in the absence of infection, other molecules that could contribute to cGAS activation are mtDNA or dsRNA released from inside the mitochondria to the cell cytosol, due to mitochondrial damage[117]. Q-VD-OPh treatment induced mitochondrial depolarization in our *ex vivo* culture, which suggests that the drug is able to induce a decrease in mitochondrial membrane potential. This sublethal mitochondrial damage would result in mtDNA or dsRNA release, activation of cGAS-STING pathway and the subsequent activation of the type-I IFN pathway (**Figure 1**)[71].

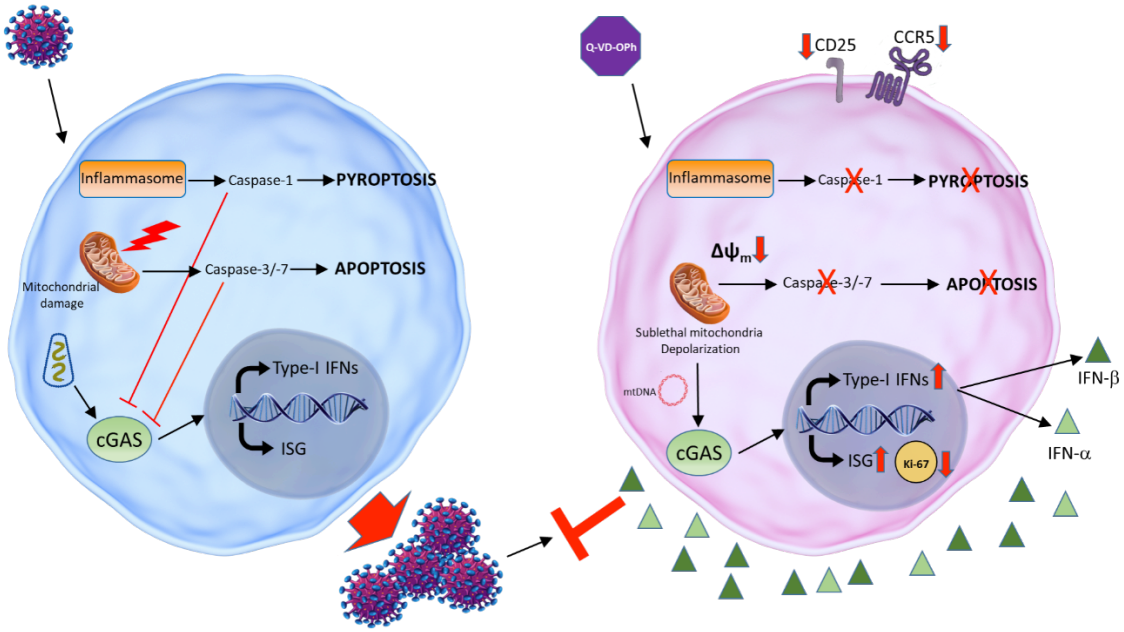

Figure 1. Proposed mechanism of action of Q-VD-OPh. Schematic representation of a HIV infected cell and a Q-VD-OPh treated cell. **a)** HIV-1 activates inflammasome formation and induces mitochondrial damage, which activates caspase-1 (pyroptosis) and caspase-3/7 (apoptosis), respectively. Caspase-1 and caspase-3/7 production inhibit the virus-induced cGAS-STING pathway, decreasing type-I IFN and ISGs production and allowing viral replication. **b)** In the treated cell, Q-VD-OPh blocks caspase activity and consequently, pyroptosis and apoptosis. Sublethal mitochondrial depolarization induced by Q-VD-OPh allows mtDNA release, which will activate cGAS-STING pathway and the production of type-I IFNs and ISGs activation. The innate immune response induced will then be able to inhibit HIV-1 infection. The decline in cellular activation, by a decrease in CD25, CCR5 and Ki-67 expression, will enhance the cellular antiviral state and help to the inhibition.

Long-term treatment with Q-VD-OPh or chronic IFN signaling could play a detrimental role during HIV infection, or any other infection produced by another pathogen, since a long-term production of IFN could drive to cellular immune exhaustion and immune activation[106, 196]. Also,

long-term treatment could disturb the homeostatic balance by avoiding natural cell death, and thus, keeping cells in the body leading to autoimmunity, cancer, or other immunological diseases. Nevertheless, an intermittent administration of Q-VD-OPh would be more appropriate for treatment during long periods of time, and thus, keeping the cellular balance. However, further studies need to be performed.

The use of interferon as a treatment against infections has been used previously. Since its early discovery, interferons have been used to treat different infectious diseases, like common colds[197], several herpes viruses[198, 199] and hepatitis B[200] and C virus infections[201]; showing a potent antiviral activity and interfering with its viral replication. Moreover, in the current SARS-CoV-2 (Covid-19) pandemic, interferon treatment is being tested to decrease the durability of detectable virus in the respiratory tract of infected patients[202]. More recently, it has also been demonstrated the use of various interferon molecules to treat cancer. In breast cancer, it has been observed that tumor cells reverse interferon expression to facilitate metastasis. Therefore, an increase of interferon expression would reduce the spread of these cancer cells[203]. Some groups also have confirmed that interferons trigger the activation of apoptosis in tumor cells[204], thus, interferon treatment could be used to remove cancer malignancies. Also, in multiple sclerosis has been observed that interferon treatment helps to reduce the relapse of the disease[205].

At the same time, it must be considered the potential to produce novel therapies through the modulation of caspase activity, since it is evident by the beneficial therapeutic effects observed upon administration. However, there are a number of challenges in the development of safe and effective drugs. One major obstacle is the lack of knowledge regarding the role of caspases in certain apoptosis-associated diseases, and an incomplete understanding of the different cell death pathways that contribute to these diseases. Information regarding the therapeutic window for administration is also required. Administration of caspase therapeutics without this information may have deleterious effects to patients. Another challenge facing the use of caspase therapeutics is the development of adverse effects upon treatment. Off-target effects may occur due to lack of drug specificity leading to the modulation of non-target caspases or indeed unrelated proteins. Additionally, interference with non-apoptotic or non-inflammatory roles of caspases may result in adverse effects and must also be considered. Research relating to the long-term consequences of caspase inhibition, in particular for the treatment of chronic conditions, is required to determine the safety of these drugs and the future of caspase therapeutics. Furthermore, a very significant advance in the world of caspase inhibition has emerged recently. Efficacy of the pan-caspase inhibitor Emricasan has been tested as a

treatment for different liver diseases in several clinical trials, suggesting that treatment with caspase inhibitors could be used in the clinic, since no adverse effects have been detected[130-135]. However, more studies should be performed to confirm these results and to further evaluate Emricasan as a potential drug.

In conclusion, all these data suggest that new approaches could be taken into consideration in the fight against HIV. Up to 26% of people initiating treatment are infected with a virus carrying resistance to first-line drugs[206]. The modulation of cellular pathways instead of targeting the virus could be a potential approach to avoid resistance to antiretroviral treatments and to treat individuals carrying resistant viruses. In addition, this therapeutic approach could improve $CD4^+$ T cell recovery, avoiding its depletion in lymphoid tissue. So, this opens a broad range of possibilities, since new autophagy modulators or pan-caspase inhibitors could be used to fight a wide variety of infectious and non-infectious diseases.

CONCLUSIONS

OBJECTIVE 1.

- Human lymphoid aggregate cultures (HLACs) from tonsils display a fully functional autophagic pathway.

OBJECTIVE 2.

- HIV infection of HLACs is associated with a significant increase in autophagy, however, this increase is not correlated with a loss of pathway functionality.

OBJECTIVE 3.

- Autophagy modulation, by either induction or inhibition, blocks HIV replication. These data suggest that HIV uses strategies to fine tune autophagy to its own benefit, and *in vivo*, a modulating therapy of this pathway would be a promising therapeutic approach.

OBJECTIVE 4.

- *Ex vivo* cultures of human lymphoid tissues are a suitable model to obtain further insights into HIV and its intricate relationship with autophagy, and hence to unlock the full therapeutic potential of autophagy modulators.
- In *ex vivo* human lymphoid tissue cultures, HIV infection induces both pyroptosis and apoptosis.

OBJECTIVE 5.

- Treatment with the pan-caspase inhibitor Q-VD-OPh prevent HIV-induced $CD4^+$ T cell depletion and reduces viral replication and HIV DNA (total and integrated). The inhibition is caspase-dependent and envelope-independent.

OBJECTIVE 6.

- In lymphoid tissue, Q-VD-OPh treatment is associated with a decrease in cellular activation, with a reduction in the expression of CCR5, CD25 and Ki-67 in both $CD4^+$ and $CD8^+$ T cells. In addition, treatment with Q-VD-OPh induces cell cycle arrest, sub-lethal decrease in mitochondrial membrane potential and induces an increase in type-I IFN production and interferon gene activation. All these data suggest that Q-VD-OPh is inducing a cellular antiviral state.

Overall, our data suggest that host-directed therapies, as autophagy and caspase modulators, are a promising emerging approach in addressing infectious diseases, and may have the potential to both interfere with host cell mechanisms hijacked by viruses for productive infection and boost innate immune defense mechanisms.

PUBLICATIONS

Martínez R, Tapia G, De Muga S, Hernández A, Cao MG, Teixidó C, Urrea V, García E, **Pedreño-López S**, Ibarz L, Blanco J, Clotet B, Cabrera C. **(2019)**. *Combined assessment of peritumoral Th1/Th2 polarization and peripheral immunity as a new biomarker in the prediction of BCG response in patients with high-risk NMIBC*. Oncoimmunology.
doi: 10.1080/2162402X.2019.1602460.

Gutiérrez-Chamorro L, Riveira-Muñoz E, Palau V, Nevot M, **Pedreño-López S**, Senserrich J, Barrios C, Massanella M, Clotet B, Cabrera C, Mitjà O, Crespo M, Pascual J, Riera M, Ballana E. **(2021)**. *SARS-CoV-2 infection modulates ACE2 function and subsequent inflammatory responses in swabs and plasma of COVID-19 patients.* Viruses.
doi: doi.org/10.3390/v13091715.

Pedreño- López S, García E, Guerrero D, Gómez-Mora E, Senserrich J, Clotet B, Cabrera C. **(2021)**. *Modulation of the autophagic pathway inhibits HIV-1 infection in human lymphoid tissue cultured ex vivo.* Autophagy.
Submitted.

REFERENCES

1. Barre-Sinoussi, F., Chermann, J.C., Rey, F., Nugeyre, M.T., Chamaret, S., Gruest, J., et al. (1983). Isolation of a T-lymphotropic retrovirus from a patient at risk for acquired immune deficiency syndrome (AIDS). Science *220*: 868-871.
2. Powell, M.K., Benkova, K., Selinger, P., Dogosi, M., Kinkorova Lunackova, I., Koutnikova, H., et al. (2016). Opportunistic Infections in HIV-Infected Patients Differ Strongly in Frequencies and Spectra between Patients with Low CD4+ Cell Counts Examined Postmortem and Compensated Patients Examined Antemortem Irrespective of the HAART Era. PLoS One *11*: e0162704.
3. Sharp, P.M., and Hahn, B.H. (2011). Origins of HIV and the AIDS pandemic. Cold Spring Harb Perspect Med *1*: a006841.
4. UNAIDS (2020). UNAIDS Report on the global AIDS epidemic.
5. Checkley, M.A., Luttge, B.G., and Freed, E.O. (2011). HIV-1 envelope glycoprotein biosynthesis, trafficking, and incorporation. J Mol Biol *410*: 582-608.
6. Cervera, L., Godia, F., Tarres-Freixas, F., Aguilar-Gurrieri, C., Carrillo, J., Blanco, J., et al. (2019). Production of HIV-1-based virus-like particles for vaccination: achievements and limits. Appl Microbiol Biotechnol *103*: 7367-7384.
7. German Advisory Committee Blood, S.A.o.P.T.b.B. (2016). Human Immunodeficiency Virus (HIV). Transfus Med Hemother *43*: 203-222.
8. Engelman, A., and Cherepanov, P. (2012). The structural biology of HIV-1: mechanistic and therapeutic insights. Nat Rev Microbiol *10*: 279-290.
9. NIH. Clinical Info HIV.gov.
10. Veazey, R.S., DeMaria, M., Chalifoux, L.V., Shvetz, D.E., Pauley, D.R., Knight, H.L., et al. (1998). Gastrointestinal tract as a major site of CD4+ T cell depletion and viral replication in SIV infection. Science *280*: 427-431.
11. Brenchley, J.M., Schacker, T.W., Ruff, L.E., Price, D.A., Taylor, J.H., Beilman, G.J., et al. (2004). CD4+ T cell depletion during all stages of HIV disease occurs predominantly in the gastrointestinal tract. J Exp Med *200*: 749-759.
12. Fulop, T., Franceschi, C., Hirokawa, K., and Pawelec, G. (2009). Handbook on Immunosenescence: Basic Understanding and Clinical Applications. Springer.
13. Garg, H., and Blumenthal, R. (2008). Role of HIV Gp41 mediated fusion/hemifusion in bystander apoptosis. Cell Mol Life Sci *65*: 3134-3144.
14. Forsman, A., and Weiss, R.A. (2008). Why is HIV a pathogen? Trends Microbiol *16*: 555-560.
15. Appay, V., and Sauce, D. (2008). Immune activation and inflammation in HIV-1 infection: causes and consequences. J Pathol *214*: 231-241.
16. Glushakova, S., Baibakov, B., Margolis, L.B., and Zimmerberg, J. (1995). Infection of human tonsil histocultures: a model for HIV pathogenesis. Nat Med *1*: 1320-1322.
17. Grivel, J.C., and Margolis, L. (2009). Use of human tissue explants to study human infectious agents. Nat Protoc *4*: 256-269.
18. Jekle, A., Keppler, O.T., De Clercq, E., Schols, D., Weinstein, M., and Goldsmith, M.A. (2003). In vivo evolution of human immunodeficiency virus type 1 toward increased pathogenicity through CXCR4-mediated killing of uninfected CD4 T cells. J Virol *77*: 5846-5854.
19. Audige, A., Schlaepfer, E., Bonanomi, A., Joller, H., Knuchel, M.C., Weber, M., et al. (2004). HIV-1 does not provoke alteration of cytokine gene expression in lymphoid tissue after acute infection ex vivo. J Immunol *172*: 2687-2696.
20. Doitsh, G., Cavrois, M., Lassen, K.G., Zepeda, O., Yang, Z., Santiago, M.L., et al. (2010). Abortive HIV infection mediates CD4 T cell depletion and inflammation in human lymphoid tissue. Cell *143*: 789-801.
21. Homann, S., Tibroni, N., Baumann, I., Sertel, S., Keppler, O.T., and Fackler, O.T. (2009). Determinants in HIV-1 Nef for enhancement of virus replication and depletion of CD4+ T lymphocytes in human lymphoid tissue ex vivo. Retrovirology *6*: 6.

22. Margolis, L.B., Glushakova, S., Baibakov, B., and Zimmerberg, J. (1995). Syncytium formation in cultured human lymphoid tissue: fusion of implanted HIV glycoprotein 120/41-expressing cells with native CD4+ cells. AIDS Res Hum Retroviruses *11*: 697-704.
23. Glushakova, S., Grivel, J.C., Fitzgerald, W., Sylwester, A., Zimmerberg, J., and Margolis, L.B. (1998). Evidence for the HIV-1 phenotype switch as a causal factor in acquired immunodeficiency. Nat Med *4*: 346-349.
24. Kinter, A., Moorthy, A., Jackson, R., and Fauci, A.S. (2003). Productive HIV infection of resting CD4+ T cells: role of lymphoid tissue microenvironment and effect of immunomodulating agents. AIDS Res Hum Retroviruses *19*: 847-856.
25. Penn, M.L., Grivel, J.C., Schramm, B., Goldsmith, M.A., and Margolis, L. (1999). CXCR4 utilization is sufficient to trigger CD4+ T cell depletion in HIV-1-infected human lymphoid tissue. Proc Natl Acad Sci U S A *96*: 663-668.
26. Fulda, S., Gorman, A.M., Hori, O., and Samali, A. (2010). Cellular stress responses: cell survival and cell death. Int J Cell Biol *2010*: 214074.
27. Levine, B., and Klionsky, D.J. (2004). Development by self-digestion: molecular mechanisms and biological functions of autophagy. Dev Cell *6*: 463-477.
28. Huang, J., and Brumell, J.H. (2014). Bacteria-autophagy interplay: a battle for survival. Nat Rev Microbiol *12*: 101-114.
29. Glick, D., Barth, S., and Macleod, K.F. (2010). Autophagy: cellular and molecular mechanisms. J Pathol *221*: 3-12.
30. Hurley, J.H., and Young, L.N. (2017). Mechanisms of Autophagy Initiation. Annu Rev Biochem *86*: 225-244.
31. Kageyama, S., Gudmundsson, S.R., Sou, Y.S., Ichimura, Y., Tamura, N., Kazuno, S., et al. (2021). p62/SQSTM1-droplet serves as a platform for autophagosome formation and anti-oxidative stress response. Nat Commun *12*: 16.
32. Rusten, T.E., and Stenmark, H. (2010). p62, an autophagy hero or culprit? Nat Cell Biol *12*: 207-209.
33. Fleming, A., Noda, T., Yoshimori, T., and Rubinsztein, D.C. (2011). Chemical modulators of autophagy as biological probes and potential therapeutics. Nat Chem Biol *7*: 9-17.
34. Rubinsztein, D.C., Codogno, P., and Levine, B. (2012). Autophagy modulation as a potential therapeutic target for diverse diseases. Nat Rev Drug Discov *11*: 709-730.
35. Galluzzi, L., Bravo-San Pedro, J.M., Levine, B., Green, D.R., and Kroemer, G. (2017). Pharmacological modulation of autophagy: therapeutic potential and persisting obstacles. Nat Rev Drug Discov *16*: 487-511.
36. Towers, C.G., and Thorburn, A. (2016). Therapeutic Targeting of Autophagy. EBioMedicine *14*: 15-23.
37. Levine, B., Packer, M., and Codogno, P. (2015). Development of autophagy inducers in clinical medicine. J Clin Invest *125*: 14-24.
38. Li, J., Kim, S.G., and Blenis, J. (2014). Rapamycin: one drug, many effects. Cell Metab *19*: 373-379.
39. Cheng, Y., Ren, X., Hait, W.N., and Yang, J.M. (2013). Therapeutic targeting of autophagy in disease: biology and pharmacology. Pharmacol Rev *65*: 1162-1197.
40. Cuomo, F., Altucci, L., and Cobellis, G. (2019). Autophagy Function and Dysfunction: Potential Drugs as Anti-Cancer Therapy. Cancers (Basel) *11*.
41. Wu, Y.T., Tan, H.L., Shui, G., Bauvy, C., Huang, Q., Wenk, M.R., et al. (2010). Dual role of 3-methyladenine in modulation of autophagy via different temporal patterns of inhibition on class I and III phosphoinositide 3-kinase. J Biol Chem *285*: 10850-10861.
42. Dai, S., Wang, B., Li, W., Wang, L., Song, X., Guo, C., et al. (2016). Systemic application of 3-methyladenine markedly inhibited atherosclerotic lesion in ApoE(-/-) mice by modulating autophagy, foam cell formation and immune-negative molecules. Cell Death Dis *7*: e2498.

43. Cheong, H., Lu, C., Lindsten, T., and Thompson, C.B. (2012). Therapeutic targets in cancer cell metabolism and autophagy. Nat Biotechnol *30*: 671-678.
44. Mauthe, M., Orhon, I., Rocchi, C., Zhou, X., Luhr, M., Hijlkema, K.J., et al. (2018). Chloroquine inhibits autophagic flux by decreasing autophagosome-lysosome fusion. Autophagy *14*: 1435-1455.
45. Mitja, O., Corbacho-Monne, M., Ubals, M., Tebe, C., Penafiel, J., Tobias, A., et al. (2020). Hydroxychloroquine for Early Treatment of Adults with Mild Covid-19: A Randomized-Controlled Trial. Clin Infect Dis.
46. Redmann, M., Benavides, G.A., Berryhill, T.F., Wani, W.Y., Ouyang, X., Johnson, M.S., et al. (2017). Inhibition of autophagy with bafilomycin and chloroquine decreases mitochondrial quality and bioenergetic function in primary neurons. Redox Biol *11*: 73-81.
47. Pivtoraiko, V.N., Harrington, A.J., Mader, B.J., Luker, A.M., Caldwell, G.A., Caldwell, K.A., et al. (2010). Low-dose bafilomycin attenuates neuronal cell death associated with autophagy-lysosome pathway dysfunction. J Neurochem *114*: 1193-1204.
48. Loos, B., du Toit, A., and Hofmeyr, J.H. (2014). Defining and measuring autophagosome flux-concept and reality. Autophagy *10*: 2087-2096.
49. Musiwaro, P., Smith, M., Manifava, M., Walker, S.A., and Ktistakis, N.T. (2013). Characteristics and requirements of basal autophagy in HEK 293 cells. Autophagy *9*: 1407-1417.
50. Killian, M.S. (2012). Dual role of autophagy in HIV-1 replication and pathogenesis. AIDS Res Ther *9*: 16.
51. Cabrera-Rodriguez, R., Perez-Yanes, S., Estevez-Herrera, J., Marquez-Arce, D., Cabrera, C., Espert, L., et al. (2021). The Interplay of HIV and Autophagy in Early Infection. Front Microbiol *12*: 661446.
52. Espert, L., Codogno, P., and Biard-Piechaczyk, M. (2008). What is the role of autophagy in HIV-1 infection? Autophagy *4*: 273-275.
53. Wang, X., Gao, Y., Tan, J., Devadas, K., Ragupathy, V., Takeda, K., et al. (2012). HIV-1 and HIV-2 infections induce autophagy in Jurkat and CD4+ T cells. Cell Signal *24*: 1414-1419.
54. Zhou, D., and Spector, S.A. (2008). Human immunodeficiency virus type-1 infection inhibits autophagy. AIDS *22*: 695-699.
55. Espert, L., Varbanov, M., Robert-Hebmann, V., Sagnier, S., Robbins, I., Sanchez, F., et al. (2009). Differential role of autophagy in CD4 T cells and macrophages during X4 and R5 HIV-1 infection. PLoS One *4*: e5787.
56. Denizot, M., Varbanov, M., Espert, L., Robert-Hebmann, V., Sagnier, S., Garcia, E., et al. (2008). HIV-1 gp41 fusogenic function triggers autophagy in uninfected cells. Autophagy *4*: 998-1008.
57. Van Grol, J., Subauste, C., Andrade, R.M., Fujinaga, K., Nelson, J., and Subauste, C.S. (2010). HIV-1 inhibits autophagy in bystander macrophage/monocytic cells through Src-Akt and STAT3. PLoS One *5*: e11733.
58. Izquierdo-Useros, N., Lorizate, M., McLaren, P.J., Telenti, A., Krausslich, H.G., and Martinez-Picado, J. (2014). HIV-1 capture and transmission by dendritic cells: the role of viral glycolipids and the cellular receptor Siglec-1. PLoS Pathog *10*: e1004146.
59. Dinkins, C., Pilli, M., and Kehrl, J.H. (2015). Roles of autophagy in HIV infection. Immunol Cell Biol *93*: 11-17.
60. Nardacci, R., Amendola, A., Ciccosanti, F., Corazzari, M., Esposito, V., Vlassi, C., et al. (2014). Autophagy plays an important role in the containment of HIV-1 in nonprogressor-infected patients. Autophagy *10*: 1167-1178.
61. Gomez-Mora, E., Robert-Hebmann, V., Garcia, E., Massanella, M., Clotet, B., Cabrera, C., et al. (2017). Brief Report: Impaired CD4 T-Cell Response to Autophagy in Treated HIV-1-Infected Individuals. J Acquir Immune Defic Syndr *74*: 201-205.

62. Gupta, M.K., Kaminski, R., Mullen, B., Gordon, J., Burdo, T.H., Cheung, J.Y., et al. (2017). HIV-1 Nef-induced cardiotoxicity through dysregulation of autophagy. Sci Rep *7*: 8572.
63. Zhou, D., Masliah, E., and Spector, S.A. (2011). Autophagy is increased in postmortem brains of persons with HIV-1-associated encephalitis. J Infect Dis *203*: 1647-1657.
64. Galluzzi, L., Vitale, I., Aaronson, S.A., Abrams, J.M., Adam, D., Agostinis, P., et al. (2018). Molecular mechanisms of cell death: recommendations of the Nomenclature Committee on Cell Death 2018. Cell Death Differ *25*: 486-541.
65. Kesavardhana, S., Malireddi, R.K.S., and Kanneganti, T.D. (2020). Caspases in Cell Death, Inflammation, and Pyroptosis. Annu Rev Immunol *38*: 567-595.
66. Li, J., and Yuan, J. (2008). Caspases in apoptosis and beyond. Oncogene *27*: 6194-6206.
67. You, Y., Cheng, A.C., Wang, M.S., Jia, R.Y., Sun, K.F., Yang, Q., et al. (2017). The suppression of apoptosis by alpha-herpesvirus. Cell Death Dis *8*: e2749.
68. Osellame, L.D., Blacker, T.S., and Duchen, M.R. (2012). Cellular and molecular mechanisms of mitochondrial function. Best Pract Res Clin Endocrinol Metab *26*: 711-723.
69. Pena-Blanco, A., and Garcia-Saez, A.J. (2018). Bax, Bak and beyond - mitochondrial performance in apoptosis. FEBS J *285*: 416-431.
70. McArthur, K., Whitehead, L.W., Heddleston, J.M., Li, L., Padman, B.S., Oorschot, V., et al. (2018). BAK/BAX macropores facilitate mitochondrial herniation and mtDNA efflux during apoptosis. Science *359*.
71. Riley, J.S., Quarato, G., Cloix, C., Lopez, J., O'Prey, J., Pearson, M., et al. (2018). Mitochondrial inner membrane permeabilisation enables mtDNA release during apoptosis. EMBO J *37*.
72. Dewson, G., and Kluck, R.M. (2009). Mechanisms by which Bak and Bax permeabilise mitochondria during apoptosis. J Cell Sci *122*: 2801-2808.
73. Miao, E.A., Rajan, J.V., and Aderem, A. (2011). Caspase-1-induced pyroptotic cell death. Immunol Rev *243*: 206-214.
74. Bergsbaken, T., Fink, S.L., and Cookson, B.T. (2009). Pyroptosis: host cell death and inflammation. Nat Rev Microbiol *7*: 99-109.
75. den Hartigh, A.B., and Fink, S.L. (2018). Pyroptosis Induction and Detection. Curr Protoc Immunol *122*: e52.
76. Fink, S.L., and Cookson, B.T. (2006). Caspase-1-dependent pore formation during pyroptosis leads to osmotic lysis of infected host macrophages. Cell Microbiol *8*: 1812-1825.
77. Li, P., Allen, H., Banerjee, S., Franklin, S., Herzog, L., Johnston, C., et al. (1995). Mice deficient in IL-1 beta-converting enzyme are defective in production of mature IL-1 beta and resistant to endotoxic shock. Cell *80*: 401-411.
78. Kuida, K., Lippke, J.A., Ku, G., Harding, M.W., Livingston, D.J., Su, M.S., et al. (1995). Altered cytokine export and apoptosis in mice deficient in interleukin-1 beta converting enzyme. Science *267*: 2000-2003.
79. Brennan, M.A., and Cookson, B.T. (2000). Salmonella induces macrophage death by caspase-1-dependent necrosis. Mol Microbiol *38*: 31-40.
80. Hilbi, H., Moss, J.E., Hersh, D., Chen, Y., Arondel, J., Banerjee, S., et al. (1998). Shigella-induced apoptosis is dependent on caspase-1 which binds to IpaB. J Biol Chem *273*: 32895-32900.
81. Bergsbaken, T., and Cookson, B.T. (2007). Macrophage activation redirects yersinia-infected host cell death from apoptosis to caspase-1-dependent pyroptosis. PLoS Pathog *3*: e161.
82. Jesenberger, V., Procyk, K.J., Yuan, J., Reipert, S., and Baccarini, M. (2000). Salmonella-induced caspase-2 activation in macrophages: a novel mechanism in pathogen-mediated apoptosis. J Exp Med *192*: 1035-1046.

83. Cervantes, J., Nagata, T., Uchijima, M., Shibata, K., and Koide, Y. (2008). Intracytosolic Listeria monocytogenes induces cell death through caspase-1 activation in murine macrophages. Cell Microbiol *10*: 41-52.
84. Lim, S.G., Condez, A., Lee, C.A., Johnson, M.A., Elia, C., and Poulter, L.W. (1993). Loss of mucosal CD4 lymphocytes is an early feature of HIV infection. Clin Exp Immunol *92*: 448-454.
85. Okoye, A.A., and Picker, L.J. (2013). CD4(+) T-cell depletion in HIV infection: mechanisms of immunological failure. Immunol Rev *254*: 54-64.
86. Alimonti, J.B., Ball, T.B., and Fowke, K.R. (2003). Mechanisms of CD4+ T lymphocyte cell death in human immunodeficiency virus infection and AIDS. J Gen Virol *84*: 1649-1661.
87. Meyaard, L., Otto, S.A., Jonker, R.R., Mijnster, M.J., Keet, R.P., and Miedema, F. (1992). Programmed death of T cells in HIV-1 infection. Science *257*: 217-219.
88. Cassol, E., Alfano, M., Biswas, P., and Poli, G. (2006). Monocyte-derived macrophages and myeloid cell lines as targets of HIV-1 replication and persistence. J Leukoc Biol *80*: 1018-1030.
89. Cotton, M.F., Ikle, D.N., Rapaport, E.L., Marschner, S., Tseng, P.O., Kurrle, R., et al. (1997). Apoptosis of CD4+ and CD8+ T cells isolated immediately ex vivo correlates with disease severity in human immunodeficiency virus type 1 infection. Pediatr Res *42*: 656-664.
90. Gougeon, M.L., and Montagnier, L. (1993). Apoptosis in AIDS. Science *260*: 1269-1270.
91. Garg, H., Mohl, J., and Joshi, A. (2012). HIV-1 induced bystander apoptosis. Viruses *4*: 3020-3043.
92. Garg, H., and Joshi, A. (2017). Host and Viral Factors in HIV-Mediated Bystander Apoptosis. Viruses *9*.
93. Herbeuval, J.P., Grivel, J.C., Boasso, A., Hardy, A.W., Chougnet, C., Dolan, M.J., et al. (2005). CD4+ T-cell death induced by infectious and noninfectious HIV-1: role of type 1 interferon-dependent, TRAIL/DR5-mediated apoptosis. Blood *106*: 3524-3531.
94. Schindler, M., Munch, J., Kutsch, O., Li, H., Santiago, M.L., Bibollet-Ruche, F., et al. (2006). Nef-mediated suppression of T cell activation was lost in a lentiviral lineage that gave rise to HIV-1. Cell *125*: 1055-1067.
95. Blanco, J., Barretina, J., Ferri, K.F., Jacotot, E., Gutierrez, A., Armand-Ugon, M., et al. (2003). Cell-surface-expressed HIV-1 envelope induces the death of CD4 T cells during GP41-mediated hemifusion-like events. Virology *305*: 318-329.
96. Cunyat, F., Curriu, M., Marfil, S., Garcia, E., Clotet, B., Blanco, J., et al. (2012). Evaluation of the cytopathicity (fusion/hemifusion) of patient-derived HIV-1 envelope glycoproteins comparing two effector cell lines. J Biomol Screen *17*: 727-737.
97. Sousa, A.E., Carneiro, J., Meier-Schellersheim, M., Grossman, Z., and Victorino, R.M. (2002). CD4 T cell depletion is linked directly to immune activation in the pathogenesis of HIV-1 and HIV-2 but only indirectly to the viral load. J Immunol *169*: 3400-3406.
98. Feria, M.G., Taborda, N.A., Hernandez, J.C., and Rugeles, M.T. (2018). HIV replication is associated to inflammasomes activation, IL-1beta, IL-18 and caspase-1 expression in GALT and peripheral blood. PLoS One *13*: e0192845.
99. Marchetti, G., Bellistri, G.M., Borghi, E., Tincati, C., Ferramosca, S., La Francesca, M., et al. (2008). Microbial translocation is associated with sustained failure in CD4+ T-cell reconstitution in HIV-infected patients on long-term highly active antiretroviral therapy. AIDS *22*: 2035-2038.
100. Merlini, E., Bai, F., Bellistri, G.M., Tincati, C., d'Arminio Monforte, A., and Marchetti, G. (2011). Evidence for polymicrobic flora translocating in peripheral blood of HIV-infected patients with poor immune response to antiretroviral therapy. PLoS One *6*: e18580.
101. Nowroozalizadeh, S., Mansson, F., da Silva, Z., Repits, J., Dabo, B., Pereira, C., et al. (2010). Microbial translocation correlates with the severity of both HIV-1 and HIV-2 infections. J Infect Dis *201*: 1150-1154.

102. Silvestri, G., Sodora, D.L., Koup, R.A., Paiardini, M., O'Neil, S.P., McClure, H.M., et al. (2003). Nonpathogenic SIV infection of sooty mangabeys is characterized by limited bystander immunopathology despite chronic high-level viremia. Immunity *18*: 441-452.
103. Doitsh, G., and Greene, W.C. (2016). Dissecting How CD4 T Cells Are Lost During HIV Infection. Cell Host Microbe *19*: 280-291.
104. Galloway, N.L., Doitsh, G., Monroe, K.M., Yang, Z., Munoz-Arias, I., Levy, D.N., et al. (2015). Cell-to-Cell Transmission of HIV-1 Is Required to Trigger Pyroptotic Death of Lymphoid-Tissue-Derived CD4 T Cells. Cell Rep *12*: 1555-1563.
105. Doitsh, G., Galloway, N.L., Geng, X., Yang, Z., Monroe, K.M., Zepeda, O., et al. (2014). Cell death by pyroptosis drives CD4 T-cell depletion in HIV-1 infection. Nature *505*: 509-514.
106. Cheng, L., Yu, H., Li, G., Li, F., Ma, J., Li, J., et al. (2017). Type I interferons suppress viral replication but contribute to T cell depletion and dysfunction during chronic HIV-1 infection. JCI Insight *2*.
107. Cox, A.L., and Siliciano, R.F. (2014). HIV: Not-so-innocent bystanders. Nature *505*: 492-493.
108. Shalini, S., Dorstyn, L., Dawar, S., and Kumar, S. (2015). Old, new and emerging functions of caspases. Cell Death Differ *22*: 526-539.
109. Cheng, Z., Dai, T., He, X., Zhang, Z., Xie, F., Wang, S., et al. (2020). The interactions between cGAS-STING pathway and pathogens. Signal Transduct Target Ther *5*: 91.
110. Chen, Q., Sun, L., and Chen, Z.J. (2016). Regulation and function of the cGAS-STING pathway of cytosolic DNA sensing. Nat Immunol *17*: 1142-1149.
111. Kwon, J., and Bakhoum, S.F. (2020). The Cytosolic DNA-Sensing cGAS-STING Pathway in Cancer. Cancer Discov *10*: 26-39.
112. Cosentino, K., and Garcia-Saez, A.J. (2018). MIM through MOM: the awakening of Bax and Bak pores. EMBO J *37*.
113. Wang, Y., Ning, X., Gao, P., Wu, S., Sha, M., Lv, M., et al. (2017). Inflammasome Activation Triggers Caspase-1-Mediated Cleavage of cGAS to Regulate Responses to DNA Virus Infection. Immunity *46*: 393-404.
114. Wu, B., and Hur, S. (2015). How RIG-I like receptors activate MAVS. Curr Opin Virol *12*: 91-98.
115. Chau, T.L., Gioia, R., Gatot, J.S., Patrascu, F., Carpentier, I., Chapelle, J.P., et al. (2008). Are the IKKs and IKK-related kinases TBK1 and IKK-epsilon similarly activated? Trends Biochem Sci *33*: 171-180.
116. Barnes, P., Drazen, J., Rennard, S., and Thomson, N. (2008). Asthma and COPD 2nd Edition. Elsevier.
117. Riley, J.S., and Tait, S.W. (2020). Mitochondrial DNA in inflammation and immunity. EMBO Rep *21*: e49799.
118. Ning, X., Wang, Y., Jing, M., Sha, M., Lv, M., Gao, P., et al. (2019). Apoptotic Caspases Suppress Type I Interferon Production via the Cleavage of cGAS, MAVS, and IRF3. Mol Cell *74*: 19-31 e17.
119. White, M.J., McArthur, K., Metcalf, D., Lane, R.M., Cambier, J.C., Herold, M.J., et al. (2014). Apoptotic caspases suppress mtDNA-induced STING-mediated type I IFN production. Cell *159*: 1549-1562.
120. Imre, G. (2020). Cell death signalling in virus infection. Cell Signal *76*: 109772.
121. Fadeel, B., and Orrenius, S. (2005). Apoptosis: a basic biological phenomenon with wide-ranging implications in human disease. J Intern Med *258*: 479-517.
122. Favaloro, B., Allocati, N., Graziano, V., Di Ilio, C., and De Laurenzi, V. (2012). Role of apoptosis in disease. Aging (Albany NY) *4*: 330-349.
123. Ratziu, V., Sheikh, M.Y., Sanyal, A.J., Lim, J.K., Conjeevaram, H., Chalasani, N., et al. (2012). A phase 2, randomized, double-blind, placebo-controlled study of GS-9450 in subjects with nonalcoholic steatohepatitis. Hepatology *55*: 419-428.

124. McCall, M.D., Maciver, A.M., Kin, T., Emamaullee, J., Pawlick, R., Edgar, R., et al. (2012). Caspase inhibitor IDN6556 facilitates marginal mass islet engraftment in a porcine islet autotransplant model. Transplantation *94*: 30-35.
125. Callus, B.A., and Vaux, D.L. (2007). Caspase inhibitors: viral, cellular and chemical. Cell Death Differ *14*: 73-78.
126. Ekert, P.G., Silke, J., and Vaux, D.L. (1999). Caspase inhibitors. Cell Death Differ *6*: 1081-1086.
127. Chauvier, D., Ankri, S., Charriaut-Marlangue, C., Casimir, R., and Jacotot, E. (2007). Broad-spectrum caspase inhibitors: from myth to reality? Cell Death Differ *14*: 387-391.
128. Keoni, C.L., and Brown, T.L. (2015). Inhibition of Apoptosis and Efficacy of Pan Caspase Inhibitor, Q-VD-OPh, in Models of Human Disease. J Cell Death *8*: 1-7.
129. Caserta, T.M., Smith, A.N., Gultice, A.D., Reedy, M.A., and Brown, T.L. (2003). Q-VD-OPh, a broad spectrum caspase inhibitor with potent antiapoptotic properties. Apoptosis *8*: 345-352.
130. Mu, L.Y., Li, S.Q., Tang, L.X., and Li, R. (2021). Efficacy and Safety of Emricasan in Liver Cirrhosis and/or Fibrosis. Clinics (Sao Paulo) *76*: e2409.
131. Frenette, C.T., Morelli, G., Shiffman, M.L., Frederick, R.T., Rubin, R.A., Fallon, M.B., et al. (2019). Emricasan Improves Liver Function in Patients With Cirrhosis and High Model for End-Stage Liver Disease Scores Compared With Placebo. Clin Gastroenterol Hepatol *17*: 774-783 e774.
132. Garcia-Tsao, G., Bosch, J., Kayali, Z., Harrison, S.A., Abdelmalek, M.F., Lawitz, E., et al. (2020). Randomized placebo-controlled trial of emricasan for non-alcoholic steatohepatitis-related cirrhosis with severe portal hypertension. J Hepatol *72*: 885-895.
133. Mehta, G., Rousell, S., Burgess, G., Morris, M., Wright, G., McPherson, S., et al. (2018). A Placebo-Controlled, Multicenter, Double-Blind, Phase 2 Randomized Trial of the Pan-Caspase Inhibitor Emricasan in Patients with Acutely Decompensated Cirrhosis. J Clin Exp Hepatol *8*: 224-234.
134. Valentino, K.L., Gutierrez, M., Sanchez, R., Winship, M.J., and Shapiro, D.A. (2003). First clinical trial of a novel caspase inhibitor: anti-apoptotic caspase inhibitor, IDN-6556, improves liver enzymes. Int J Clin Pharmacol Ther *41*: 441-449.
135. Pockros, P.J., Schiff, E.R., Shiffman, M.L., McHutchison, J.G., Gish, R.G., Afdhal, N.H., et al. (2007). Oral IDN-6556, an antiapoptotic caspase inhibitor, may lower aminotransferase activity in patients with chronic hepatitis C. Hepatology *46*: 324-329.
136. Schmidt, A., Huber, J.E., Sercan Alp, O., Gurkov, R., Reichel, C.A., Herrmann, M., et al. (2020). Complex human adenoid tissue-based ex vivo culture systems reveal anti-inflammatory drug effects on germinal center T and B cells. EBioMedicine *53*: 102684.
137. Leisching, G.R., Loos, B., Botha, M.H., and Engelbrecht, A.M. (2015). The role of mTOR during cisplatin treatment in an in vitro and ex vivo model of cervical cancer. Toxicology *335*: 72-78.
138. Wu, M., Lao, Y., Xu, N., Wang, X., Tan, H., Fu, W., et al. (2015). Guttiferone K induces autophagy and sensitizes cancer cells to nutrient stress-induced cell death. Phytomedicine *22*: 902-910.
139. Campbell, G.R., and Spector, S.A. (2011). Hormonally active vitamin D3 (1alpha,25-dihydroxycholecalciferol) triggers autophagy in human macrophages that inhibits HIV-1 infection. J Biol Chem *286*: 18890-18902.
140. Gorshkov, K., Chen, C.Z., Bostwick, R., Rasmussen, L., Xu, M., Pradhan, M., et al. (2020). The SARS-CoV-2 cytopathic effect is blocked with autophagy modulators. bioRxiv.
141. Sharma, N., Thomas, S., Golden, E.B., Hofman, F.M., Chen, T.C., Petasis, N.A., et al. (2012). Inhibition of autophagy and induction of breast cancer cell death by mefloquine, an antimalarial agent. Cancer Lett *326*: 143-154.

142. Parks, A., Charest-Morin, X., Boivin-Welch, M., Bouthillier, J., and Marceau, F. (2015). Autophagic flux inhibition and lysosomogenesis ensuing cellular capture and retention of the cationic drug quinacrine in murine models. PeerJ *3*: e1314.
143. Fourrier, C., Bryksin, V., Hattersley, K., Hein, L.K., Bensalem, J., and Sargeant, T.J. (2021). Comparison of chloroquine-like molecules for lysosomal inhibition and measurement of autophagic flux in the brain. Biochem Biophys Res Commun *534*: 107-113.
144. Curriu, M., Carrillo, J., Massanella, M., Garcia, E., Cunyat, F., Pena, R., et al. (2012). Susceptibility of human lymphoid tissue cultured ex vivo to xenotropic murine leukemia virus-related virus (XMRV) infection. PLoS One *7*: e37415.
145. Cicala, C., Arthos, J., Rubbert, A., Selig, S., Wildt, K., Cohen, O.J., et al. (2000). HIV-1 envelope induces activation of caspase-3 and cleavage of focal adhesion kinase in primary human CD4(+) T cells. Proc Natl Acad Sci U S A *97*: 1178-1183.
146. Glushakova, S., Baibakov, B., Zimmerberg, J., and Margolis, L.B. (1997). Experimental HIV infection of human lymphoid tissue: correlation of CD4+ T cell depletion and virus syncytium-inducing/non-syncytium-inducing phenotype in histocultures inoculated with laboratory strains and patient isolates of HIV type 1. AIDS Res Hum Retroviruses *13*: 461-471.
147. O'Doherty, U., Swiggard, W.J., and Malim, M.H. (2000). Human immunodeficiency virus type 1 spinoculation enhances infection through virus binding. J Virol *74*: 10074-10080.
148. Guo, J., Wang, W., Yu, D., and Wu, Y. (2011). Spinoculation triggers dynamic actin and cofilin activity that facilitates HIV-1 infection of transformed and resting CD4 T cells. J Virol *85*: 9824-9833.
149. Grivel, J.C., Malkevitch, N., and Margolis, L. (2000). Human immunodeficiency virus type 1 induces apoptosis in CD4(+) but not in CD8(+) T cells in ex vivo-infected human lymphoid tissue. J Virol *74*: 8077-8084.
150. Southerland, B., Kulkarni-Datar, K., Keoni, C., Bricker, R., Grunwald, W.C., Ketcha, D.M., et al. (2010). Q-VE-OPh, a Negative Control for O-Phenoxy-Conjugated Caspase Inhibitors. Journal of Cell Death *3*: 33-40.
151. Zack, J.A., Kim, S.G., and Vatakis, D.N. (2013). HIV restriction in quiescent CD4(+) T cells. Retrovirology *10*: 37.
152. Pan, X., Baldauf, H.M., Keppler, O.T., and Fackler, O.T. (2013). Restrictions to HIV-1 replication in resting CD4+ T lymphocytes. Cell Res *23*: 876-885.
153. Biancotto, A., Iglehart, S.J., Vanpouille, C., Condack, C.E., Lisco, A., Ruecker, E., et al. (2008). HIV-1 induced activation of CD4+ T cells creates new targets for HIV-1 infection in human lymphoid tissue ex vivo. Blood *111*: 699-704.
154. Hashimoto, T., Kikkawa, U., and Kamada, S. (2011). Contribution of caspase(s) to the cell cycle regulation at mitotic phase. PLoS One *6*: e18449.
155. Hashimoto, T., Yamauchi, L., Hunter, T., Kikkawa, U., and Kamada, S. (2008). Possible involvement of caspase-7 in cell cycle progression at mitosis. Genes Cells *13*: 609-621.
156. Chen, H., Ning, X., and Jiang, Z. (2017). Caspases control antiviral innate immunity. Cell Mol Immunol *14*: 736-747.
157. Rongvaux, A., Jackson, R., Harman, C.C., Li, T., West, A.P., de Zoete, M.R., et al. (2014). Apoptotic caspases prevent the induction of type I interferons by mitochondrial DNA. Cell *159*: 1563-1577.
158. Churchill, M.J., Deeks, S.G., Margolis, D.M., Siliciano, R.F., and Swanstrom, R. (2016). HIV reservoirs: what, where and how to target them. Nat Rev Microbiol *14*: 55-60.
159. Gougeon, M.L., and Piacentini, M. (2009). New insights on the role of apoptosis and autophagy in HIV pathogenesis. Apoptosis *14*: 501-508.
160. Haase, A.T. (1999). Population biology of HIV-1 infection: viral and CD4+ T cell demographics and dynamics in lymphatic tissues. Annu Rev Immunol *17*: 625-656.
161. Banga, R., Munoz, O., and Perreau, M. (2021). HIV persistence in lymph nodes. Curr Opin HIV AIDS *16*: 209-214.

162. Gerland, L.M., Genestier, L., Peyrol, S., Michallet, M.C., Hayette, S., Urbanowicz, I., et al. (2004). Autolysosomes accumulate during in vitro CD8+ T-lymphocyte aging and may participate in induced death sensitization of senescent cells. Exp Gerontol *39*: 789-800.
163. Brass, A.L., Dykxhoorn, D.M., Benita, Y., Yan, N., Engelman, A., Xavier, R.J., et al. (2008). Identification of host proteins required for HIV infection through a functional genomic screen. Science *319*: 921-926.
164. Kyei, G.B., Dinkins, C., Davis, A.S., Roberts, E., Singh, S.B., Dong, C., et al. (2009). Autophagy pathway intersects with HIV-1 biosynthesis and regulates viral yields in macrophages. J Cell Biol *186*: 255-268.
165. Nardacci, R., Ciccosanti, F., Marsella, C., Ippolito, G., Piacentini, M., and Fimia, G.M. (2017). Role of autophagy in HIV infection and pathogenesis. J Intern Med *281*: 422-432.
166. Randow, F., and Munz, C. (2012). Autophagy in the regulation of pathogen replication and adaptive immunity. Trends Immunol *33*: 475-487.
167. Sagnier, S., Daussy, C.F., Borel, S., Robert-Hebmann, V., Faure, M., Blanchet, F.P., et al. (2015). Autophagy restricts HIV-1 infection by selectively degrading Tat in CD4+ T lymphocytes. J Virol *89*: 615-625.
168. Heredia, A., Amoroso, A., Davis, C., Le, N., Reardon, E., Dominique, J.K., et al. (2003). Rapamycin causes down-regulation of CCR5 and accumulation of anti-HIV beta-chemokines: an approach to suppress R5 strains of HIV-1. Proc Natl Acad Sci U S A *100*: 10411-10416.
169. Cloherty, A.P.M., van Teijlingen, N.H., Eisden, T., van Hamme, J.L., Rader, A.G., Geijtenbeek, T.B.H., et al. (2021). Autophagy-enhancing drugs limit mucosal HIV-1 acquisition and suppress viral replication ex vivo. Sci Rep *11*: 4767.
170. Johnson, L.S., Dunn, K.W., Pytowski, B., and McGraw, T.E. (1993). Endosome acidification and receptor trafficking: bafilomycin A1 slows receptor externalization by a mechanism involving the receptor's internalization motif. Mol Biol Cell *4*: 1251-1266.
171. Al-Bari, M.A. (2015). Chloroquine analogues in drug discovery: new directions of uses, mechanisms of actions and toxic manifestations from malaria to multifarious diseases. J Antimicrob Chemother *70*: 1608-1621.
172. Donia, M., McCubrey, J.A., Bendtzen, K., and Nicoletti, F. (2010). Potential use of rapamycin in HIV infection. Br J Clin Pharmacol *70*: 784-793.
173. Deeks, S.G., Tracy, R., and Douek, D.C. (2013). Systemic effects of inflammation on health during chronic HIV infection. Immunity *39*: 633-645.
174. Chun, T.W., Nickle, D.C., Justement, J.S., Meyers, J.H., Roby, G., Hallahan, C.W., et al. (2008). Persistence of HIV in gut-associated lymphoid tissue despite long-term antiretroviral therapy. J Infect Dis *197*: 714-720.
175. Kaufmann, S.H.E., Dorhoi, A., Hotchkiss, R.S., and Bartenschlager, R. (2018). Host-directed therapies for bacterial and viral infections. Nat Rev Drug Discov *17*: 35-56.
176. Nicoletti, F., Lapenta, C., Donati, S., Spada, M., Ranazzi, A., Cacopardo, B., et al. (2009). Inhibition of human immunodeficiency virus (HIV-1) infection in human peripheral blood leucocytes-SCID reconstituted mice by rapamycin. Clin Exp Immunol *155*: 28-34.
177. Stock, P.G., Barin, B., Hatano, H., Rogers, R.L., Roland, M.E., Lee, T.H., et al. (2014). Reduction of HIV persistence following transplantation in HIV-infected kidney transplant recipients. Am J Transplant *14*: 1136-1141.
178. Roy, J., Paquette, J.S., Fortin, J.F., and Tremblay, M.J. (2002). The immunosuppressant rapamycin represses human immunodeficiency virus type 1 replication. Antimicrob Agents Chemother *46*: 3447-3455.
179. D'Alessandro, S., Scaccabarozzi, D., Signorini, L., Perego, F., Ilboudo, D.P., Ferrante, P., et al. (2020). The Use of Antimalarial Drugs against Viral Infection. Microorganisms *8*.
180. Li, M., Liu, W., Bauch, T., Graviss, E.A., Arduino, R.C., Kimata, J.T., et al. (2020). Clearance of HIV infection by selective elimination of host cells capable of producing HIV. Nat Commun *11*: 4051.

181. Campbell, G.R., and Spector, S.A. (2021). Induction of Autophagy to Achieve a Human Immunodeficiency Virus Type 1 Cure. Cells *10*.
182. Vakifahmetoglu-Norberg, H., Xia, H.G., and Yuan, J. (2015). Pharmacologic agents targeting autophagy. J Clin Invest *125*: 5-13.
183. Vats, S., and Manjithaya, R. (2019). A reversible autophagy inhibitor blocks autophagosome-lysosome fusion by preventing Stx17 loading onto autophagosomes. Mol Biol Cell *30*: 2283-2295.
184. Church, J.A. (2014). Cell Death by Pyroptosis Drives CD4 T-Cell Depletion in HIV-1 Infection. Pediatrics *134 Suppl 3*: S184.
185. Braun, J.S., Prass, K., Dirnagl, U., Meisel, A., and Meisel, C. (2007). Protection from brain damage and bacterial infection in murine stroke by the novel caspase-inhibitor Q-VD-OPH. Exp Neurol *206*: 183-191.
186. Laforge, M., Silvestre, R., Rodrigues, V., Garibal, J., Campillo-Gimenez, L., Mouhamad, S., et al. (2018). The anti-caspase inhibitor Q-VD-OPH prevents AIDS disease progression in SIV-infected rhesus macaques. J Clin Invest *128*: 1627-1640.
187. Lim, E.J., El Khobar, K., Chin, R., Earnest-Silveira, L., Angus, P.W., Bock, C.T., et al. (2014). Hepatitis C virus-induced hepatocyte cell death and protection by inhibition of apoptosis. J Gen Virol *95*: 2204-2215.
188. Teng, X., Chen, W., Liu, Z., Feng, T., Li, H., Ding, S., et al. (2018). NLRP3 Inflammasome Is Involved in Q-VD-OPH Induced Necroptosis Following Cerebral Ischemia-Reperfusion Injury. Neurochem Res *43*: 1200-1209.
189. Scheller, C., Sopper, S., Chen, P., Flory, E., Koutsilieri, E., Racek, T., et al. (2002). Caspase inhibition activates HIV in latently infected cells. Role of tumor necrosis factor receptor 1 and CD95. J Biol Chem *277*: 15459-15464.
190. Platt, E.J., Wehrly, K., Kuhmann, S.E., Chesebro, B., and Kabat, D. (1998). Effects of CCR5 and CD4 cell surface concentrations on infections by macrophagetropic isolates of human immunodeficiency virus type 1. J Virol *72*: 2855-2864.
191. Ramilo, O., Bell, K.D., Uhr, J.W., and Vitetta, E.S. (1993). Role of CD25+ and CD25-T cells in acute HIV infection in vitro. J Immunol *150*: 5202-5208.
192. Leng, Q., Borkow, G., Weisman, Z., Stein, M., Kalinkovich, A., and Bentwich, Z. (2001). Immune activation correlates better than HIV plasma viral load with CD4 T-cell decline during HIV infection. J Acquir Immune Defic Syndr *27*: 389-397.
193. Connolly, P., Garcia-Carpio, I., and Villunger, A. (2020). Cell-Cycle Cross Talk with Caspases and Their Substrates. Cold Spring Harb Perspect Biol *12*.
194. Falk, M., Ussat, S., Reiling, N., Wesch, D., Kabelitz, D., and Adam-Klages, S. (2004). Caspase inhibition blocks human T cell proliferation by suppressing appropriate regulation of IL-2, CD25, and cell cycle-associated proteins. J Immunol *173*: 5077-5085.
195. Perng, Y.C., and Lenschow, D.J. (2018). ISG15 in antiviral immunity and beyond. Nat Rev Microbiol *16*: 423-439.
196. Teijaro, J.R., Ng, C., Lee, A.M., Sullivan, B.M., Sheehan, K.C., Welch, M., et al. (2013). Persistent LCMV infection is controlled by blockade of type I interferon signaling. Science *340*: 207-211.
197. Merigan, T.C., Reed, S.E., Hall, T.S., and Tyrrell, D.A. (1973). Inhibition of respiratory virus infection by locally applied interferon. Lancet *1*: 563-567.
198. Sundmacher, R., Neumann-Haefelin, D., and Cantell, K. (1976). Letter: Interferon treatment of dendritic keratitis. Lancet *1*: 1406-1407.
199. Arvin, A.M., Feldman, S., and Merigan, T.C. (1978). Human leukocyte interferon in the treatment of varicella in children with cancer: a preliminary controlled trial. Antimicrob Agents Chemother *13*: 605-607.
200. Greenberg, H.B., Pollard, R.B., Lutwick, L.I., Gregory, P.B., Robinson, W.S., and Merigan, T.C. (1976). Effect of human leukocyte interferon on hepatitis B virus infection in patients with chronic active hepatitis. N Engl J Med *295*: 517-522.

201. Daniels, D., Grytdal, S., Wasley, A., Centers for Disease, C., and Prevention (2009). Surveillance for acute viral hepatitis - United States, 2007. MMWR Surveill Summ *58*: 1-27.
202. Zhou, Q., Chen, V., Shannon, C.P., Wei, X.S., Xiang, X., Wang, X., et al. (2020). Interferon-alpha2b Treatment for COVID-19. Front Immunol *11*: 1061.
203. Bidwell, B.N., Slaney, C.Y., Withana, N.P., Forster, S., Cao, Y., Loi, S., et al. (2012). Silencing of Irf7 pathways in breast cancer cells promotes bone metastasis through immune escape. Nat Med *18*: 1224-1231.
204. Thyrell, L., Erickson, S., Zhivotovsky, B., Pokrovskaja, K., Sangfelt, O., Castro, J., et al. (2002). Mechanisms of Interferon-alpha induced apoptosis in malignant cells. Oncogene *21*: 1251-1262.
205. Filipi, M., and Jack, S. (2020). Interferons in the Treatment of Multiple Sclerosis: A Clinical Efficacy, Safety, and Tolerability Update. Int J MS Care *22*: 165-172.
206. Organization, W.H. (2020). World Health Organization (WHO) report.